SM 84-20

STRUCTURAL ANALYSIS OF IMPERFECT THREE-LEGGED TRUSS COLUMNS FOR LARGE SPACE STRUCTURES APPLICATIONS

Thesis by

Dov Elyada

In Partial Fulfillment of the Requirements

for the Degree of

Doctor of Philosopy

California Institute of Technology

Pasadena, California

1985

(Submitted December 7, 1984)

PREFACE AND ACKNOWLEDGEMENTS

This thesis is an outgrowth, indeed the only truly productive outcome, of a more ambitious and general research plan: Static structural stability, non-linear response and imperfection-sensitivity in reticulated-shell structures of a fairly broad, though initially undefined, class of geometries. Results were to be applied towards analysis of *Large Space Structures;* in particular, structures like the *McDonnel-Douglas geodetic-cylinder beam* [12] (see introduction, Fig. 1-3) which displays triplex modal interaction, were in mind. The approach was to be a closed-form one, leaving numerics as a last resort.

It so happened, however, that at the initial phase of the research a paper by Crawford and Benton [33] was encountered, dealing with duplex modal interaction in three-legged columns of large space structures, and which, it was thought, could be improved upon. This seemed a worthy-enough first step, and indeed, the results (which were to become Chapter 3 of this thesis) were encouraging. Still there remained a doubt as to the practical value of that analysis, in which discontinuous-pinned longerons and infinite shear rigidity were assumed. it took some work to clear the first assumption, yet the second one kept on resisting till it was recognized (in the course of assisting Ae 104 students in analyzing a rigid-jointed three-legged column with which they were experimenting during the third term of 1981/82) that another problem was involved; any practical finite-rigidity shear web was apt to introduce coupling between bending and compression, coupling which did not exist in the idealized problem, was specific to the web design details and was probably of greater importance than the finiteness of the shear rigidity.

With this recognition the three-legged column was put aside in favor of the general problem. It was soon found, however, that none of the methods that had

been applied to the three-legged column were applicable to the reticulated shell. First, reticulated shells with discontinuous-pinned members were, in general, statically-underdeterminate, and no magic shear webs could be introduced to save them. Introduction of member continuity meant that local and global displacements could no longer be sharply distinguished as they had been in the three-legged column. Most importantly, the three-legged column had a statically-determinate cross-section, meaning that it was possible to determine the *internal* forces using equilibrium only, whereas this was not the case in the reticulated shell. There, the internal forces could only be calculated from the displacements, using an *inverted* local load-displacement relation, which was unavailable in closed-form.

In view of this an altogether new approach was tried. This was based on the works of Forman and Hutchinson [27] and M.S. Anderson [28,32] who treated the bifurcation problem of *'perfect'* [1] reticulated shells in a closed-form, exact-finite-difference manner. The idea was to use the same finite-difference framework as they did to write the equations, or potential energy, of the *imperfect* system and to obtain approximate solutions using either Galerkin's or Rayleigh-Ritz's method. The major obstacle was found again to be the necessity of inverting the local load-displacement relation for each member. Though an approximate closed-form inversion was obtained, its complexity rendered it useless as a basis for successive closed-form steps.

Could the generality of the problem be sacrificed in order to avoid this inversion business? Certainly, if enough of the members in a cross-section had an already-inverted or easy-to-invert load-displacement relations, the remaining ones being as numerous as the equilibrium equations, that could have been possible. It turned out that the three-legged column - this time with a realistic

1. In [32] a special kind of *local* imperfections is also treated.

shear-web, constructed of six string diagonals in each bay - is just such a structure. Being probably of the most-immediate interest to large space structures applications, and moreover, promising to exhibit triplex modal interaction (diagonal-slackening considered as a third instability mode) this problem was tackled.

Although undertaken mainly as an exercise that lends insight into general multiplex interaction phenomena, the problem of the string-diagonaled three-legged column proved formidable enough to occupy the rest of the research period. Refraining from presentation of inconclusive phases of the work, this thesis thus covers only that problem and special cases derived from it.

The first year of the research was supported in part by the California Institute of Technology President's Fund, Grant No. PF 218. This support is gratefully acknowledged. The author wishes to express his sincere gratitude to his advisor, Professor Charles D. Babcock, for the very fruitful conversations he had with him and for his concern and attention in general. An hour of discussion with him usually turned out a problem-defogger far more efficient than two weeks of banging one's head against one's office wall. His helpfulness is very much appreciated. The author also wishes to thank Ms. Marta Nyiri for typing the horrible manuscript and for her extraordinary patience with that stubborn perfectionist. Thanks also go to Mrs. Betty Wood who helped in preparing the graphical material. Last but not least, the author is grateful to the person who sacrificed most in order to make this whole adventure possible, his wife Nora Elyada, to whom he dedicates this work with love.

D.E.,

"And thus was the work of the columns completed."

First Kings, 7:22

Pasadena,

November 1984

ABSTRACT

Three-legged truss columns are basic structural components of many envisioned large outer-space structures. They constitute three longerons ('legs') forming, in the column cross-section, the vertices of an equiliateral triangle. Their longerons are held together by uniformly spaced battens while a shear web, usually made of diagonals, restrains shear deformation.

This work deals with configurations characterized by having relatively stiff battens, longerons which are pinned to the battens and prestressed string diagonals. Considered are only simply-supported slender columns having slender longeron segments and relatively thin and lightly preloaded diagonals. The columns are allowed to have global (overall) as well as local (longeron segment) geometrical imperfections - not necessarily small ones.

Investigated is the static structural behavior of such columns when loaded by purely axial compressive concentrated forces acting at the supports. Addressed are the topics of global and local buckling, post-buckling, imperfection sensitivity, global-local mode interaction, complete non-linear response, limit loads and diagonals slackening and post-slackening.

The approach is a theoretical one; a system of non-linear, ordinary differential equations is set up which represents the column, and results, mostly in closed form, are obtained by solving that system for a variety of cases of varying generality.

First, a highly idealized case is studied in detail, in which the diagonals are removed and infinite shear rigidity is postulated instead. The results exhibit most of the essential features of the more complicated cases. Next, the case of the undeflected or only-slightly-deflected column is considered. Results include

the prebuckling behavior, slackening and local buckling loads, global buckling load, initial post-buckling behavior and imperfection sensitivities. Diagonals slackening in a deflecting column is studied next. This is done by means of slackening loci constructed in the load-deflection plane. Solutions are obtained for some special cases of a deflecting column. These include a complete analysis of the locally-perfect case and the cases of small load and high deflection. Also obtained is an engineering-oriented load-deflection working relation valid for the most general case but based on generalization rather than on rigorous solution. A torsion-compression mode, dominant in post-slackening, is also analyzed. The work is concluded by investigating the error committed in treating continuous longerons as if they were discontinuous-pinned.

TABLE OF CONTENTS

LIST OF FIGURES

NOMENCLATURE

Remark:

Nomenclature entries marked by < P> correspond to symbols which are used exclusively for physical/dimensional quantities. Nomenclature entries marked by < P/N eqn. # > , where eqn. # is an equation number, correspond to symbols which denote physical/dimensional quantities in part of the text, then change their meaning to normalized/nondimensional in another part. Eqn. # points to the equation according to which the normalization is done. No confusion should arise since nearly all the work deals with only normalized/non-dimensional quantities. The exceptions are few, short and well-defined: Sections 2.1-2.6, Section 7.1 to eqn. (7.7) and Section 8.1.1 to eqns. (8.4). Normalized quantities that must appear in these places side by side with their physical counterparts are distinguished by "hats" (^), which are later dropped. See also text in the following locations: (1) beginning of Section 2.5.1; (2) beginning of Section 2.7; (3) beginning of Section 7.1; (4) following Eqn. (7.7); (5) beginning of Section 8.1.1; and (6) following eqns. (8.4). Entries having neither < P> nor < P/N eqn. # > correspond to symbols denoting exclusively normalized/non-dimensional quantities.

a	Amplitude of column deflection, the spanwise maximum of w(x), < P/N 2.21d> .
a_{max}	Maximum of a such that the theory is still valid.
a(max)	Value of a for which $P = P_m$.
A	Longeron cross-sectional area, < P> . Also, in Section 4.7 only, a coefficient defined before eqns. (4.28).
B	A coefficient defined before eqns. (4.28).

c_1, c_2	Constants of integration, eqns. (6.12).
C	A coefficient defined before eqns. (4.28).
C_s	Slackening parameter defined by eqn. (4.6a).
C_s°	The ε-independent part of C_s, eqn. (4.6b).
D	Defined by eqn. (6.11g).
e	Global imperfection parameter, the amplitude of $w_o(x)$, <P/N 2.30>.
e*	Equivalent e for third bifurcation, eqn (6.15).
E	Young's modulus of longeron material, <P>.
E_t	Segment "tangent modulus", $d(p/A)/d(\delta)$, eqn. (2.10), <P>.
E_1, E_2	Eqns. (6.11e,f).
$(EA)_d$	Diagonal extensional stiffness, <P>.
$f(\alpha)$	A certain function of α, eqn. (3.31b) and Figure 3-7.
$f_1(\alpha)$	A certain function of α, eqn. (3.25) and Figure 3-7.
$f_2(\alpha)$	A certain function of α, eqn. (3.26).
$f_{CB}(\alpha)$	Crawford and Benton-implied $f(\alpha)$, eqn. (3.36), Figure 3-7.
$g(\alpha)$	A function of α to be identified (=1).
$g_1(\chi)$	Function of χ, eqn. (8.7a).
$g_2(\chi)$	Function of χ, eqn. (8.7b).
h	Standard of smallness (2nd paragraph of Section 2.5).
$h_1(\chi)$	Function of χ, eqn. (8.9a).
$h_2(\chi)$	Function of χ, eqn. (8.9b).

H	In Chapter 2: Heaviside's step function; in Chapter 3: P_E/P.
i	Unit vector in the x direction, Figures 2-5, 7-1.
I	Longeron bending-related cross sectional second moment of area, < P> .
j	Unit vector in the y direction, Figure 7-1.
k	Unit vector in the z direction, Figures 2-5, 7-1.
K	In Chapter 3: $\varepsilon^2/(1-P)^3$; in Chapter 4: $\lambda^2 B/4AC$.
l	Bay length, longeron segment length, Figure 1-6, < P> .
$\mathbf{l}_{mn}$	Vector associated with bay member mn (Section 2.2), < P> .
l_{mn}	Length of $\mathbf{l}_{mn}$, < P> .
L	Overall column length, Figure 1-6, < P> .
m_i^b	End bending moment of longeron segment at batten i, Figure 8-1, < P/N 8.4f> .
N	Number of bays in complete column.
o, O	Order symbols, eqns. (2.12).
p(x)	Local (longeron) compressive force in general.
p_e	Simply-supported longeron segment Euler buckling load, $\pi^2 EI/l^2$, < P> .
p_i	Compressive force in longeron segment i, Figure 8-1, < P/N 8.4a> .
p_o	Longeron segment compressive preload, < P/N 2.14d> .

$\mathbf{p}_{mn}$	Internal force vector associated with bay member mn, < P> .
p_{mn}	Magnitude of $\mathbf{p}_{mn}$, eqn (2.7), < P/N 2.14a> or < P/N 2.17a> .
$\bar{p}$	Mean longeron compressive force, eqn. (4.1).
$\bar{p}_b$	$\bar{p}$ at global buckling.
$\bar{p}_r$	Auxiliary longeron force for calculating paths using eqns. (6.27).
P	Column external compressive force, Figure 6-1, < P/N 2.24> .
P_b	P of global buckling (first bifurcation).
P_c	P of local buckling (second bifurcation).
P_E	Perfect-ideal column global Euler-buckling load, eqn. (2.22).
P_m	Column maximum load-carrying capacity, limit load.
P_p	Nominal (perfect column) maximum load-carrying capacity.
P_s	P of diagonal slackening in an undeflected column.
P_{ES}	Eqn. (4.36).
P^*	Critical (third bifurcation) load of the undeflected column, eqn. (4.4a).
P_c^*	Critical (third bifurcation) load of the deflected column.
P_E^*	Perfect-non-ideal column global Euler buckling load, eqn. (4.20a).
q	General quantity.
q_i	General quantity corresponding to longeron segment i.

q_i^b	General quantity corresponding to batten i.
$\mathbf{r}_o, \mathbf{r}_m, \mathbf{r}_{mn}$	Lever-arm vectors, < P> .
R	Radius of circle circumscribed about column cross-section, Figure 1-6, < P> .
t	Integration dummy variable.
$u(x), u_i$	Axial displacement, ith bay node axial displacement, Figure 2-3, < P/N 2.21c> .
u_i^b	Axial (x) displacement of ith batten centroid, < P/N 2.21c> .
$v(\xi)$	Longeron segment deflection, Figure 8-1, < P/N 8.4d> .
$v_o(\xi)$	Longeron segment imperfection deflection, Figure 8-1.
$v_i'^b$	Longeron segment end slope ($dv/d\xi$) at batten i.
$w(x), w_i$	Column deflection, ith bay node transverse displacement, Figure 2-3, < P/N 2.21d> .
w_i^b	Transverse (z) displacement of ith batten centroid, < P/N 2.21d> .
$w_i''^b$	Column curvature referred to a batten point, Figure 8-2, eqn. (8.13).
x	Global spanwise coordinate axis, Figure 2-2, < P/N 2.21a> .
x_i	x-coordinate of ith bay node in ref. state, Figure 2-3, < P/N 2.21a> .
x_j^b	x-coordinate of ith batten in ref. state < P/N 2.21a> .
x_c	x-coordinate of transition point between critical and sub-critical column stretches.
x_{lb}	x-coordinate of locally-buckled spanwise point.

x_s	x-coordinate of slackening onset point.
x_{sP}	P-dependent x_s.
y	Global transverse coordinate axis, Figure 2-4, < P> .
z	Global transverse coordinate axis, Figure 2-2, < P> .

Greek Symbols:

α	Load-deflection variable, amplitude of $\varphi(x)$, eqn. (3.3b).
α_r	Auxiliary α for calculating equilibrium paths using eqns. (6.27).
β	Bay aspect ratio parameter, eqn. (2.5).
$\gamma(x)$, γ_i	Shear deformation, ith bay shear angle, Figure 2-3, < P/N 2.21f> .
$\delta(x)$,δ_i	Longeron relative shortening, relative shortening of ith longeron segment, Figure 8-1, < P/N 8.4b> .
δ_{mn}	"Strain" of bay member mn, eqns. (2.3), < P/N 2.14b or 2.17b> .
ε	Local imperfection parameter, amplitude of $v_o(\xi)$, < P/N 2.14c, 8.4c> , (Figure 2-1).
η, η_i	Local transverse coordinate axis, transverse coordinate axis for longeron segment i, Figures 8-1, 8-2, < P> .
η_1, η_2	Eqns. (6.11c,d).
$\vartheta(x)$,ϑ_i	Bending deformation, ith bay bisector rotation, Figure 2-3, < P/N 2.21e> .

ϑ_i^b	Rotation of the ith batten around the y axis, < P/N 2.21e> .
ϑ_o	In Chapter 3: $\varphi'(o)$, elsewhere: imperfection theta, < P/N 2.21e> .
κ	Normalized diagonal rigidity, eqn. (2.18).
λ	Normalized bay length, eqn. (2.25).
$\mu_1(x)$	Amplitude of alternating part of end-moment function, solution of eqn. (8.19b).
$\mu_2(x)$	Slowly-varying part of end-moment function, solution of eqn. (8.19c).
$\mu_i^{(j)b}$	Components of m_i^b according to (8.16) decomposition.
ν	Shear compliance parameter, eqn. (2.41c).
ξ,ξ_i	Local axial coordinate axis, axial coordinate axis for longeron segment i, Figures 8-1, 8-2, < P/N 8.4e> .
ρ	Longeron bending-related cross sectional radius of gyration, $\sqrt{I/A}$, < P> .
$\varphi(x)$	Load-normalized deflection, eqn. (3.3a).
$\chi(x),\chi_i$	Eqn. (8.2).
ψ^b	Rotation of a batten around the x axis < P> .
$\psi'(x),\psi_i'$	Bay twist, Figure 7-1, eqn. (7.1b), < P/N 7.7> .

Operations and Special Symbols:

$(\,)'$	Differentiation with respect to the argument, also, finite differentiations as in eqns. (2.2), (8.18), < P/N 2.21b> .
$(\,)^{\bullet}$	Differentiation with respect to $\hat{x}$. Becomes $(\,)'$ whenever "hats" are dropped, eqn. (2.21b).
$(\hat{\ })$	Temporary indication of normalized quantities.
$(\,)_o$	Imperfection displacement measures, eqn. (2.29a); exceptions: ϑ_o in Chapter 3 and p_o.
$(\bar{\ })$	$(\,)$-$(\,)_o$, deformation-constituent of a displacement measure, eqns (2.36); exceptions: $\bar{p}$ and its related quantities.
$(\,)^{(j)}$	Perturbation of order j (except in $\mu_i^{(j)b}$).
$(\,)_b$	Of global buckling.
$(\,)_i^b$	Of batten i.
LBL	Local Buckling Line.

1. INTRODUCTION

1.1 Large Space Structures and Truss Columns

In recent years a considerable amount of work has been put into the design and analysis of a novel class of structures; structures of very large dimensions to be erected, assembled, deployed or even wholly manufactured in outer space. Among the applications envisioned are space-stationed communications platforms, radio-astronomy dishes and VLBI systems, solar sail propulsion systems, solar power stations and large space stations and colonies (Figures 1-1). Dimensions are to range from a few tens of meters to a few kilometers. Some are to be built in low earth orbits and then be transferred to the geosynchronous orbit. For more details, including many graphical artist conceptions, the reader is referred to references such as [1-5].

The problems associated with materializing such systems are manifold. An appreciation of the variety of subjects involved can be gained from the above references as well as from the proceedings of the NASA-sponsored meetings [6-10] dedicated to the subject. We will only mention those problems related to structural integrity and performance. The large dimensions together with the typical low-load environment and the imperative necessity of weight optimization lead to extremely flexible structures. Thus attitude or orbit control of such structures involve also *shape control*. Thermoelastic problems arise from uneven sun-radiation absorption and poor heat conductivity and result in geometrical distortions detrimental to the performance of systems like antena dishes. For structural elements the design criterion of which is their load-carrying capacity (such as members directly connected to engines, thrusters, actuators or large concentrated masses) the typical large-space-system requirements will lead to stiffness-critical rather than strength-critical elements. In

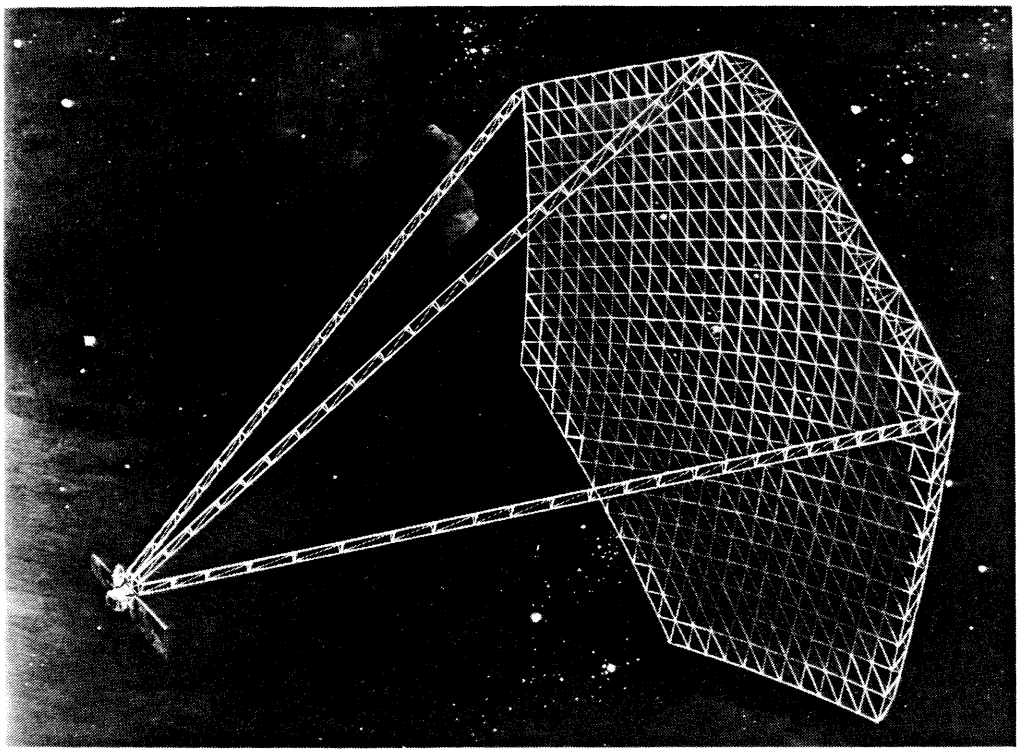

Figure 1-1a. Synchronously deployable truss antenna (NASA Langley Research Center).

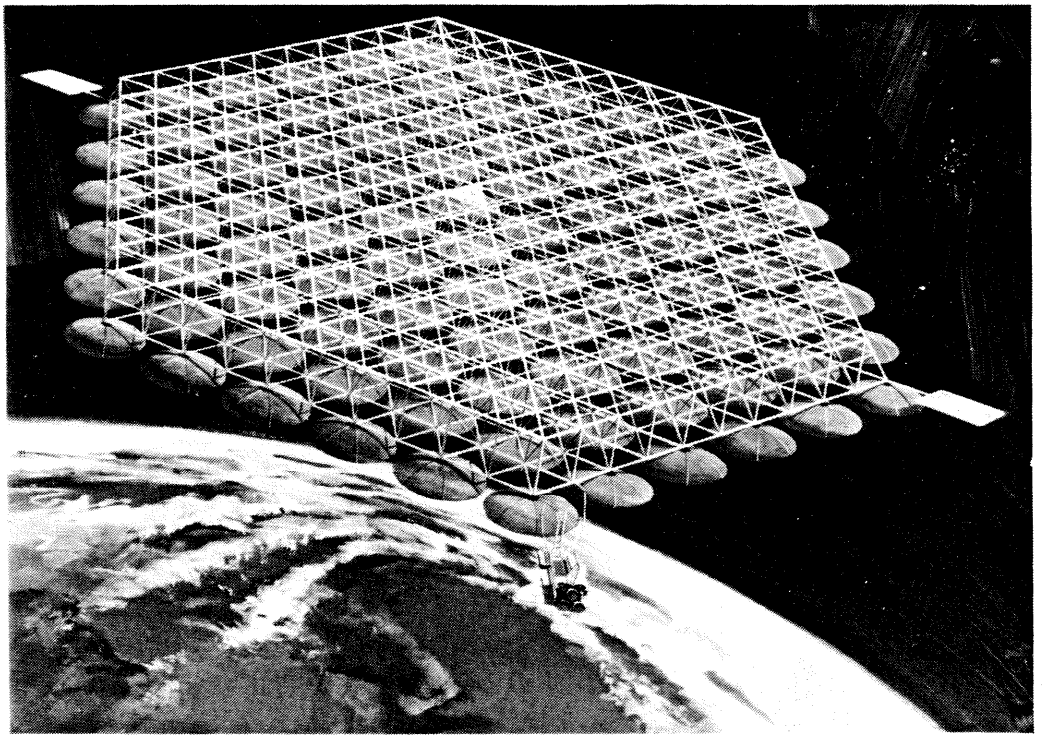

Figure 1-1b. Large space communications platform (NASA Langley Research Center).

other words, such elements will have to be designed for sufficient structural stability and buckling strength. A detailed presentation of large space structures design requirements is given by Hedgepeth [11]. In this work we will be concerned with the static structural stability aspect only.

A widely-used way of optimizing stiffness/weight ratios in structural designs is that of 'hierarchical structuring', i.e., the primary structure is constructed of a lattice of secondary members, say truss beams, each of which is itself built up of tertiary members - longerons, diagonals, battens - and, depending on the size of the primary structure, even lower-than-third-ranking members may be used. Examples of this are shown in Figures 1-2 and 1-3. No wonder, then, that apart from structural elements intended to maintain some required environment, most load-carrying elements in large space structures are designed in the above manner. It is therefore of interest to understand the behavior of such structures, and in particular that of their basic building blocks; the truss beams, truss rods and truss columns. The latter are distinguished by their being incorporated into the primary structure in such a way as to make the load acting on them a pure axial compression.

A variety of truss columns appear in large space structure concepts. They may be classified according to their number of longerons (or 'legs'), the method used to keep the longerons apart (battens), the method used to resist bending- and torsion-related shears (shear web) and the degree of fixity of their joints. Some are rigidly assembled in space whereas others (Figures 1-4, 1-5) are deployable/collapsible. The most common truss columns are the three- and four-legged ones. An extreme case is when the column has 'many' longerons, (of the order of a few tens, say). It then becomes a *cylindrical geodetic column* or, as it is sometimes called, a *cylindrical isogrid column*. An example of this kind is the column developed for in-space manufacturing by McDonnel-Douglas

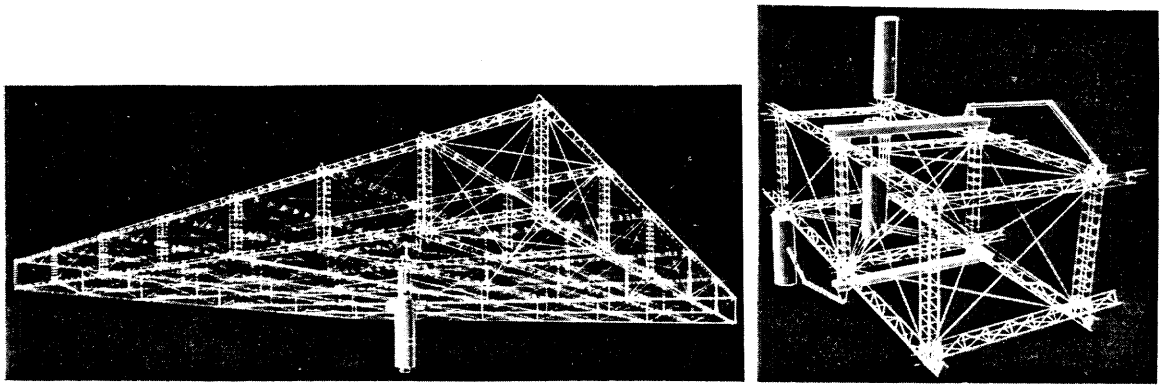

Figure 1-2. Hierarchical structuring in large space structures. (From ref. 1, courtesy of Aerospace America.)

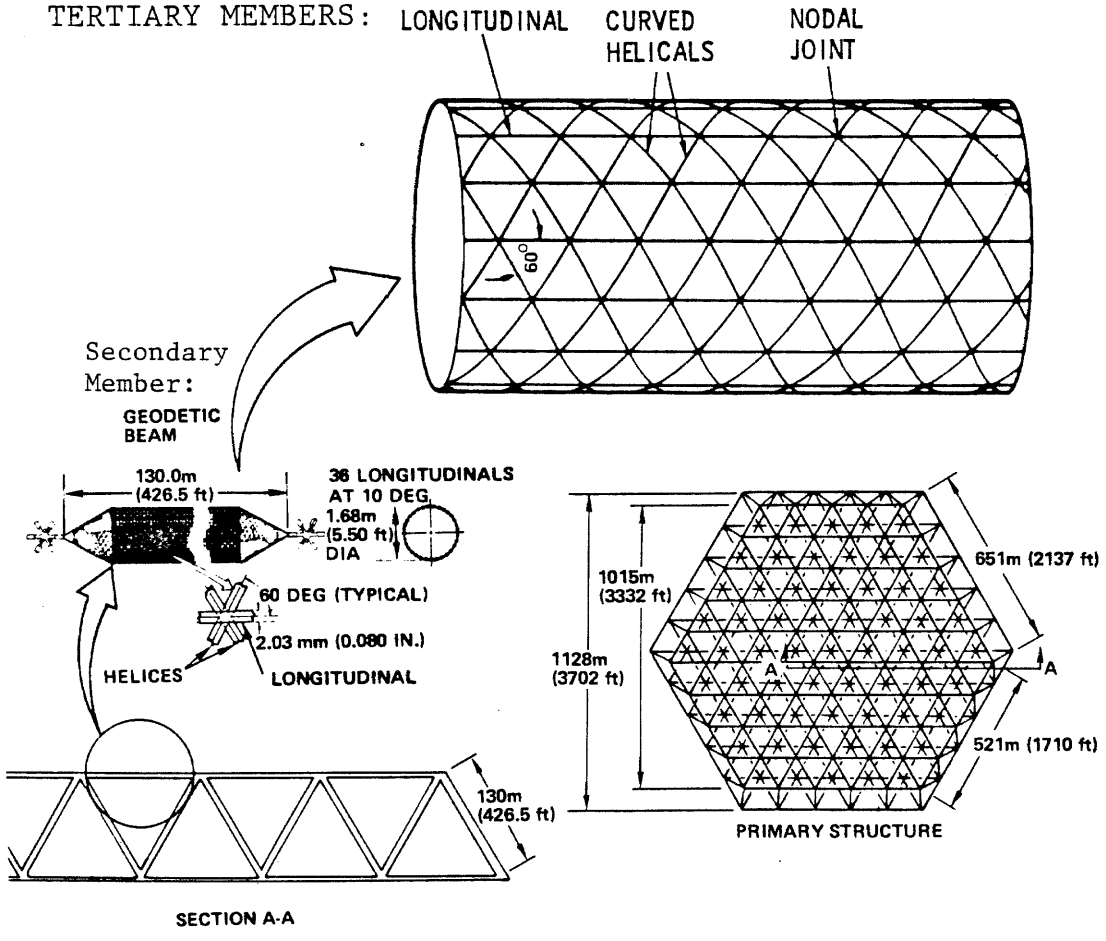

Figure 1-3. Hierarchical structuring: the McDonnel Douglas Geodetic Column [12].

Corporation [12], which is shown in Figure 1-3.

Of most immediate interest to designers is, perhaps, the three-legged column, which is the simplest and therefore the likeliest to find use in the first generation of large space structures. Two examples are shown in Figures 1-4 and 1-5. The first is a rather large design (3.66 m. transverse dimension and 203.8 m. extended length) developed by Lockheed [13] for a version of the Land-Mobile Satellite. The second is an Astromast™ (Series A15000) column produced by Astro Research Corporation. Both are deployable structures, stabilized against shear by simple string diagonals and appear to have fairly low (if at all) joints fixity. The commonality of such designs and the likelihood of their being put to actual use are among the reasons three-legged columns having string diagonals were chosen to constitute the subject of this work.

1.2 Modal Interaction and Imperfection Sensitivity in Truss Columns

It has been known for a long time that certain classes of structures, when subjected to buckling loads in a load-controlled environment, sometimes also in a displacement-controlled environment, exhibit a particularly abrupt, violent, even destructive buckling behavior. For the same structures, experimentally-obtained critical loads show an extreme degree of scatter, and values which are often only a small percentage of the calculated bifurcation-buckling loads. It was Koiter, in his classical work [14], who established that the reasons for this behavior lie in the *instability of equilibrium of the post-buckled state* and made the connection between this property and the consequential *imperfection-sensitivity* of such structures. By 'imperfection sensitivity' it is meant that even slight geometrical, material or loading variations introduced into an otherwise 'perfect' system, i.e., a system that posesses a bifurcation-type buckling, suffice to sharply reduce the load-carrying capacity of the structure below the load

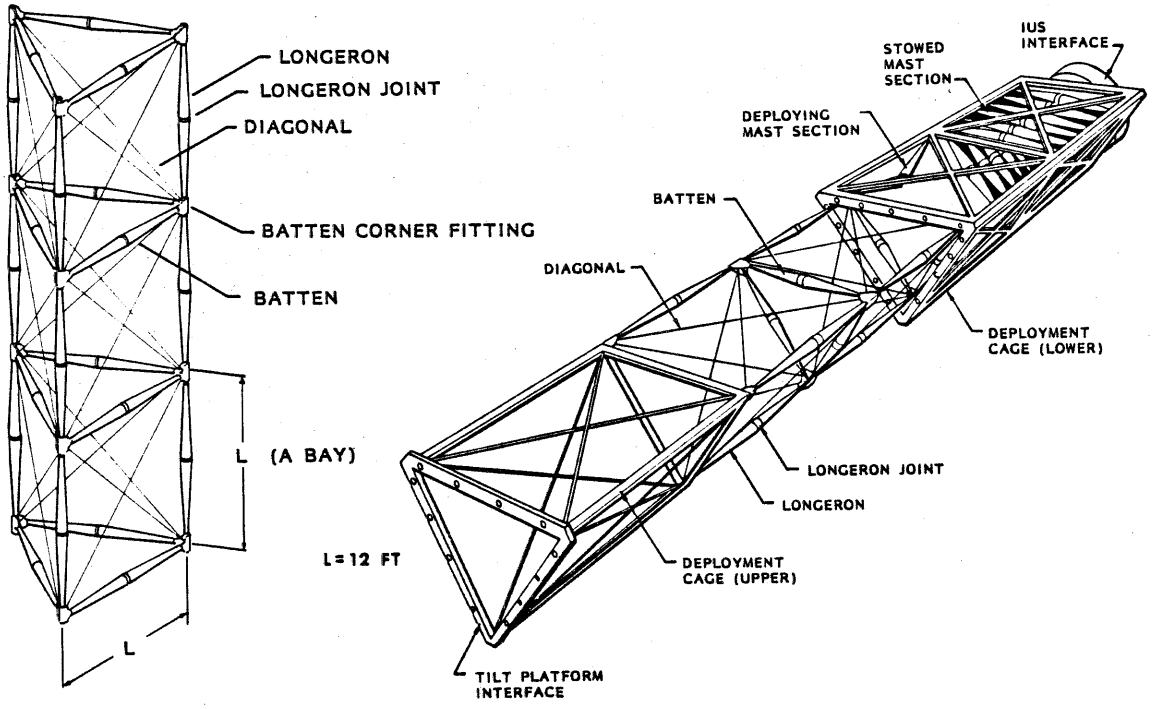

Figure 1-4. Lockheed 3-legged deployable mast for Land Mobile Satellite System [13].

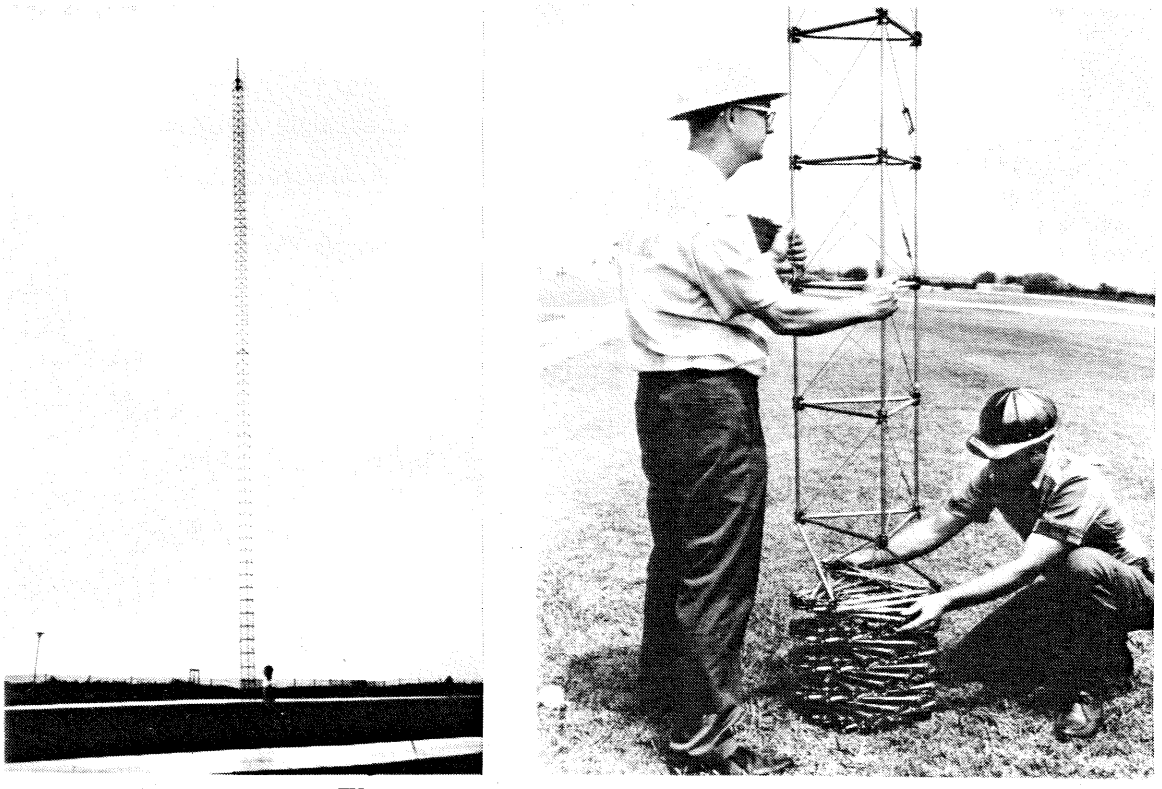

Figure 1-5. Astromast™ series A15000 deployable three-legged column, by Astro Corporation.

associated with the bifurcation condition. Koiter's discoveries stimulated an extensive research effort reviewed many times, e.g. Tvergaard [15].

As was pointed out by Koiter himself (see [15]), structures which have two or more independent buckling modes with coinciding or nearly-coinciding critical loads are particularly prone to post-buckling instability and imperfection sensitivity. Indeed, the classical example of a highly imperfection-sensitive structure - the axially-compressed cylindrical shell, with its multitude of coinciding modes (Timoshenko and Gere [16]) - is just such a structure. This phenomenon is known as *modal interaction*. The reason behind it, at least in some cases, is that the structure, buckled in one of the modes, presents a much-lower resistance to buckling in the other mode than does the nominal structure. Even though each of the interacting modes considered separately may in itself be insensitive to imperfections, their interaction produces a highly imperfection-sensitive circumstance.

A very common situation of modal interaction occurs in structures having so-called *local* and *global* buckling modes. The term 'local' usually refers to a mode of wavelength short compared with the largest structural dimension, and in which some structural detail buckles. On the other hand, the global mode wavelength is of the order of the largest structural dimension and in it some overall feature of the structure is deformed. If designed so as to have close local and global critical loads these structures may exhibit modal interaction. Indeed, starting in 1969 with van der Neut's column[1] [17,18], local-global interactions were studied by several authors (see [15]; a few recent additions may be found in [19]). Some highly idealized cases, including van der Neut's, were investigated because of their demonstrative power. Of special interest are

1. van der Neut's column is a column built-up of two spaced flanges, each of which is a simply-supported plate. 'Local' there refers to plate buckling whereas 'global' is the overall column buckling.

the examples given in the monograph by Thompson and Hunt [20]. Besides presenting van der Neut's results, they also show that similar interaction phenomena can occur not only between two buckling modes but also between a single buckling mode and a material-yield failure mode. Most importantly from our standpoint, Thompson and Hunt show that in a truss column not altogether unlike ours, modal interaction and high imperfection sensitivity do occur. There, as in our case, the global mode is an overall Euler mode of the complete column while the local mode refers to buckling between battens of longeron segments.

Thus, another dimension is added to the interest in investigating three-legged columns for large space structures applications. If weight-minimization, so important in these applications, is done using the simplistic "one-horse-shay" approach, i.e., by sizing the structure in such a way as to make it fail in the local and global modes simultaneously, then modal interaction results. As pointed out by Thompson and Hunt [20] and Thompson and Lewis [21], the extreme imperfection sensitivity thus created erodes away the column strength to such an extent as to shift the optimal design-point significantly. There is no way that either realistic load-carrying capacity estimates or valid structural optimization may be done without allowing in the analysis for modal interaction and without knowledge of the imperfection involved. Hence the interest that this work might bear towards a well-based design of large space structures.

Before leaving this subject it should be noted that interactions more complicated than simple local-global may occur in large space structures columns, e.g., in cylindrical geodetic columns, besides the Euler overall mode and the local, between-joints longeron mode, there may exist modes typical of cylindrical-shell buckling (see Anderson [28]). If they all interact we have a case of 'triplex modal interaction'. Since in three-legged columns with string diagonals

slackening of all the preloaded diagonals constitutes a third mode of failure, with a definite critical load, we can expect triplex modal interaction to occur in our subject-problem too.

1.3 Statement of the Problem, Scope

In this work we deal with structural behavior of three-legged columns having preloaded string diagonals, Figure 1-6. These are taken as being secondary members of a primary large space structure, and incorporated into it through pinned joints. Thus the column under consideration will be simply-supported at both ends and subject to a single axial compressive load acting through the supports. As is mostly the case in large space structures (resulting from the large dimensions and low-load environment) our column will be *slender*, consisting of a large number of identical bays, each of which having an aspect ratio of the order of 1. The column cross section is equilateral-triangular. Only columns in which the longeron-segments are pinned to the battens are considered.

We are interested in the complete non-linear structural behavior of the column. In particular we will treat buckling, post buckling, modal interaction, imperfection sensitivity, non-linear response, load-carrying capacity and diagonal slackening behavior. We will not, however, be interested in global modes higher than the fundamental one.

The column is allowed two modes of geometrical imperfection, each associated with one of the buckling modes. The *global imperfection* is a deviation from straightness of the (unloaded) column axis, having a half-wavelength equal to the column length, whereas the *local imperfection* is an initial waviness of the longeron segments of a half-wavelength equal to the segment length. No imperfection is allowed in either the external loading, the diagonal preloads or the materials/dimensions of the longeron segments and diagonals. Though in

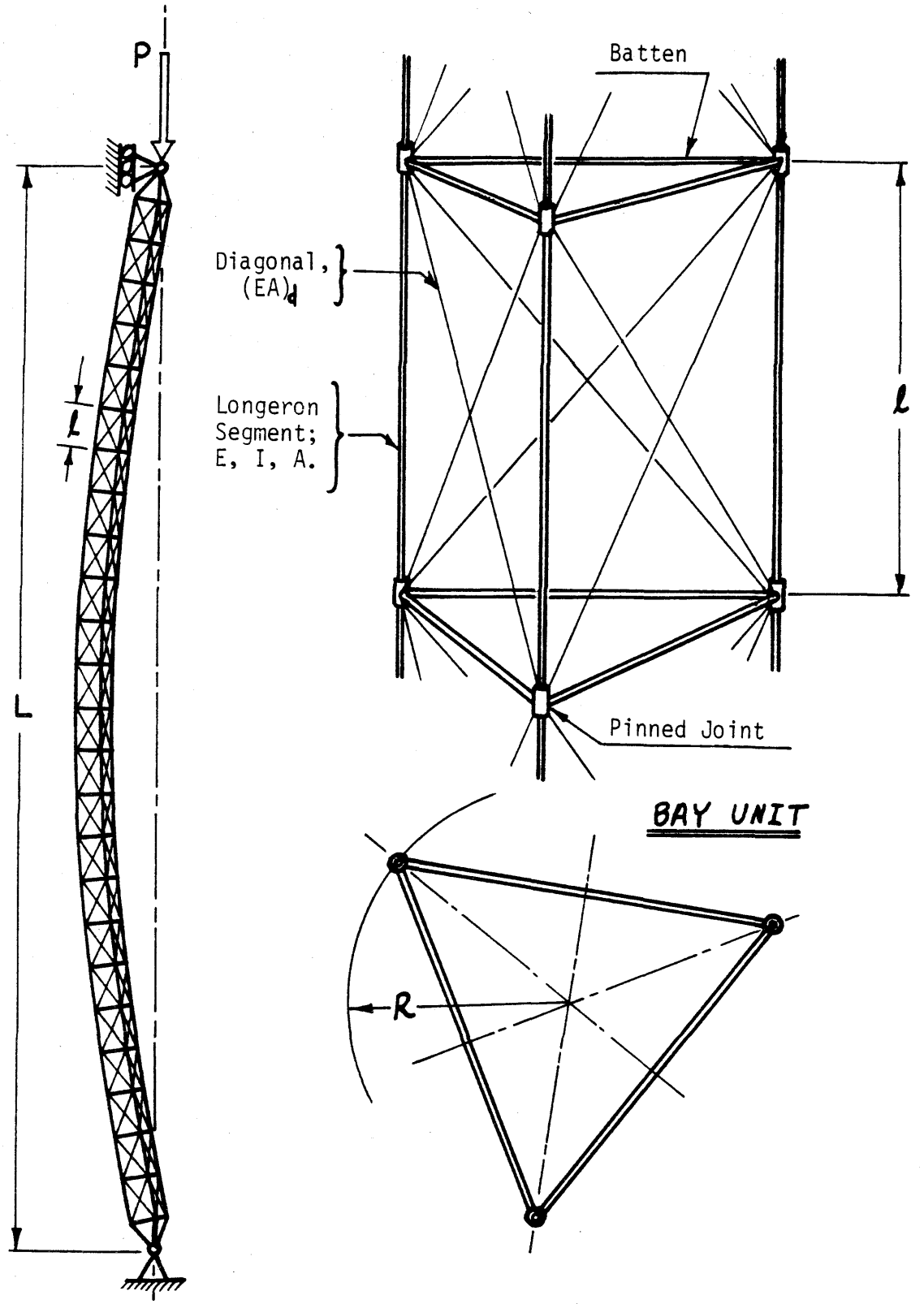

Figure 1-6. Problem definition.

practical situations actual imperfections are complicated the imperfections dealt with here are highly idealized: they are sinusoidal in shape, each mode describable in terms of a single imperfection parameter. Since in design situations the imperfections are known in advance to an extent not better than that, this poses no limitation from an engineering standpoint. The problem of how conservative the results of our analysis are with respect to 'worst-case' imperfections is not addressed. This work departs from studies using asymptotic imperfection-sensitivity approaches in its being a 'large imperfections theory'; the imperfections are allowed to assume magnitudes of the same order as the associated displacements.

1.4 Review of the State-of-the-Art

The problem of buckling of truss columns is by no means a new one. It was approached as early as 1891 by Engesser. His and subsequent works are referenced in Bleich's monograph [22]. The applications of interest were heavy terrestrial structures, and it proved sufficient to analyze them as columns of solid cross sections with finite shear rigidity, the latter determined from the particular shear web (lacing) design. See also Timoshenko and Gere [16]. Approximate methods were used to predict *local* buckling of truss members, e.g., Bleich [22]. The family of modern methods, referenced by Noor in [8], in which the lattice structure is replaced by an equivalent continuum structure, can be viewed as being, in some sense, an extension of that method.

With today's availability of finite element codes capable of handling large stability problems, a rigorous treatment as frameworks of truss columns having many degrees of freedom can in principle be done. However, when the number of degrees of freedom becomes large - as is mostly the case in large space structures applications - these essentially non-linear analyses become prohibitively

expensive. Reduction methods, in which a relatively small set of assumed modes is used to reduce the number of degrees of freedom of the finite element model, were introduced by Noor (e.g., [8,23]) in order to overcome this problem.

A third approach is one employing the calculus of finite differences. In repetitive structures, exact finite difference equations having constant coefficients can be written and sometimes solved for unknowns defined at discrete equispaced points. This approach, which can be traced to Bleich and Melan [24], was used in stability problems by von Karman and Biot [25] for a truss shear column, by Wah [26] for a planar beam gridwork and by Forman and Hutchinson [27] for repetitive reticulated shells. More recently M.S. Anderson [28] modified the method of Forman and Hutchinson and applied it to, among other cases, a cylindrical geodetic column and a certain kind of three-legged column.

The works and methods mentioned above do not treat modal interaction or imperfection-sensitivity, at least not explicitely. The first to do that with regard to truss columns were Thompson and Hunt [20]. Theirs is an idealized two-legged column that serves to demonstrate the global-local interaction phenomenon. Only local imperfections are considered and only the bifurcation point is sought. (For discussion of their results see Section 3.3.) Later, Crawford and Hedgepeth [29] treated the optimal design problem associated with Thompson and Hunt's column. Byskov [30] studies the same column, but with continuous longerons, using the method of Koiter and Kuiken [18] and also an asymptotic method deviced by himself and Hutchinson. A case of a column having global but not local imperfections was treated by Mikulas [31]. A restricted type of local imperfections (which do not result in prebuckling joint rotations) was introduced by M.S. Anderson [32] into his analysis of cylindrical geodetic columns.

Because of the high degree of idealization in Thompson and Hunt's column the results of the studies related to it could not have readily been applied to actual situations. The first step in this direction was taken by Crawford and Benton [33]. They generalized the Thompson and Hunt approach to a three-legged case having global as well as local imperfections.

And here we arrive at another motivation for the present work. It was felt that the power of Thompson and Hunt method cannot be rigorously extended to post-buckling and non-linear response problems. In doing that extension Crawford and Benton had to introduce certain hypotheses, the validity of which could not be verified without further analysis. (See later, Section 3.9.) Since in the present work the approach is fundamental, resort to uncertain assumptions is kept to a minimum.

Two more obstacles stood between Crawford and Benton's analysis and application to actual situations. These were the assumptions, borrowed from Thompson and Hunt's model, of discontinuous-pinned longerons and of infinite-rigidity non-coupling shear web. The present work goes some steps further towards applicability in that (1) although retaining the first assumption, it proves its appropriateness and (2) it replaces the idealized shear web by a practical one.

1.5 Approach and Structure of the Present Work.

The approach to the problem under consideration is a fundamental one: A system of algebraic equations, the unknowns of which are a set of displacement measures, and which incorporates geometry, material properties and static equilibrium conditions, is written for a single bay. Since this system involves changes in displacement measures that occur across a bay, then, viewed from a global standpoint, it constitutes a system of differential-like equations, in fact a somewhat unconventional finite-difference system, for the complete column.

Investigation of the column behavior is then done by studying this system and its solutions. An aim is to obtain as much of the behavior as possible in closed form.

The column equations are derived for a particular (likeliest) plane of deflection. Also assumed in the derivation is that longeron continuity is of no important consequence. The theory to be developed is a 'first-order theory' in the sense that only first-order terms in the displacement measures and in other small quantities are included. In this respect the level of approximation is the same as that of an Euler-Timoshenko column. In contrast to asymptotic post-buckling and imperfection-sensitivity approaches we will be able to obtain results valid for a relatively wide range of displacements and their associated imperfections (e.g. global deflections of the order of the column transverse dimensions); a range limited only by the 'first-orderness' of the theory.

The column equations are derived in Chapter 2. Then, in Chapter 3, they are reduced to the special case of an infinite-rigidity non-coupling shear web (the 'ideal column') to reveal the major features of the column behavior. We then return to the general case and in Chapter 4 we analyze phenomena related to its undeflected or slightly deflected state - slackening, local buckling, global buckling and initial post-buckling. Chapter 5 is devoted to the analysis of diagonal slackening while in Chapter 6 we deal with solutions and equilibrium paths in the deflected state. A special buckling mode, which involves pure torsion-compression, and which is associated with diagonal slackening in the absence of bending and global imperfection is discussed in Chapter 7. Lastly, in Chapter 8 the error caused by neglecting longeron continuity (in cases where the longerons are indeed continuous) is estimated and shown to be reasonably small.

2. COLUMN EQUATIONS

We approach the column problem by establishing a system of differential-like equations governing its behavior. First the assumptions employed are stated. Counterparts of the ordinary three groups of relations - strain-displacement, constitutive and equilibrium - are then derived. Using order-of-magnitude estimation techniques these relations are normalized and simplified. The concept of spanwise diagonal-slackening regions is introduced to set up regional displacement equations. The finite difference nature of these equations, and the implications of treating them as differential are discussed.

2.1 Assumptions

We place the following restrictions on the configuration of the column considered. In many envisioned large space structures applications these restrictions are reasonably met.

1. The column is simply-supported at both ends and is loaded by only a compressive force P acting at the supports (Figure 1-6).
2. The column is slender: its characteristic transverse dimension R (Figure 1-6) is much smaller than its length L.
3. The column is constructed of a sufficiently large number of identical bays so that the length of each, l (Figure 1-6), is much smaller than L. However, the bay aspect ratio l /R is considered to be still of order 1.
4. The longeron segment of length l is itself slender: its effective bending-related cross sectional radius of gyration, ρ, is small compared to l.
5. The longerons are pinned to the battens; no moments are transferred across the column from one longeron to its neighbors.

6. The diagonals cannot take compression and are therefore preloaded. The compressive preload thereby induced in the longerons, p_o, is small compared with the longeron segment Euler buckling load, $p_e = \pi^2 EI/l^2$. It is the same in all three longerons and does not change from bay to bay. During column loading diagonal slackening is allowed.

7. The diagonal extensional stiffness, $(EA)_d$, is much smaller than that of the longeron, EA; small enough so as to render the shear deformations important, still large enough so as to leave bending deformations dominant.

8. Both the longerons and diagonals are made of linearly-elastic materials.

9. The global imperfection is taken formally to have components associated with each displacement degree of freedom, components which are spanwise-smooth and slowly-varying. In specific treatments, however, those will invariably be specialized to exact replicas, in shape as well as in direction, of the components of the fundamental initial global buckling mode; the deflection having a sine shape of amplitude e and half-wavelength L.

10. The local imperfection has also a sine shape, with an amplitude ε and a half-wavelength l (Figure 2-1). ε is the same in all three longerons and does not change from bay to bay. (The increase in segment deflection due to the preload is *not* included in ε).

11. The imperfection parameters e and ε are allowed to be of the same orders of magnitude as ρ and R respectively.

We also make the following prejudgements concerning the actual behavior of the system, with the intention of simplifying the mathematical treatment:

12. We assume that batten deformations are so small as to not to affect the system behavior. Thus we will treat the battens as if they were rigid frames.

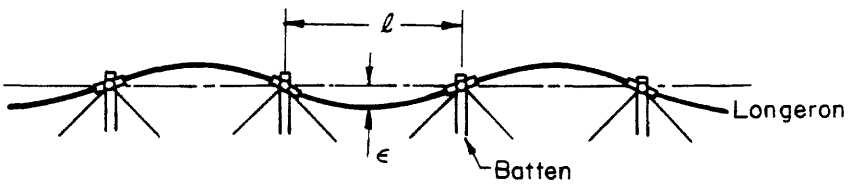

Figure 2-1. The local imperfection.

13. We will treat the longerons as if they were discontinuous, their segments being pinned to each other as well as to the battens. The reason is that the segment end-moments obviously vanish when no global deflection is present, and are expected to have a negligibly small effect in the case of slowly-varying global deflection. A quantitative justification of this assumption is the subject of Chapter 8, where the approximation involved is analyzed.

14. We assume that the column deflects in a plane which is one of the planes of symmetry of the column cross section, and in a direction away from the longeron contained in that plane (i.e. the positive z direction, see Figure 2-2). Crawford and Benton [33] have calculated that deflection in this direction has the most deleterious effect on the global bending rigidity. Hence it is plausible (though not proven in this work) that the post-buckling load is lower for this direction than it is for any other one (in a $\pm$ 60° sector) and that in the absence of global imperfection and cross sectional asymmetries a column will actually buckle in this direction. It is also assumed that the battens undergo no rotation around the column axis. This assumption, however, is relaxed in Chapter 7 where we investigate a pure, torsion-compression mode that under certain conditions becomes possible.

15. We will deal with global deflection amplitudes, a, of the order of R at most. It turns out that this is quite enough because all the interesting phenomena occur at amplitudes smaller than R.

16. Notwithstanding assumption (15) we will further restrict the range of a as necessary for the local longeron deflection to be of the order of ρ at most. Thus we will treat the individual segment as a simply-supported Euler column and also neglect terms of the order of the segment shortening compared to its length.

The system of coordinates in use is shown in Figure 2-2.

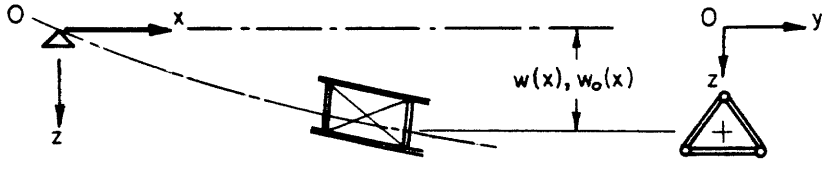

Figure 2-2. Global coordinate system, plane and direction of global deflection and global imperfection.

2.2 'Strain-Displacement' Relations

In this section kinematic relations are established between global displacement measures which we term 'displacements' and bay-members shortening/elongation we refer to as 'strains'. It is stressed that these quantities are only analogous to their continuum mechanics counterparts, an analogy that stems from treating the *bay* as the basic element instead of the infinitesimal cube of continuum mechanics.

Figure 2-3 depicts a bay in its deformed and reference states. The reference state is that occupied by the externally unloaded, internally preloaded globally-perfect column. We choose a reference point - the bay node - as the point bisecting the straight line segment passing through the adjoining batten centroids. Let x_i be the x-coordinate of the reference-state node. Let u_i^b, w_i^b and ϑ_i^b be respectively the x-displacement, z-displacement and angular rotation (positive as in the figure) of the batten centroid immediately to the right of x_i.

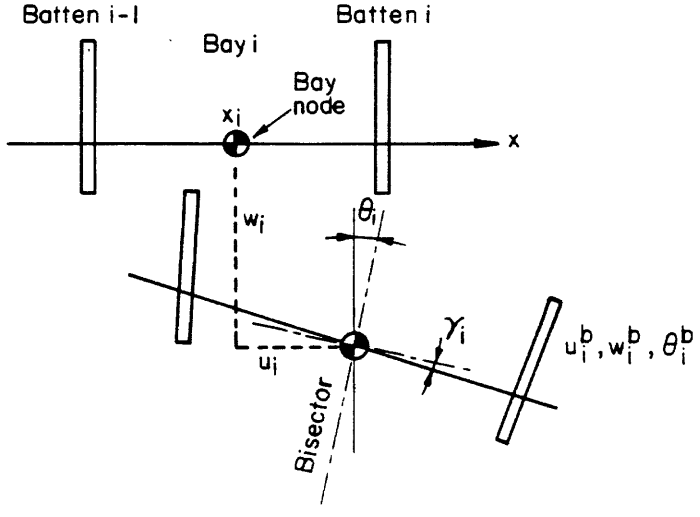

Figure 2-3. Bay displacement measures.

We define the four bay displacement measures, u_i, w_i, ϑ_i and γ_i as follows:

$$u_i \equiv \frac{1}{2}(u_i^b + u_{i-1}^b); \quad \text{x–displacement of node} \tag{2.1a}$$

$$w_i \equiv \frac{1}{2}(w_i^b + w_{i-1}^b); \quad \text{z–displacement of node} \tag{2.1b}$$

$$\vartheta_i \equiv \frac{1}{2}(\vartheta_i^b + \vartheta_{i-1}^b); \quad \text{rotation of bay bisector} \tag{2.1c}$$

$$\gamma_i \equiv w'_i - \vartheta_i; \quad \text{bay shear deformation} \tag{2.1d}$$

where w'_i and other primed quantities are 'derivatives' in a finite-difference sense:

$$u'_i \equiv \frac{1}{l}(u_i^b - u_{i-1}^b) \tag{2.2a}$$

$$w'_i \equiv \frac{1}{l}(w_i^b - w_{i-1}^b) \tag{2.2b}$$

$$\vartheta'_i \equiv \frac{1}{l}(\vartheta_i^b - \vartheta_{i-1}^b) \tag{2.2c}$$

In the following the bay subscript i will usually be omitted.

The 'strain-displacement' relations are derived in the following manner. Each bay member (longeron segment or diagonal) is designated as in Figure 2-4. Members 11, 22, and 33 are longeron segments, 11 being on the convex side (see Figure 2-2). Members having two distinct subscripts are diagonals: 12 and 21 are the left hand diagonals, 13 and 31 are the right hand diagonals and 23 and 32 are called the back diagonals. The coordinates of the bay vertices 1, 2, 3, 1', 2', 3' are calculated, using the bay geometry and eqns. (2.1)-(2.2), for the reference as well as for the deformed states. With each member mn a vector $\mathbf{l}_{mn}$ is associated, which represents its length and direction and which is formed from those coordinates. A member elongation is then found from the difference in length of the associated vector in the deformed and reference states. In doing this 2nd order terms in u', w', ϑ, Rϑ' and γ are neglected compared to 1. Defining the 'strain' of member mn as

δ_{mn} = (member elongation or shortening) / (member length in ref. state) (2.3a)

and introducing the sign convention

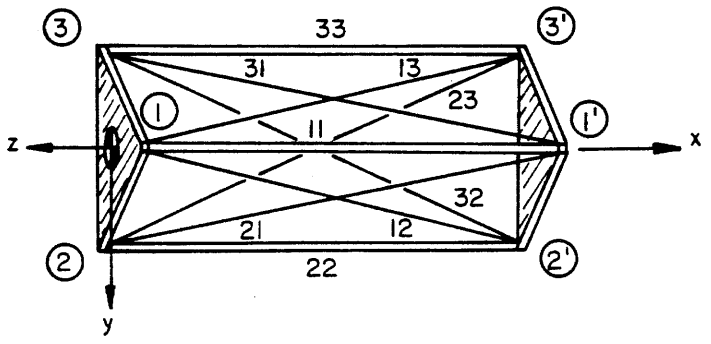

Figure 2-4. Bay members designation.

Longerons 'strains' $\delta_{11},\delta_{22},\delta_{33}$: positive in shortening
Diagonal 'strains' δ_{12},δ_{21},etc.: positive in elongation } (2.3b)

we obtain the desired 'strain-displacement' relations in the form

$$\delta_{11} = -u' - R\vartheta' \tag{2.4a}$$

$$\delta_{12} = \delta_{13} = \beta^2(u' + \frac{R}{4}\vartheta' + \frac{3R}{2l}\gamma) \tag{2.4b}$$

$$\delta_{21} = \delta_{31} = \beta^2(u' + \frac{R}{4}\vartheta' - \frac{3R}{2l}\gamma) \tag{2.4c}$$

$$\delta_{22} = \delta_{33} = -u' + \frac{R}{2}\vartheta' \tag{2.4d}$$

$$\delta_{23} = \delta_{32} = \beta^2(u' - \frac{R}{2}\vartheta') \tag{2.4e}$$

where β is a bay aspect ratio parameter

$$\beta \equiv \frac{1}{\sqrt{1 + 3(R/l)^2}} = \text{cosine} < \text{longeron,diagonal} > \tag{2.5}$$

Note that the 'strain-displacement' relations are linear. Any non-linear column behavior will have to stem from somewhere else.

2.3 Column Equilibrium Relations

The equilibrium relations to be derived here are the analogues of the twice-integrated Bernoulli-Euler beam-column equation EIw'' + Pw = 0. They are obtained by considering the static equilibrium of a complete column section - from an end-support to some station x - rather than that of an isolated bay. This allows the introduction of the destabilizing terms missing from the strain-displacement relations by means of regarding the equilibrium of the deformed state. The price paid is that we are no longer able to prescribe any desired boundary conditions at one of the column supports; the bending moments and shears (perpendicular to the x-axis) must vanish there.

With every bay member mn an internal force vector $\mathbf{p}_{mn}$ is associated,

$$\mathbf{p}_{mn} = (p_{mn} / l_{mn})\, \mathbf{l}_{mn} \tag{2.6}$$

where $\mathbf{l}_{mn}$ is the deformed-state member geometrical vector of Section 2.2 and l_{mn} is its length. The quantities p_{mn} - the magnitudes of $\mathbf{p}_{mn}$ - are the internal member compressive or tensile loads, and are acting in the present work as stress measures. We will refer to them as 'stresses' in analogy to their continuum mechanics counterparts. The following sign convention is maintained:

$$\left.\begin{array}{l} \text{Longeron 'Stresses' } p_{11}, p_{22}, p_{33} \text{ : positive in compression.} \\ \text{Diagonal 'Stresses' } p_{12}, p_{21}, \text{etc. : positive in tension.} \end{array}\right\} \tag{2.7}$$

The components of each $\mathbf{l}_{mn}$ relative to an orthogonal basis associated with the global coordinate system, and its length l_{mn}, are borrowed from Section 2.2. The components of each $\mathbf{p}_{mn}$ are then written according to (2.6). Next, the equilibrium of the column section of Figure 2-5, loaded by the external load P and cut through the bay i is considered:

$$P + \sum_{mn} \mathbf{p}_{mn} \cdot \mathbf{i} = 0, \qquad \sum_{mn} \mathbf{p}_{mn} \cdot \mathbf{k} = 0, \qquad -w^{b}_{i-1} P \mathbf{j} + \sum_{mn} (\mathbf{r}_{mn} - \mathbf{r}_{o}) \times \mathbf{p}_{mn} = 0 .$$

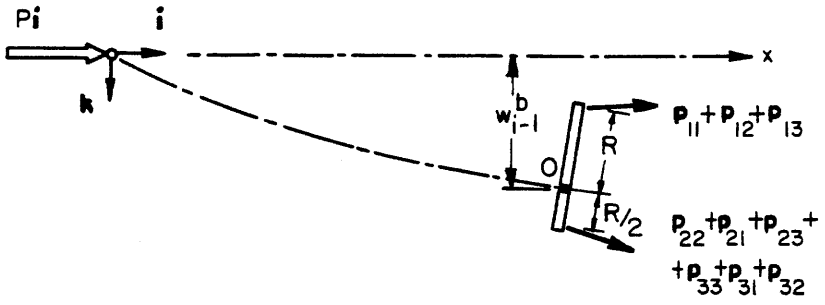

Figure 2-5. Global equilibrium.

i,**j**, and **k** are the base vectors associated with the coordinate axes x, y, and z respectively and $\mathbf{r}_{mn}$ and $\mathbf{r}_o$ are the position vectors of the points of application of $\mathbf{p}_{mn}$ and of the point 0 (Figure 2-5) respectively. In this way the following equilibrium relations are obtained:

$$p_{33} = p_{22} \tag{2.8a}$$

$$p_{13} = p_{12} \tag{2.8b}$$

$$p_{31} = p_{21} \tag{2.8c}$$

$$p_{32} = p_{23} \tag{2.8d}$$

$$p_{11} - 2\beta\left[1 + (1-\beta^2)\left(u' + \frac{R}{4}\vartheta'\right) - \frac{3R}{2l}(\vartheta + \beta^2\gamma)\right]p_{12} = \frac{1}{3}\left(1 + \frac{2w - l w'}{R}\right)P \tag{2.8e}$$

$$\left.\begin{aligned} p_{22} - \beta\left[1 + (1-\beta^2)\left(u' + \frac{R}{4}\vartheta'\right) + \frac{3R}{2l}(\vartheta + \beta^2\gamma)\right]p_{21} \\ + \beta\left[1 + (1-\beta^2)\left(u' - \frac{R}{2}\vartheta'\right)\right]p_{23} = \frac{1}{3}\left(1 - \frac{2w - l w'}{2R}\right)P \end{aligned}\right\} \tag{2.8f}$$

$$\beta\left[1 - \beta^2\left(u' + \frac{R}{4}\vartheta' + \frac{3R}{2l}\gamma\right)\right]p_{12} - \beta\left[1 - \beta^2\left(u' + \frac{R}{4}\vartheta' - \frac{3R}{2l}\gamma\right)\right]p_{21} = \frac{l w'}{3R}P \tag{2.8g}$$

In deriving these w^b_{i-1} was replaced by $w_i - (l/2)w'_i$ according to (2.1)-(2.2).

2.4 The 'Constitutive Relations'

By the term 'constitutive relations' we mean relations between the 'strains' δ_{mn} of equations (2.4) and the 'stresses' p_{mn} of equations (2.8). These relations are again only analogues of their continuum mechanics counterparts, and confusion between the two must not arise.

Corresponding to the two types of bay members - longerons and diagonals - we have two types of constitutive relations, both highly non-linear. For a longeron of length, l, bending rigidity EI, longitudinal rigidity EA and imperfection parameter ε, and under assumptions (4), (10), and (16) of Section 2.1 and definitions (2.3) and (2.7), the 'strain' δ_{mn}, *referred to the unstressed state*, is readily obtained as

$$\delta_{mm} = \frac{\pi^2(\varepsilon/l)^2}{4}\left[\frac{1}{(1-p_{mm}/p_e)^2} - 1\right] + \frac{p_{mm}}{EA}$$

where, we recall, $p_e \equiv \pi^2 EI/l^2$. The first term is the shortening due to bending whereas the second term is due to axial compression. Our reference state is, however, not the unstressed one but the one in which the longeron is preloaded by an amount p_o. The longeron constitutive relation then becomes

$$\delta_{mm} = \frac{\pi^2(\varepsilon/l)^2}{4}\left[\frac{1}{(1-p_{mm}/p_e)^2} - \frac{1}{(1-p_o/p_e)^2}\right] + \frac{p_{mm}-p_o}{EA}. \qquad (2.9)$$

It is important to note that this is the only place where the local deflections (implicitely) and the local imperfection parameter ε enter the theory. The assumption of pinned segments allows the local behavior to be completely absorbed in the 'constitutive relations', and turns ε into just another structural parameter. Mathematical treatment of the problem is in this way facilitated inasmuch as approaches applicable to single-mode problems may be used. Global displacements alone will suffice to characterize the column motion com-

pletely and the modal interaction behavior will emerge without being addressed explicitely.

Another interesting quantity is the segment 'tangent modulus', $d(p_{mm}/A)/d(\delta_{mm})$. We obtain from (2.9), in agreement with Thompson and Hunt [20]

$$\left(\frac{E}{E_t}\right)_{mm} = 1 + \frac{(\varepsilon/\rho)^2/2}{(1 - p_{mm}/p_e)^3}. \tag{2.10}$$

The diagonal constitutive law is complicated by the fact that it cannot carry compression. Also, the diagonal in the reference state is preloaded by an amount determined from internal equilibrium to be $p_o/2\beta$. The following expression represents all these features:

$$p_{mn} = \left[\frac{p_o}{2\beta} + (EA)_d\,\delta_{mn}\right] \cdot H\left(\frac{p_o}{2\beta(EA)_d} + \delta_{mn}\right), \quad m \neq n, \tag{2.11}$$

where $(EA)_d$ is the diagonal tensile stiffness and $H(\cdot)$ is Heaviside's step function. The two constitutive laws (2.9) and (2.11) are shown graphically in Figure 2-6.

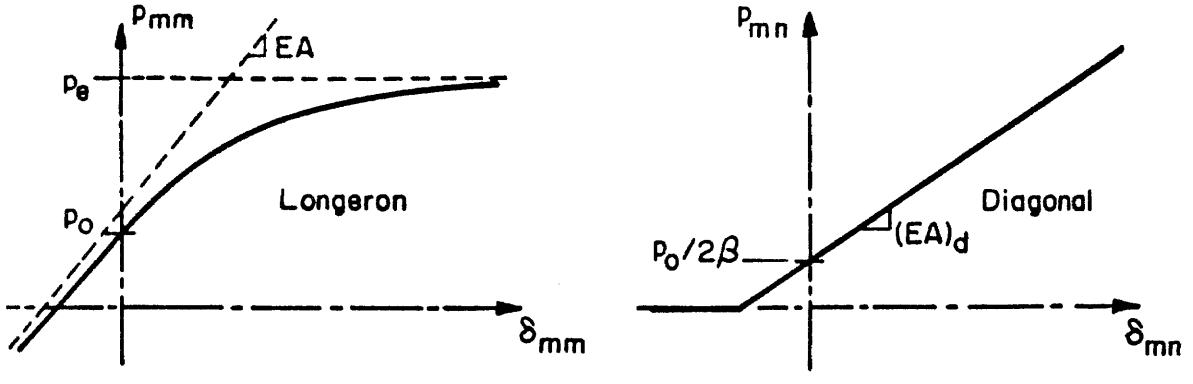

Figure 2-6. The constitutive relations.

2.5 Normalization, Order Estimation, and Simplification

In this section we employ the assumptions of Sec. 2.1 in order to estimate the orders of magnitude of the various terms in the strain-displacement, equilibrium and constitutive relations. The results indicate what terms can be safely neglected, and how best can the quantities involved be normalized. We then proceed to write the simplified relations involving only normalized non-dimensional quantities.

Let h be a typically-small positive constant, satisfying to some desired extent the relation $h << 1$. h plays in this work the role of *a standard of smallness* by comparison to which we decide whether, say, a structural parameter is small or not. The choice of h depends on the level of accuracy we require from our results. In general, terms of order h^2 will be neglected with respect to terms of order 1 and in this sense our theory will be a uniform first-order-in-h theory. The order symbols $o(\cdot)$ and $O(\cdot)$ will be used in the following (perhaps uncommon) meaning. For some quantity q we will write

$$q = o(h^n) \quad \text{if} \quad 0 \leq |q| \leq h^{n-\frac{1}{2}}, \tag{2.12a}$$

$$q = O(h^n) \quad \text{if} \quad h^{n+\frac{1}{2}} \leq |q| \leq h^{n-\frac{1}{2}}. \tag{2.12b}$$

We are now equipped to give precise mathematical meanings to the assumptions of Section 2.1

$$\text{Assumption(2):} \quad R/L = o(h), \tag{2.13a}$$

$$\text{Assumption(3):} \quad l/L = o(h), \quad l/R = O(1), \tag{2.13b,c}$$

$$\text{Assumption(4):} \quad \rho/l = o(h), \tag{2.13d}$$

$$\text{Assumption(6):} \quad p_o/p_e = o(h), \tag{2.13e}$$

$$\text{Assumption(7)}: \quad \frac{(EA)_d}{EA} = O(h) . \tag{2.13f}$$

Note that (2.5) and (2.13c) imply also

$$\beta = O(1) , \quad 1 - \beta = O(1) . \tag{2.13g}$$

The assumptions regarding the orders of magnitude of the deflections and imperfections translate to:

$$\text{Assumption(11)}: \quad e/R = o(1) , \quad \varepsilon/\rho = o(1) , \tag{2.13h,i}$$

$$\text{Assumption(15)}: \quad w/R = o(1) , \tag{2.13j}$$

$$\text{Assumption(16)}: \quad \delta_{mm} = o(h^2) . \tag{2.13k}$$

The last of these can be verified by noting that the bending term in a segment shortening arises from integration of a square of a 1st order quantity.

2.5.1 Normalization of the Constitutive Relations: Define the following non-dimensional quantities, the orders of magnitude of which are in accordance with eqns. (2.13). (We will use, temporarily, 'hats' over letters to denote normalized counterparts of non-normalized quantities. Those hats will later be dropped.)

$$\hat{p}_{mm} \equiv p_{mm}/p_e = p_{mm} l^2/(\pi^2 EI) = o(1) , \tag{2.14a}$$

$$\hat{\delta}_{mm} \equiv \delta_{mm}(l^2/\pi^2\rho^2) = o(1) , \tag{2.14b}$$

$$\hat{\varepsilon} \equiv \varepsilon/(\sqrt{2}\rho) = o(1) ,^1 \tag{2.14c}$$

$$\hat{p}_o \equiv p_o/p_e = o(h) . \tag{2.14d}$$

The longeron-segment constitutive relations (2.9) and (2.10) can now be written as

1. The reason behind this normalization is the simplicity it induces in (2.15b). Also, for thin-walled tubular cross-sections, $\sqrt{2}\rho$ equals the mean wall radius.

$$\hat{\delta}_{mm} = \frac{\hat{\varepsilon}^2}{2}\left[\frac{1}{(1-\hat{p}_{mm})^2} - \frac{1}{(1-\hat{p}_o)^2}\right] + (\hat{p}_{mm} - \hat{p}_o)\,, \tag{2.15a}$$

$$\left(\frac{E}{E_t}\right)_{mm} = 1 + \frac{\hat{\varepsilon}^2}{(1-\hat{p}_{mm})^3}\,. \tag{2.15b}$$

It is important to note that the restriction of small local deflections, Assumption (16), can now be expressed as a constraint on the relation between ε and p_{mm} in any longeron segment; eqns. (2.15a), (2.14b), and (2.13k) give

$$\frac{\hat{\varepsilon}^2/2}{(1-\hat{p}_{mm})^2} = o(1) \tag{2.16}$$

It will be seen later (Section 3.2.1) that equilibrium translates this further into a restriction on the global deflection amplitude.

For normalizing the diagonal constitutive relation we choose

$$\hat{p}_{mn} \equiv \beta\, p_{mn}/p_e, \qquad m \neq n\,; \tag{2.17a}$$

$$\hat{\delta}_{mn} \equiv \frac{1}{\beta^2}\delta_{mn}(l^2/\pi^2\rho^2) = o(1), \qquad m \neq n\,. \tag{2.17b}$$

(These choices are suggested by the fact that only combinations βp_{mn} and δ_{mn}/β^2 appear in the equilibrium and strain-displacement relations (2.8) and (2.4).) Also define *normalized diagonal rigidity*

$$\kappa \equiv \beta^3\,\frac{(EA)_d}{EA} = o(h) \tag{2.18}$$

to get the normalized form of the diagonal constitutive relation (2.11)

$$\hat{p}_{mn} = \left(\frac{1}{2}\hat{p}_o + \kappa\hat{\delta}_{mn}\right)\cdot H\left(\frac{1}{2}\hat{p}_o + \kappa\hat{\delta}_{mn}\right), \quad m \neq n\,. \tag{2.19}$$

2.5.2 Displacements Order Estimation: From (2.13k) and (2.4a,d) we conclude immediately

$$u' = o(h^2), \qquad R\vartheta' = o(h^2)\,. \tag{2.20a,b}$$

Provided w_i is a slowly-varying sequence - which excludes high wave-number

modes - we are justified in claiming that $w' = o(w/L)$, $\vartheta' = o(\vartheta/L)$ and $u' = o(u/L)$. Hence, by (2.13a,j) and (2.20a,b)

$$\frac{u}{L} = o(h)\,, \qquad \frac{w}{L} = o(h)\,, \qquad w' = o(h)\,, \qquad \vartheta = o(h)\,. \tag{2.20c,d,e,f}$$

There remains to find out the order of γ. Physically, γ is determined by transverse equilibrium, represented by eqn. (2.8g). Let us therefore begin by writing down a simplified form of (2.8g), one in which u' and $R\vartheta'$ are already neglected according to (2.20a,b) and p_{21} vanishes (diagonal 21 slackened, worst case for γ)

$$(1 - \beta^2 \frac{3R}{2l}\gamma)\,\frac{p_{12}}{P} = \frac{l\,w'}{3R\beta}\,.$$

By (2.13c,g) and (2.20e) the right hand side of this is clearly $o(h)$. Hence we find that the diagonal loads are generally small:

$$p_{mn}/P = o(h)\,. \tag{2.20g}$$

To find what this has in store for γ form $\delta_{12} - \delta_{21}$ using eqns. (2.4) and then replace 'strains' by 'stresses' using (2.11)

$$\beta^2 \frac{3R}{2l}\gamma = \frac{p_{12}}{(EA)_d} = (\frac{p_{12}}{P})(\frac{P}{3p_e})\,\frac{3\pi^2 EA\rho^2/l^2}{(EA)_d}\,.$$

$(P/3p_e)$ is certainly of $o(1)$. Then, by (2.20g), (2.13d), and (2.13f) the extreme right hand side of the above is of $o(h^2)$. Hence,

$$\gamma = o(h^2)\,. \tag{2.20h}$$

It is seen that the shear deformation slope γ is in this theory one order of magnitude smaller than the bending-related slope ϑ. This is due mainly to assumption (7): had $(EA)_d$ been allowed to be comparable to EA, γ would have been of $o(h^3)$ and completely negligible. The opposite case, $(EA)_d/(EA) = o(h^2)$, would have caused excessive shear deformation - a situation undesirable from design

standpoint and hence of questionable practicality.

2.5.3 Simplification and Normalization of S-D and Equilibrium: The results just obtained, eqns. (2.20), will now be used to normalize the displacements and their 'derivatives' in such a way as to make them all of $o(1)$. First normalize x so that the column normalized length is π

$$\hat{x} \equiv \frac{\pi}{L}x\,, \qquad (\,)^{\bullet} \equiv \frac{L}{\pi}(\,)' = o(1)\,, \tag{2.21a,b}$$

where the 'dot' operator means differentiation - in the sense of eqns. (2.2) - with respect to $\hat{x}$. By it being of $o(1)$ we mean that the order of the 'derivative' is the same as that of the original 'function'. This is true inasmuch as that function is spanwise slowly-varying, thus treatment of high wave-number modes is excluded. Displacements normalization is done as follows:

$$\hat{u} \equiv (L/\pi R^2)u = o(1)\,, \tag{2.21c}$$

$$\hat{w} \equiv (w/R) = o(1)\,, \tag{2.21d}$$

$$\hat{\vartheta} \equiv (L/\pi R)\vartheta = o(1)\,, \tag{2.21e}$$

$$\hat{\gamma} \equiv (3L^2/2\pi^2 R\ell)\gamma = o(1)\,. \tag{2.21f}$$

Define also the quantity P_E as the square of the ratio of the local and global slenderness ratios. (The reason for this notation will soon become clear):

$$P_E \equiv \frac{1}{2}\frac{(\ell/\rho)^2}{(L/R)^2} = O(1)\,. \tag{2.22}$$

Using eqns. (2.14b), (2.17b), (2.21), and (2.22) the 'strain-displacement' relations (2.4) take on the following normalized forms

$$\hat{\delta}_{11} = \quad 2P_E\,(-\hat{u}^{\bullet} - \hat{\vartheta}^{\bullet})\,, \tag{2.23a}$$

$$\hat{\delta}_{22} = \hat{\delta}_{33} = 2P_E\,(-\hat{u}^{\bullet} + \tfrac{1}{2}\hat{\vartheta}^{\bullet})\,, \tag{2.23b}$$

$$\hat{\delta}_{12} = \hat{\delta}_{13} = 2P_E\,(\ \hat{u}^{\bullet} + \tfrac{1}{4}\hat{\vartheta}^{\bullet} + \hat{\gamma})\,, \tag{2.23c}$$

$$\hat{\delta}_{21} = \hat{\delta}_{31} = 2P_E\,(\ \hat{u}^{\bullet} + \tfrac{1}{4}\hat{\vartheta}^{\bullet} - \hat{\gamma})\,, \tag{2.23d}$$

$$\hat{\delta}_{23} = \hat{\delta}_{32} = 2P_E\,(\ \hat{u}^{\bullet} - \tfrac{1}{2}\hat{\vartheta}^{\bullet})\,. \tag{2.23e}$$

Two more nondimensional quantities are defined: the normalized external load $\hat{P}$ and the normalized bay length λ

$$\hat{P} \equiv P/(3p_e) = o(1)\,, \tag{2.24}$$

$$\lambda \equiv (\pi/L)\,l = o(h)\,. \tag{2.25}$$

Note that the number of bays in the column, N, satisfies

$$N = \frac{L}{l} = \frac{\pi}{\lambda}\,. \tag{2.26}$$

The significance of the normalization (2.24) lies in the fact that, disregarding the diagonal forces, local buckling in the unbent column occurs for $\hat{P} = 1$ exactly. On the other hand, P_E of equation (2.22) is nothing but the global (Euler) buckling load of the ***perfect*** column (again diagonals ignored) normalized by the same $3p_e$.

Neglecting terms of $o(h^2)$ compared to terms of $O(1)$ the equilibrium relations (2.8) simplify considerably. The only remnants of the deformed state derivation are the wP and w'P terms on the right hand sides. (From this standpoint our column is equivalent to a Timoshenko beam column.) The normalization is done using eqns. (2.14a), (2.17a), (2.21b,d), (2.24), and (2.25). The resulting normalized equilibrium relations (omitting the symmetry relations) are

$$\hat{p}_{11} - 2\hat{p}_{12} = (1 + 2\hat{w} - \lambda\hat{w}^{\bullet})\,\hat{P}\,, \tag{2.27a}$$

$$\hat{p}_{22} - \hat{p}_{21} - \hat{p}_{23} = (1 - \hat{w} + \frac{\lambda}{2}\hat{w}^{\bullet})\,\hat{P}\,, \tag{2.27b}$$

$$\hat{p}_{12} - \hat{p}_{21} = \lambda\hat{w}^{\bullet}\,\hat{P}\,. \tag{2.27c}$$

There remains the compatibility relation (2.1d), the normalized form of which is (using eqns. (2.21))

$$\hat{w}^{\bullet} = \hat{\vartheta} + \frac{2}{3}\lambda\hat{\gamma}\,. \tag{2.28}$$

Since $\lambda = o(h)$ this shows clearly that in our theory the contribution of shear deformation to the deflection slope is small compared to that of bending.

2.6 Introduction of Global Imperfections

The effect of global imperfections, disregarded in the preceding derivations, will now be introduced. Formally, we assign to every displacement component a corresponding imperfection component. Thus we have an imperfection quadruplet

$$u_o(x_i)\,, \quad w_o(x_i)\,, \quad \vartheta_o(x_i)\,, \quad \gamma_o(x_i)\,, \tag{2.29a}$$

[2]

defined kinematically similar to the total displacements, eqns. (2.1). Normalization of these quantities is done in the same manner as in eqns. (2.21) to obtain

$$\hat{u}_o(\hat{x}_i)\,, \quad \hat{w}_o(\hat{x}_i)\,, \quad \hat{\vartheta}_o(\hat{x}_i)\,, \quad \hat{\gamma}_o(\hat{x}_i)\,. \tag{2.29b}$$

The global imperfection parameter e, the maximum of w_o, is normalized similar to w

$$\hat{e} \equiv e/R\,. \tag{2.30}$$

---

2. In specific applications u_o will be taken as zero and w_o, ϑ_o, and γ_o as a replica of their spanwise distribution in the fundamental initial buckling mode. For the time being we will maintain the more general situation. (u_o can be interpreted as an initial unevenness in the bay-length distribution.)

Recall that our reference state is the one occupied by the externally unloaded, internally preloaded globally perfect column. Therefore, the displacements quadruple u, w, ϑ, and γ already incorporates kinematically the imperfections u_o, w_o, ϑ_o, and γ_o. The latter are distinguished from the former by the sole trait that they do not produce 'strains'. Hence, the only gate through which the global imperfections enter the picture is the 'strain-displacement' relations. All that has to be done is to replace in them $\hat{u}$, $\hat{w}$, $\hat{\vartheta}$, and $\hat{\gamma}$ by the strain-producing constituents $\hat{u}-\hat{u}_o$, $\hat{w}-\hat{w}_o$, $\hat{\vartheta}-\hat{\vartheta}_o$, $\hat{\gamma}-\hat{\gamma}_o$.

2.7 The Column Equations

We are now in a position to summarize the column equations. For simplicity of notation let us from now on omit 'hats' over letters, agreeing that all quantities to be dealt with, except when otherwise explicitely stated, are the normalized ones. We also return to the ( )' notation for 'differentiation' with respect to $\hat{x}$. The equations to be summarized are (2.23), (2.27), (2.28), (2.15), and (2.19) and we introduce the following changes: (1) global imperfections according to the discussion in Section 2.6; (2) other than (2.27) linear combinations for the equilibrium relations; (3) matrix form for the S-D relations; (4) symmetry relations, e.g., $\delta_{12} = \delta_{13}$, are henceforth omitted.

STRAIN-DISPLACEMENT:

$$\begin{Bmatrix} \delta_{11} \\ \delta_{22} \\ \delta_{12} \\ \delta_{21} \\ \delta_{23} \end{Bmatrix} = 2P_E \begin{bmatrix} -1 & -1 & 0 \\ -1 & 1/2 & 0 \\ 1 & 1/4 & 1 \\ 1 & 1/4 & -1 \\ 1 & -1/2 & 0 \end{bmatrix} \begin{Bmatrix} u' - u'_o \\ \vartheta' - \vartheta'_o \\ \gamma - \gamma_o \end{Bmatrix} \tag{2.31}$$

EQUILIBRIUM:

$$p_{11} - (p_{12} + p_{21}) = (1 + 2w)P \tag{2.32a}$$

$$p_{22} - \frac{1}{2}(p_{12} + p_{21}) - p_{23} = (1 - w)P \tag{2.32b}$$

$$p_{12} - p_{21} = \lambda w' P \tag{2.32c}$$

BENDING-SHEAR-DEFLECTION COMPATIBILITY:

$$w' = \vartheta + \frac{2}{3}\lambda\gamma \tag{2.33}$$

CONSTITUTIVE RELATIONS:

$$\delta_{mm} = \frac{\varepsilon^2}{2}\left[\frac{1}{(1-p_{mm})^2} - \frac{1}{(1-p_o)^2}\right] + (p_{mm} - p_o)\,, \tag{2.34a}$$

$$p_{mn} = (\frac{1}{2}p_o + \kappa\delta_{mn}) \cdot H(\frac{1}{2}p_o + \kappa\delta_{mn})\,, \quad m \neq n\,. \tag{2.34b}$$

Notably, we have eleven unknowns and a non-linear system of eleven equations.

2.7.1 Diagonal Slackening Regions: The step-function non-linearity of (2.34b) is inconvenient to carry around, let alone do analysis with. To avoid this we introduce the concept of spanwise diagonal-slackening regions. It is easy to conceive of whole spanwise stretches along which the state of the diagonals is unchanging - either diagonal 12 or 21 or none are slack.[3] These stretches, designated 'Region I', 'Region II', and 'Region III', are defined in Figure 2-7. A batten that separates between adjacent regions will be called a 'region transition point'.

The partition of the span into regions allows writing a separate system of equations for each region, a system in which the diagonals constitutive relations are linear. The appeal of this stems from the expectation that region-

3. Other slackening combinations, except 12-23-31, turn out unstable or otherwise impractical, hence undeserving designation. The 12-23-31 unloading leads to a torsional mode which is analyzed in Chapter 7.

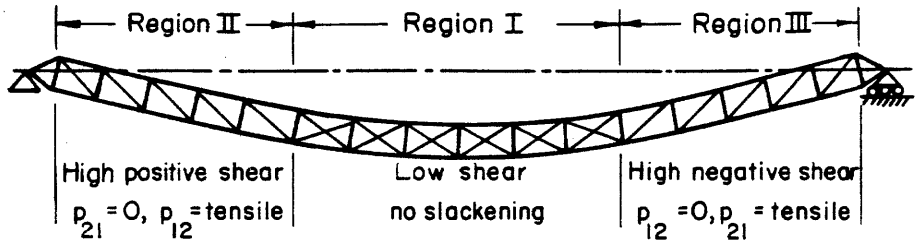

Figure 2-7. Diagonal slackening regions.

transitions are *few*. Their spanwise locations, however, become additional unknowns which have to be determined from the following *region conditions*, derivable from (2.34b):

$$\left.\begin{array}{lll} \text{Region I}: & p_{12} \geq 0; & \delta_{12} \geq -p_o/2\kappa \\ & p_{21} \geq 0; & \delta_{21} \geq -p_o/2\kappa \end{array}\right\} \qquad (2.35a,b)$$

$$\left.\begin{array}{lll} \text{Region II}: & p_{12} \geq 0; & \delta_{12} \geq -p_o/2\kappa \\ & p_{21} = 0; & \delta_{21} \leq -p_o/2\kappa \end{array}\right\} \qquad (2.35c,d)$$

$$\left.\begin{array}{lll} \text{Region III}: & p_{12} = 0; & \delta_{12} \leq -p_o/2\kappa \\ & p_{21} \geq 0; & \delta_{21} \geq -p_o/2\kappa \end{array}\right\} \qquad (2.35e,f)$$

2.7.2 The Column Regional Displacements Equations: With the help of the regions concept and of eqns. (2.35) we now proceed to eliminate all the 'stress' and 'strain' unknowns from the regional systems of equations. (We will still retain p_{11} and p_{12} as convenient notations for certain displacement combinations.) The algebraic process involving eqns. (2.31)-(2.35), results in four displacement equations for the unknowns u, w, ϑ, and γ. For notational brevity define

$$\bar{u} \equiv u - u_o\,, \quad \bar{w} \equiv w - w_o\,, \quad \bar{\vartheta} \equiv \vartheta - \vartheta_o\,, \quad \bar{\gamma} \equiv \gamma - \gamma_o\,. \qquad (2.36a,b,c,d)$$

The column regional displacement equations are:

REGION I DISPLACEMENT EQUATIONS

$$P_E\left(1+\frac{\kappa}{2}\right)\bar{\vartheta}' + wP + \frac{\varepsilon^2}{6}\left[\frac{1}{(1-p_{11})^2} - \frac{1}{(1-p_{22})^2}\right] = 0\,, \tag{2.37a}$$

$$2P_E(1+2\kappa)\bar{u}' + P + \frac{\varepsilon^2}{6}\left[\frac{1}{(1-p_{11})^2} + \frac{2}{(1-p_{22})^2} - \frac{3}{(1-p_o)^2}\right] = 0, \tag{2.37b}$$

$$4\kappa P_E\bar{\gamma} - \lambda P w' = 0\,, \tag{2.37c}$$

$$w' - \vartheta - \frac{2}{3}\lambda\gamma = 0\,; \tag{2.37d}$$

$$\left.\begin{aligned} \text{where: } p_{11} &= (1+2w)P + 4\kappa P_E\left(\bar{u}' + \frac{1}{4}\bar{\vartheta}'\right) + p_o\,, \\ p_{22} &= (1-w)P + 4\kappa P_E\left(\bar{u}' - \frac{1}{8}\bar{\vartheta}'\right) + p_o\,. \end{aligned}\right\} \tag{2.37e,f}$$

$$\left.\begin{aligned} \text{Region I conditions: } \bar{u}' + \frac{1}{4}\bar{\vartheta}' - \bar{\gamma} &\geq -\frac{p_o}{4\kappa P_E} \quad \text{(not II)}\,, \\ \bar{u}' + \frac{1}{4}\bar{\vartheta}' + \bar{\gamma} &\geq -\frac{p_o}{4\kappa P_E} \quad \text{(not III)}\,. \end{aligned}\right\} \tag{2.37g,h}$$

REGION II/III DISPLACEMENT EQUATIONS (upper sign for region II)

$$P_E\left[\left(1+\frac{\kappa}{2}\right)\bar{\vartheta}' \pm \frac{2}{3}\kappa\bar{\gamma}\right] + \left(w \mp \frac{\lambda}{6}w'\right)P + \frac{\varepsilon^2}{6}\left[\frac{1}{(1-p_{11})^2} - \frac{1}{(1-p_{22})^2}\right] = 0\,, \tag{2.38a}$$

$$2P_E\left[(1+2\kappa)\bar{u}' \pm \frac{4}{3}\kappa\bar{\gamma}\right] + \left(1 \mp \frac{2\lambda}{3}w'\right)P + \frac{\varepsilon^2}{6}\left[\frac{1}{(1-p_{11})^2} + \frac{2}{(1-p_{22})^2} - \frac{3}{(1-p_o)^2}\right] = 0\,, \tag{2.38b}$$

$$2\kappa P_E\left(\bar{u}' + \frac{1}{4}\bar{\vartheta}' \pm \bar{\gamma}\right) \mp \lambda P w' + \frac{1}{2}p_o = 0\,, \tag{2.38c}$$

$$w' - \vartheta - \frac{2}{3}\lambda\gamma = 0\,; \tag{2.38d}$$

$$\left.\begin{aligned} \text{where: } p_{11} &= (1+2w)P + 2\kappa P_E\left[\bar{u}' + \frac{1}{4}\bar{\vartheta}' \pm \bar{\gamma}\right] + \frac{1}{2}p_o\,, \\ p_{22} &= (1-w)P + 3\kappa P_E\left[\bar{u}' - \frac{1}{4}\bar{\vartheta}' \pm \frac{1}{3}\bar{\gamma}\right] + \frac{3}{4}p_o\,. \end{aligned}\right\} \tag{2.38e,f}$$

$$\text{Region II/III Conditions:} \quad \pm w' > 0\,, \quad \bar{u}' + \frac{1}{4}\bar{\vartheta}' \mp \bar{\gamma} \leq -\frac{p_o}{4\kappa P_E} \tag{2.38g,h}$$

Upon inspection of these equations the following are noted before any analysis:

1. The systems are first-order 'differential' in w and ϑ and algebraic in u' and γ. Thus only two boundary conditions need and can be specified.

2. The first region I equation is essentially a bending equation, the second is a compression one whereas the third governs mainly the shear deformation. The fourth equation is the bending-shear-deflection compatibility condition. (This is seen clearly if one overlooks $o(h)$ coupling terms). The situation is less clear in regions II/III because (2.38b) and (2.38c) are strongly coupled through $\bar{u}'$.

3. The bending and compression equations are non-linear, the non-linearity arising exclusively from the longeron constitutive behavior. The non-linear terms are not necessarily small (for any p_{11} and p_{22}) because $\varepsilon = o(1)$.

4. For certain load-displacement combinations, those that give $p_{11} = 1$ or $p_{22} = 1$, the bending and compression equations become singular. These situations clearly correspond to longeron-segment buckling - 'local buckling'.

5. Region I bending and compression equations are coupled through the $o(h)$ quantity κ in eqns. (2.37e,f). This $o(h)$ coupling is not always weak since $(1-p_{11})$ or $(1-p_{22})$ may themselves become small. Besides the strong $\bar{u}'$ coupling mentioned in (2), regions II/III equations are coupled in the same way as those of region I and also by weak $\bar{\gamma}$ terms. The more extensive coupling in these regions arises from the asymmetry in internal loading due to asymmetric diagonal slackening.

6. As expected, Regions II and III are mutually antisymmetric with respect to γ, ϑ, and w'.

7. Letting $\bar{\gamma} = 0$ (infinite shear rigidity) and $\varepsilon = 0$, $p_{11} \neq 1$, $p_{22} \neq 1$ (locally-perfect column) eqn. (2.37a) reduces to the familiar, twice-integrated Euler column equation. The factor $(1 + \kappa/2)$ represents the increase in the effective global bending rigidity due to the presence of diagonals in the cross-section; similarly $(1 + 2\kappa)$ in (2.37b) represents the effect of the same on the longitudinal rigidity.

8. Using eqns. (2.38c), (2.1b), and (2.2b) it is found that (2.38e) may be written (for region II) as

$$p_{11} = [\, 1 + 2(w + \frac{\lambda}{2} w') \,] P = (1 + 2 w_i^b) P \qquad (2.39)$$

(for region III i has to be replaced by i-1). This means that in a bay where a diagonal is slack, the only displacement component on which p_{11} depends is the deflection of an adjoining batten.

2.7.3 Boundary Conditions: As said in (1) above, only two boundary conditions are to be specified. Because of the particular way the equilibrium equations were derived no shear and moments are allowed at the end x=0. This leaves us with only the following practically-significant conditions:

$$w^b(0) = 0\,, \qquad w^b(\pi) = 0\,; \qquad (2.40a,b)$$

$$w^b(\pi) = 0\,, \qquad \vartheta^b(\pi) = 0\,; \qquad (2.40c,d)$$

The first line of these represents the simply-supported case whereas the second describes a clamped-free column. According to assumption (1) of Section 2.1 only the simply-supported case will be treated in this work.

2.7.4 Partially-Decoupled Region I Equations: The linearity and simplicity of eqns. (2.37c,d), together with the fact that they are algebraic in w', ϑ, and γ, allow for expressing γ and ϑ in terms of w' and thus eliminating them from the

system. Noting that w_o', ϑ_o and γ_o and therefore also $\bar{w}'$, $\bar{\vartheta}$ and $\bar{\gamma}$ satisfy kinematic relations such as (2.37d) we obtain first

$$\bar{\vartheta} = (1-\nu\frac{P}{P_E})w'-w_o' = \bar{w}'-\nu\frac{P}{P_E}w' = (1-\nu\frac{P}{P_E})\bar{w}'-\nu\frac{P}{P_E}w_o' , \tag{2.41a}$$

$$\bar{\gamma} = \frac{\lambda}{4\kappa}(\frac{P}{P_E})w' = \frac{\lambda}{4\kappa}(\frac{P}{P_E})(\bar{w}' + w_o') , \tag{2.41b}$$

where ν is another $o(h)$ column parameter:

$$\nu \equiv \frac{\lambda^2}{6\kappa} = o(h) . \tag{2.41c}$$

We now have to 'differentiate' (2.41a) in order to substitute for $\bar{\vartheta}'$ in eqns. (2.37). The meaning for the left hand side of this differentiation is fixed by eqn. (2.2c) and by writing formally

$$\bar{\vartheta}' = (1-\nu\frac{P}{P_E})w''-w_o'' = \bar{w}''-\nu\frac{P}{P_E}w'' = (1-\nu\frac{P}{P_E})\bar{w}''-\nu\frac{P}{P_E}w_o'' \tag{2.41d}$$

a specific meaning in terms of the w's (which is not simple) is lended to w''. We will not concern ourselves with determining the proper w'' definition[4] since it is of no consequence in this work, but proceed to eliminate $\bar{\vartheta}'$ from eqns. (2.37) using (2.41d). In this way the ***partially-decoupled region I displacement equations*** take the form

$$P_E(1+\frac{\kappa}{2})(1-\nu\frac{P}{P_E})w'' + Pw + \frac{\varepsilon^2}{6}\left[\frac{1}{(1-p_{11})^2} - \frac{1}{(1-p_{22})^2}\right] = P_E(1+\frac{\kappa}{2})w_o'' , \tag{2.42a}$$

$$2P_E(1+2\kappa)\bar{u}' + P + \frac{\varepsilon^2}{6}\left[\frac{1}{(1-p_{11})^2} + \frac{2}{(1-p_{22})^2} - \frac{3}{(1-p_o)^2}\right] = 0 , \tag{2.42b}$$

$$\bar{\vartheta} = (1-\nu\frac{P}{P_E})w' - w_o' , \tag{2.42c}$$

4. If, for example, we define $w''_i = (w'_{i+1} - w'_{i-1})/2\lambda$ the left hand side will not be $\bar{\vartheta}'$ of (2.2c) but $(\bar{\vartheta}_{+1} - \bar{\vartheta}_{-1})/4$ which, in turn, is equal to $(1/4)\bar{\vartheta}' + (3/4)[(\bar{\vartheta}^b_{+1} - \bar{\vartheta}^b_{-2})/3\lambda]$.

$$\bar{\gamma} = \frac{\lambda}{4\kappa}\left(\frac{P}{P_E}\right)w' = \frac{3}{2}\left(\frac{\nu}{\lambda}\right)\left(\frac{P}{P_E}\right)w' \; ; \tag{2.42d}$$

$$\left.\begin{aligned} \text{where: } 1-p_{11} &= [\,(1-P)-2wP\,]-4\kappa P_E\left(\bar{u}'+\frac{1}{4}\bar{w}''\right)+\frac{\lambda^2}{6}Pw''-p_o\,, \\ 1-p_{22} &= [\,(1-P)+\;wP\,]-4\kappa P_E\left(\bar{u}'-\frac{1}{8}\bar{w}''\right)-\frac{\lambda^2}{12}Pw''-p_o\,. \end{aligned}\right\}^5 \tag{2.42e,f}$$

The first two equations can be solved for $\bar{u}'$ and w. Then $\bar{\vartheta}$ and $\bar{\gamma}$ can be determined from the second two.

2.8 The De-Discretization Error

The column equations derived in this chapter establish relations between bay-quantities - the displacements and their 'derivatives' - defined by eqns. (2.1) and (2.2) at only discrete x-values. They are sequences rather than functions and the equations are therefore, by nature, finite difference equations. No error is committed if they are integrated as such, and good use can be made of this fact in numerical treatments. For closed-form treatment, however, it is quite advantageous to regard these equations as if they were differential and to integrate them accordingly. It is then that an error is committed; the one known as truncation or discretization error but in the opposite sense.[6] A general estimate of this error will not be attempted in this work, although consistency of the finite difference and differential approaches can readily be proven. It will be seen later (Section 4.7) that at least for the global buckling case the error is $o(\lambda^2) = o(h^2)$. Hence treating the column equations as if they were differential is consistent with the other approximations of the present theory.

Let us therefore redefine the 'prime' operators acting on u, w, ϑ, and γ as fol-

5. We are not at liberty to neglect the $o(h^2)$ λ^2-terms since the square-brackets may themselves get small.

6. The situation here is exactly the opposite of that commonly encountered in finite difference analyses. There we usually have a differential equation that, for the sake of ease of numerical treatment, is traded for a less exact finite-difference one. Here it is the finite-difference equation which is the more exact.

lows:

$$( )' \equiv d( )/dx\,, \qquad ( )'' \equiv d^2( )/dx^2\,. \tag{2.43a,b}$$

Henceforth, unless explicitly stated, we will use them in this meaning.

The continuum counterparts of the boundary conditions (2.40a,b) are clearly

$$w(0) = 0\,, \qquad w(\pi) = 0\,. \tag{2.44a,b}$$

3. THE IDEAL COLUMN

Consider a three-legged truss column having all the features introduced so far except for those related to the diagonals. Instead, let the diagonals be replaced by an unspecified shear-resisting web distinguished by the following properties: (a) infinite shear rigidity, (b) shear web loading does not induce longeron loading. (In the following this property will be referred to as 'non-coupling web'.) We will call this column the 'associated ideal column'. It turns out that the ideal column bending and compression equations miss all the $o(h)$ terms and only them, and thus it is also a 'zeroth order-in-h column'.

Though a rough and maybe inadequate approximation, there are good reasons to analyze the ideal column. First, as mentioned in Chapter 1, this case (and its two-legged counterpart) has been treated by several authors and there is an interest in comparison of results. Second, designers should be made aware of the magnitude of the error involved in treating a real column as if it were an ideal one and of the unconservative nature of this error. Also, the simplicity of the case affords an approximate closed-form solution which has, at least qualitatively, most of the features of the more complex ones. Besides being quite instructive the ideal column facilitates the establishment of certain concepts that carry over to the general problem.

After reducing the column equations to the ideal case we analyze the singularity that corresponds to local buckling. Then we investigate the bifurcations and behavior of the globally-perfect and locally-perfect special cases. An exact closed-form solution is found for the globally-perfect column. Using asymptotics, this solution and the load-deflection relation associated with it are investigated. The results are then applied towards constructing an approximate, yet more useful, load-deflection relation which imitates the exact asymptotic

behavior. The general, globally-imperfect case is treated in an approximate way using a Ritz-Galerkin procedure, the results of which are then slightly modified so a to make them reducible to the globally-perfect case. The load-deflection relation is then investigated to reveal the behavior in the a-P plane and to compare it with results in the literature.

3.1 The Ideal Column Equations

Removal of the diagonals and introduction of a non-coupling web of infinite shear rigidity translate mathemaically into the following:

$$p_o = 0, \qquad \kappa = 0, \qquad \gamma = 0\,. \tag{3.1a,b,c}$$

γ being determined, eqns (2.37c) and (2.38c) should be crossed out [the latter only after substituting from it for $\lambda P w'$ in (2.38a) and (2.38b)]. Eqns. (2.37d) and (2.38d) will then yield $\bar{\vartheta}' = \bar{w}''$ and both systems will reduce to

$$P_E \bar{w}'' + P w + \frac{\varepsilon^2}{6}\left[\frac{1}{(1-P-2wP)^2} - \frac{1}{(1-P+wP)^2}\right] = 0\,, \tag{3.2a}$$

$$2P_E \bar{u}' + P + \frac{\varepsilon^2}{6}\left[\frac{1}{(1-P-2wP)^2} + \frac{2}{(1-P+wP)^2} - 3\right] = 0\,. \tag{3.2b}$$

Comparing the systems (3.2) and (2.42) we see that the reduction could have been achieved simply by letting in the latter $p_o = \kappa = \nu = 0$. Moreover, from (2.42d) it is seen that taking $\nu=0$ (keeping λ finite) amounts to taking $\bar{\gamma}=0$. We therefore conclude that of the two effects inhibited by the column idealization the coupling-web effect is represented by the parameters κ and p_o whereas the finite shear rigidity effect is represented exclusively by ν. Accordingly, we will refer to ν as the 'shear compliance parameter'.

Taking simultaneously $\nu = \kappa = 0$ while keeping λ finite may seem a contradictory operation, because $\nu \equiv \lambda^2/6\kappa$. This is, however, precisely the mathematical

parallel of the ***verbal*** operations that led to the ideal column: on one hand we removed the diagonals, which were the sole source of shear resistance, while on the other hand we postulated the latter to be infinite. The contradiction is resolved if we consider ν as a general shear compliance parameter, regardless of the shear-web design and of the way ν should be calculated; for then the ν which is made to vanish is that of the unspecified ***replacement*** web, which necessarily does not have κ in its denominator.

Examining eqns. (3.2) we see that the first one, the bending equation, is completely decoupled from the second. We can solve it independently for w(x) and then find u'(x) by direct substitution. The w(x) solution is thus enough to characterize the column behavior completely and we will confine ourselves in this chapter to dealing with it only.

It will prove advantageous to introduce into (3.2a) the following substitution:

$$\varphi(x) \equiv \frac{2P}{1-P} w(x) \,. \tag{3.3a}$$

It is important to note that φ combines load and deflection. Although it has the same shape as w, its amplitude depends on P in an entirely different manner. If we denote by a the amplitude of w and by α the amplitude of φ then

$$\alpha = \frac{2P}{1-P} a \,. \tag{3.3b}$$

The mathematical formulation of the ideal column problem may now be written as follows:

$$\varphi = \varphi(x) \leq \alpha, \qquad 0 \leq x \leq \pi \,; \tag{3.4a}$$

$$P_E(\varphi'' - \varphi_o'') + P\varphi + \frac{\varepsilon^2 P}{3(1-P)^3}\left\{\frac{1}{(1-\varphi)^2} - \frac{1}{(1+\varphi/2)^2}\right\} = 0, \quad 0 < x < \pi \,; \tag{3.4b}$$

$$\varphi(0) = 0\ ; \tag{3.4c}$$

$$\varphi(\pi) = 0\ . \tag{3.4d}$$

Note that of all six structural and imperfection parameters of the general problem (P_E, φ_o, ε, λ, κ, and p_o) only the first three survive.

3.2 The Local Buckling Line and Related Phenomena

By setting the diagonal loads to zero, equilibrium relations (2.32a,b) are reduced to the ideal column case:

$$1-p_{11} = 1-P-2wP\ , \qquad 1-p_{22} = 1-P+wP, \tag{3.5a,b}$$

and expressed in terms of φ they become

$$1-p_{11} = (1-P)\,(1-\varphi), \qquad 1-p_{22} = (1-P)\,(1+\varphi/2)\ . \tag{3.6a,b}$$

Eqn. (3.4b) is evidently singular for φ=1 and φ=−2. By (3.6) these singularities are seen to correspond to the conditions p_{11}=1 and p_{22}=1 respectively, i.e. to the condition of buckling of the longeron segments at spanwise points where φ=1 or φ=−2. Intending to deal with only positive deflections (assumption 14 of Section 2.1) the singularity at φ=−2 is of no consequence. That at φ=1, however, will first come into play when the spanwise maximum of φ, namely α, becomes equal to 1. We will call the locus in the a-P plane along which α=1 the *local buckling line* (LBL). By (3.3b)

$$\text{LBL:}\quad \alpha = 1\ , \qquad P = \frac{1}{1+2a}\ . \tag{3.7a,b}$$

The LBL will play a major role in the present theory. Its most striking feature is its independence of any structural or imperfection parameter and of the shape of w(x). We shall see that the essence of this feature is carried over to the general column. Clearly, all *actual* (equilibrium) a-P combinations must fall below or on the LBL, thus, the LBL together with assumption (14) of Section 2.1

restrict the a-P region in which such combinations may occur to

$$0 \leq \alpha \leq 1 . \tag{3.8}$$

This region and the LBL itself are depicted in Figure 3-1.

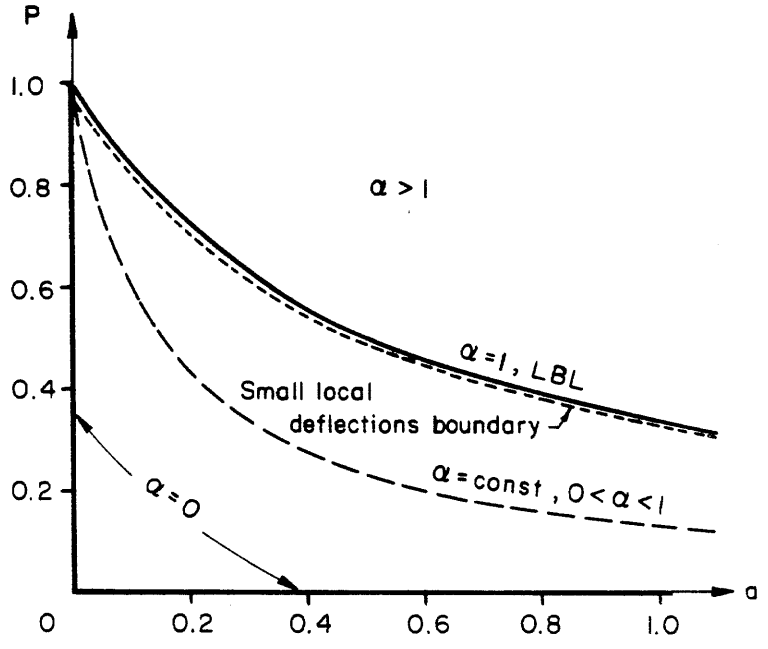

Figure 3-1. The local buckling line and α-range.

3.2.1 The Restriction on Local Deflections: We are now in a position to translate that restriction, imposed by assumption (16) of Section 2.1 and expressed mathematically by (2.16), into a restriction on the ***global*** deflection amplitude a, at least for the ideal case. When substituting (3.5) into (2.16) the maximum of the latter (for $w \geq 0$) is seen to occur for m=1 and for w=a. Using the 'o' symbol definition (2.12a) to replace the order expression by an inequality we obtain the global deflection restriction in the form

$$a \leq \frac{1-P}{2P} - \frac{\varepsilon h}{2\sqrt{2}P}, \qquad \alpha \leq 1 - \frac{\varepsilon h}{2\sqrt{2}(1-P)}. \tag{3.9a,b}$$

The first term in (3.9a) is clearly the value of a on the LBL. The second term, then, expresses the distance from the LBL that has to be maintained if the $o(h)$ theory is to be valid. As long as $\varepsilon/P = o(1)$ this distance is seen to be itself of $o(h)$. A typical ε=const. boundary obtained from the equality in (3.9a) is also depicted in Figure 3-1. Considering that the equilibrium paths in the a-P plane will turn out asymptotic to the LBL as $a \to \infty$ and also that any possible violations of (3.9) will turn out to be of very small spanwise extent we see that assumption (16) is not much of a restriction.

3.2.2 The LBL as a Limit Equilibrium Path; The Local Mode: Next we investigate the consequences of φ attaining the value 1 at a single spanwise point x_{lb}; $\varphi(x_{lb})=1=\alpha$. Consider an interval $x_1 \leq x < x_{lb}$ such that in it $0 \leq \varphi(x) < 1$. Then by (3.4b) $\varphi''-\varphi_o''$ is negative, single valued and bounded everywhere in the interval, and hence $\varphi'-\varphi_o'$ must be differentiable and monotonously decreasing there . These facts lead to the conclusion that $\varphi'(x_{lb})$ must be ***bounded.***[1] A similar argument applies to the other side of x_{lb}, using an interval $x_{lb} < x \leq x_2$.

Let us now multiply (3.4b) through by $2\varphi'/P_E$ and integrate. We obtain

$$\varphi'^2 + \frac{P}{P_E}\varphi^2 + \frac{2}{3}\frac{P/P_E}{(1-P)^3}\varepsilon^2\left[\frac{1}{1-\varphi} + \frac{2}{1+\varphi/2}\right] = \int^{x} \varphi_o(t)\varphi'(t)dt\,. \tag{3.10}$$

It is seen that as $x \to x_{lb}$ the only possibility for φ' to remain bounded is when $\varepsilon^2 P=0$. But if this is so, the third term of (3.10) becomes indeterminate and that equation can be satisfied at x_{lb} for any P and φ' .[2] It is therefore possible to

1. $\varphi_o'(x)$ is assumed bounded.
2. In other words, one can always take $\varepsilon^2 P$ and $1-\alpha$ to zero in such a way that

$$\lim_{\varepsilon^2 P \to 0,\, \alpha \to 1}\left\{\frac{\varepsilon^2 P}{1-\alpha}\right\} = \frac{3}{2}P_E(1-P)^3\left[\int^{x_{lb}} \varphi_o(t)\,\varphi'(t)\,dt - \varphi'^2(x_{lb}) - \frac{P}{P_E}\right]$$

and thereby satisfy (3.10) in the limit.

choose on both sides of x_{lb} φ'-values such that the boundary conditions (3.4c,d) are satisfied too. This means that if $\varepsilon^2 P=0$, any a-P point that lies on the line $\alpha = 1$ is consistent with the system (3.4) or, in the usual terminology, belongs to an *equilibrium path*. Since $\alpha=1$, $P\to 0$ imply $a\to\infty$ we arrive at the conclusion

> For any $w_o(x)$ having a bounded first derivative the LBL is an equilibrium path in the limit $\varepsilon\to 0$ for any $a> 0$ and in the limit $a\to\infty$ for any ε.

The second part of this means that *all* equilibrium paths tend to the LBL as $a\to\infty$.

From the above discussion we can further conclude that the point x_{lb} is undetermined and also that φ' is in general discontinuous and changes sign across x_{lb}. The function φ will satisfy the piecewise equations

$$\varphi = \varphi_1(x), \quad 0 \le x \le x_{lb}\,; \qquad \varphi = \varphi_2(x), \quad x_{lb} \le x \le \pi\,; \tag{3.11a,b}$$

$$P_E(\varphi''_1 - \varphi''_o) + P\varphi_1 = 0\,, \qquad 0 < x < x_{lb}\,; \tag{3.11c}$$

$$P_E(\varphi''_2 - \varphi''_o) + P\varphi_2 = 0\,, \qquad x_{lb} < x < \pi\,; \tag{3.11d}$$

$$\varphi_1(o) = 0\,, \quad \varphi_2(\pi) = 0\,, \quad \varphi_1(x_{lb}) = \varphi_2(x_{lb}) = 1\,; \tag{3.11e,f,g,h}$$

the solution of which, for the case $\varphi_o = 0$, is given by

$$\varphi(x) = \begin{cases} \sin\sqrt{\dfrac{P}{P_E}}\,x \,/\, \sin\sqrt{\dfrac{P}{P_E}}\,x_{lb}\,, & 0 \le x \le x_{lb}\,; \\ \sin\sqrt{\dfrac{P}{P_E}}\,(\pi - x) \,/\, \sin\sqrt{\dfrac{P}{P_E}}\,(\pi - x_{lb})\,, & x_{lb} \le x \le \pi\,; \end{cases} \tag{3.11i}$$

and is shown qualitatively in Figure 3-2. We will refer to it as the *'local mode'*. Also shown in that figure is a special case of later interest; the case $a\to\infty$ $(P\to 0)$, $x_{lb}=\pi/2$. From (3.11c,d) we see that for P=0 the sine segments reduce to straight line segments, thus the local mode shape becomes triangular at this limit.

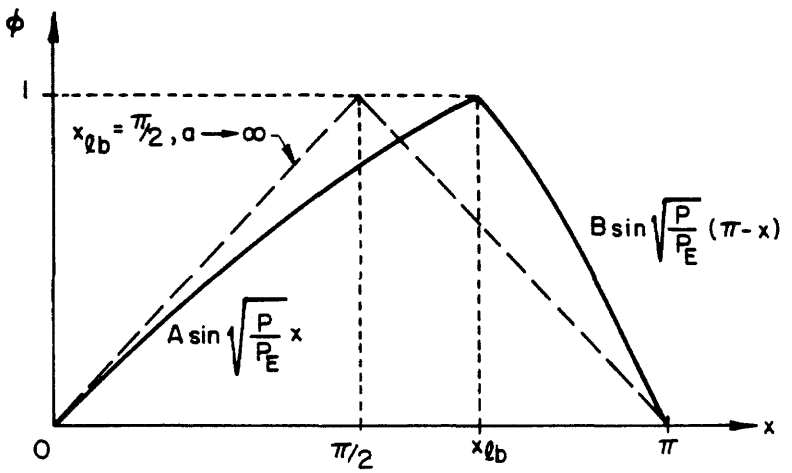

Figure 3-2. The local mode.

3.3 Global Buckling

In this section we will be concerned with the bifurcation of eqns. (3.4) -- $\varphi_o(x)$ set to zero -- from the trivial solution $\varphi=0$. To distinguish this bifurcation from others to come we will refer to it as the *'1st bifurcation'*. When it happens, the (globally-perfect) column is said to undergo *'global buckling'*.

We proceed as usual by taking the first perturbation $\varphi^{(1)}(x)$ around the pre-buckling (trivial) solution $\varphi^{(o)}=0$. The system for $\varphi^{(1)}$ is just the linearized (3.4)

$$P_E \varphi^{(1)''} + P[\, 1 + \frac{\varepsilon^2}{(1-P)^3}] \varphi^{(1)} = 0 \, ; \tag{3.12a}$$

$$\varphi^{(1)}(o) = 0 \, , \qquad \varphi^{(1)}(\pi) = 0 \, . \tag{3.12b,c}$$

The non-trivial solution is immediate (fundamental mode only)

$$\varphi = \alpha \sin x \,, \tag{3.13a}$$

$$(P_E - P_b)(1 - P_b)^3 - \varepsilon^2 P_b = 0 \,, \tag{3.13b}$$

where P_b is the value of P required for the bifurcation to occur. We will call it the *'global buckling load'* and the mode (3.13a) the fundamental initial global buckling mode or, in short, the *'global mode'*.

The root P_b of (3.13b) is shown graphically as function of P_E and ε in Figures 3-3a,b. Note the huge drop in the buckling load that is caused by even slight ε's, especially for P_E values near 1. (E.g., for P_E=1 and for rectangular cross-section longerons, imperfection the size of the cross-section width causes a drop of almost 90%.)

Of special interest are the local imperfection sensitivity power laws, derivable from (3.13b). For $\varepsilon \to 0$

$$P_b \sim P_E[1 - \varepsilon^2/(1-P_E)^3], \qquad 0 < (1 - P_E) = O(1) \,; \tag{3.14a}$$

$$P_b \sim 1 - \varepsilon^{1/2}, \qquad |1 - P_E| = o(\varepsilon) \,; \tag{3.14b}$$

$$P_b \sim 1 - (P_E - 1)^{-1/3} \varepsilon^{2/3}, \qquad 0 < (P_E - 1) = O(1) \,. \tag{3.14c}$$

Note the increased sensitivity as $P_E \to 1$ from either side.

Results to the same effect were obtained by other authors and it is of interest to compare them with ours. In their book [20] Thompson and Hunt treat a two-legged ideal column. Later, Crawford and Hedgepeth [29] employed the same method to draw conclusions about optimal design. The approach is to use the tangent modulus given by (2.15b) in a Shanley buckling formula, $P_b = \pi^2 E_t I_c / L^2$ (I_c being the *global* 2nd moment of area). In our notation this results in

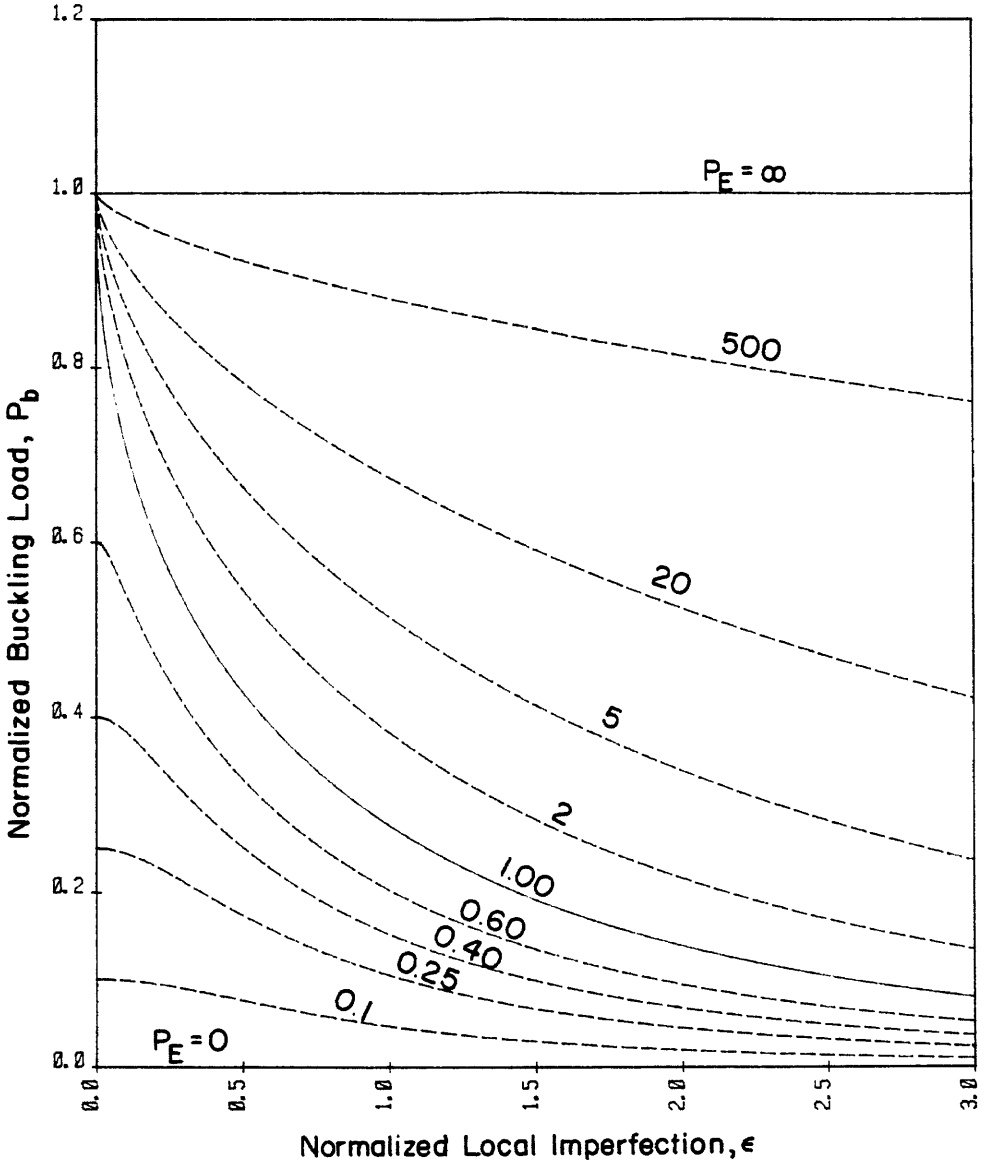

Figure 3-3a. Normalized buckling load in the first bifurcation.

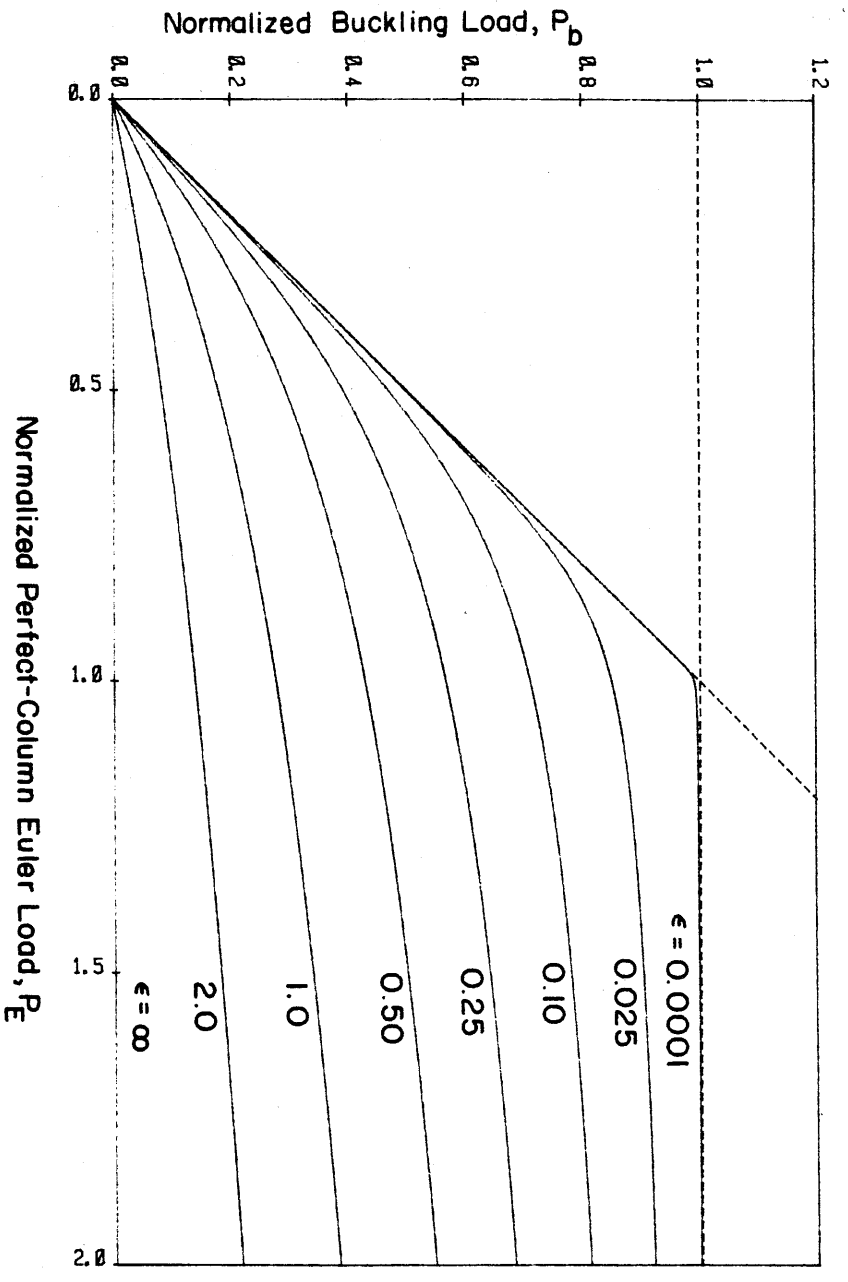

Figure 3-3b. Normalized buckling load in the first bifurcation.

$$P_b = P_E \cdot \frac{E_t}{E} = P_E / \left(1 + \frac{\varepsilon^2}{(1-P_b)^3}\right)$$

which is identical to (3.13b). In this context it is worth noting that (3.12a) can be written, using (2.15b), as

$$(E_t/E)\, P_E \varphi^{(1)\prime\prime} + P \varphi^{(1)} = 0$$

which points at the appropriateness in this case of the Shanley formula approach.

Byskov [30] derives a formula for global buckling of a two-legged ideal column having *continuous* longerons. Using the Koiter and Kuiken [18] asymptotic approach, which appeals to the idea of slowly-varying local amplitudes, he obtains

$$(P_E - P_b)(1 - P_b)^3 - (\varepsilon P_b)^2 P_b = 0$$

in sharp contrast to (3.13b). This discordance can be settled, however, if we note that Byskov's result, being of asymptotic origin, is strictly valid only in the limit $\varepsilon \to 0$. From Figure 3-3a we see that in this limit either $P_b \to 1$ or $\partial P_b/\partial \varepsilon \to 0$, in which cases the disagreement vanishes. (The imperfection sensitivity power laws associated with Byskov's result are identical with eqns. (3.14) except for the $o(\varepsilon^2)$ term in (3.14a), which is multiplied by P_E). The fact that result was obtained for continuous longerons supports assumption (13) of Section 2.1 and seems to contest the assertion in [30] that by neglecting longeron continuity "an essential feature" is lost.

3.4 The Locally-Perfect Ideal Column

The equation for the locally-perfect ideal column is obtained from (3.4b) by setting ε=0. Note that in this case the boundary (3.9) coincides with the LBL and the restriction associated with it disappears. In contrast with Section 3.2.2 we

now investigate the case $\alpha \neq 1$. As is the rule in this work (Assumption 9 of Section 2.1) we restrict the choice of the global imperfection to a replica of the associated buckling mode, given in this case by (3.13a)

$$w_o(x) = e \sin x. \tag{3.15}$$

Taking $\varepsilon = 0$, $\alpha \neq 1$, the nonlinear term in (3.4b) vanishes leaving behind the classical Euler column equation and its well-known solution

$$w(x) = a \sin x, \qquad a = \frac{e}{1 - P/P_E}. \text{ [3]} \tag{3.16a,b}$$

The mode (3.16a) is recognized as the global mode. We will refer to the line in the a-P plane given by (3.16b) as the *'global line'*. Two global line cases are shown in Figure 3-4.

There is nothing, however, in eqns. (3.16) that excludes them from the point α=1. Indeed, the absence of local imperfections or any other stimulus makes it possible for the longeron segments ***not*** to buckle at the LBL. At the point of intersection of the global line and the LBL both modes, the global (eqn 3.16a) and the local (eqn. 3.11i) coexist, thereby characterizing it as a bifurcation point. To distinguish it from the 1st bifurcation point discussed in Section 3.3, we will call it the *'2nd bifurcation point'*, (Figure 3-4). Since the global mode has a midspan maximum, it is plausible that upon bifurcation from global to local x_{lb} will be determined as $\pi/2$.

The value of P in the second bifurcation, denoted by P_c, is obtained from intersecting (3.16b) with (3.7b)

$$P_c = \frac{1}{2}\left[\, 1+P_E(1+2e) - |1-P_E| \sqrt{1+4eP_E[1+(1+e)P_E]/(1-P_E)^2} \,\right]. \tag{3.16c}$$

This was obtained by Mikulas [31] for the case P_E=1. Figures 3-5a,b depict the

3. The ground for the notation P_E in (2.22) is now obvious.

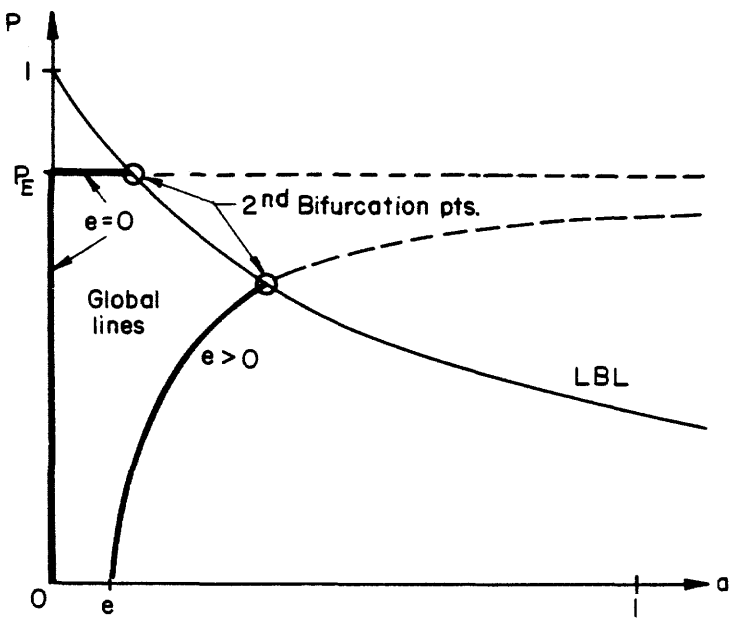

Figure 3-4. Global lines and 2nd bifurcation.

behavior of P_c with changing e and P_E. The global imperfection sensitivity power laws, for $e \to 0$ are

$$P_c \sim P_E[1-2eP_E/(1-P_E)], \qquad 0 < (1-P_E)/P_E = O(1)\,; \tag{3.16d}$$

$$P_c \sim 1-\sqrt{2e}, \qquad |1-P_E| = o(\varepsilon)\,; \tag{3.16e}$$

$$P_c \sim 1-2eP_E/(P_E-1), \qquad 0 < (P_E-1)/P_E = O(1)\,. \tag{3.16f}$$

It is seen that except for the case $P_E=1$ the imperfection-sensitivity of the second bifurcation load is milder than that of the first bifurcation.

3.5 Exact Postbuckling Solution for the Globally-Perfect Case

In this section we will follow the globally-perfect solution that bifurcates from

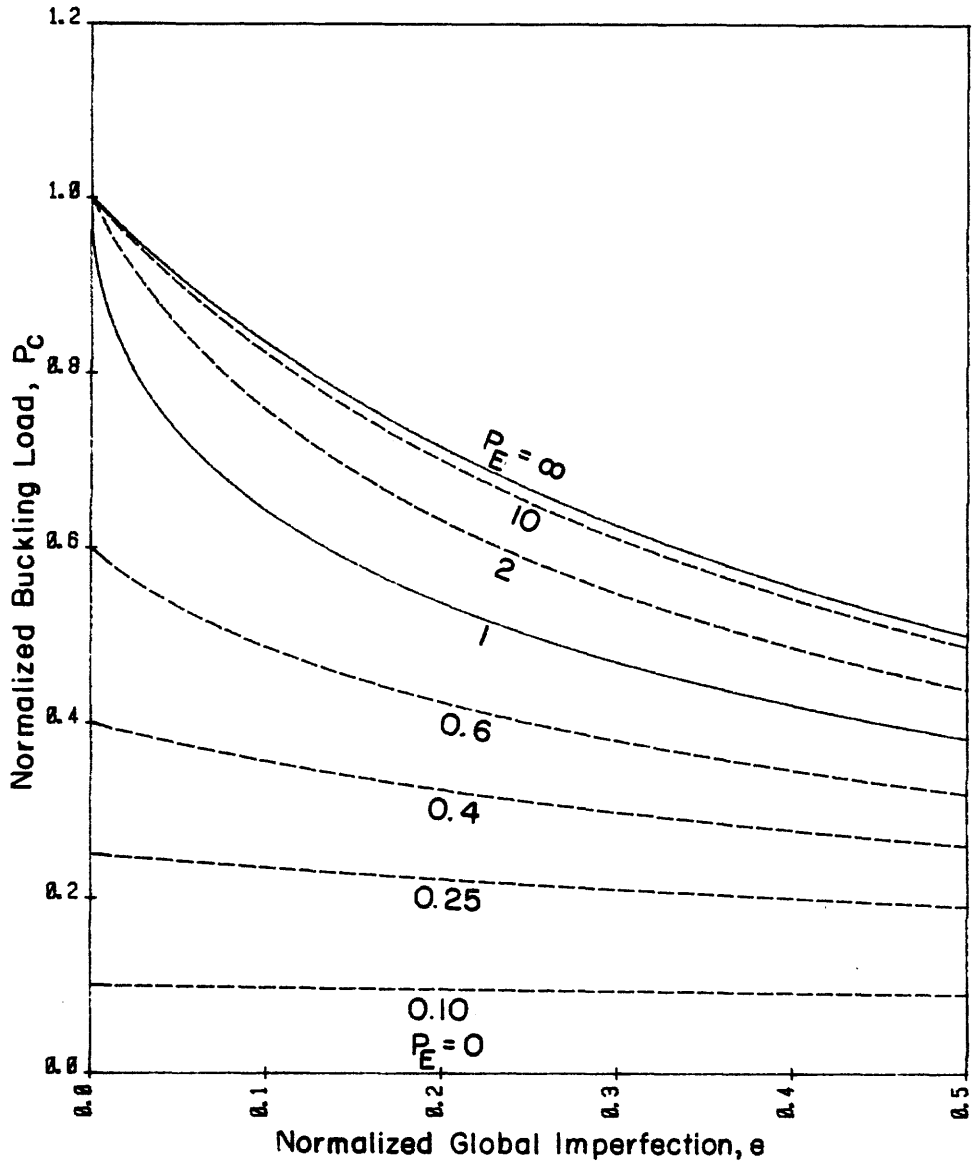

Figure 3-5a. Normalized buckling load in the second bifurcation.

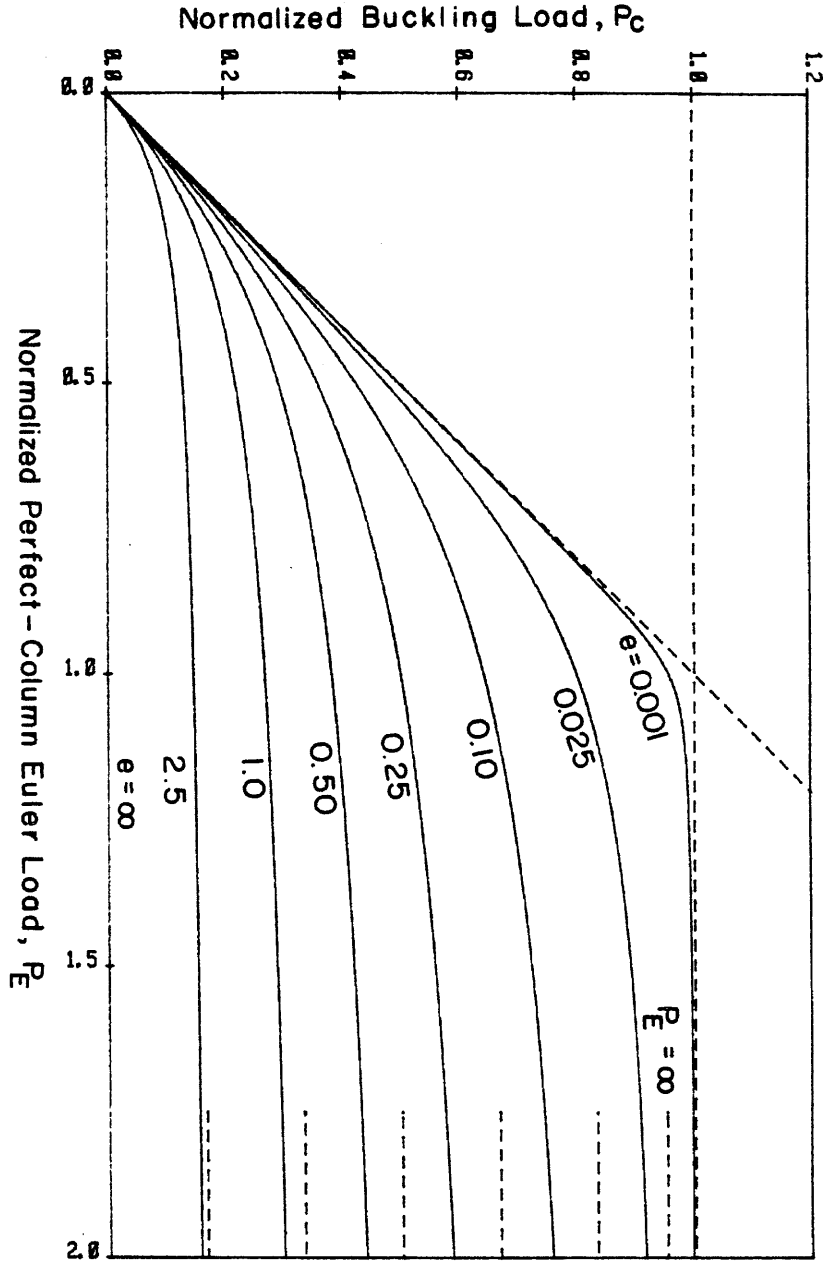

Figure 3-5b. Normalized buckling load in the second bifurcation.

the trivial one at the 1st bifurcation point as it changes with increasing α. In the process we will obtain the *'post-buckling equilibrium path'* relation, which describes a line in the a-P plane - the *'post-buckling line'*. The results of Section 3.3 allow us to assume that the solution has a single relative extremum in $[0, \pi]$ and that that extremum is a maximum. We will also assume that the solution is twice differentiable in $[0, \pi]$.

We start from the once-integrated equation (3.10) replacing the right-hand side by a constant of integration. In accordance with the above assumptions, $\varphi'=0$ implies $\varphi=\alpha$ and vice versa. We can use this to express the constant of integration in terms of α

$$\varphi' = \pm\sqrt{\frac{P}{P_E}\,(\alpha^2-\varphi^2) + \frac{\varepsilon^2}{(1-P)^3}\left[\frac{\alpha^2}{(1-\alpha)(1+\alpha/2)} - \frac{\varphi^2}{(1-\varphi)(1+\varphi/2)}\right]}\,. \qquad (3.17)$$

This can now be integrated a second time to give x as a function of φ. However, since φ has a maximum, $x(\varphi)$ is double valued and only one branch of it can in this way be obtained. By choosing the lower limit of integration as $\varphi=0$ we make this branch satisfy the boundary condition (3.4c). Accordingly, and in order to be consistent with $\alpha > 0$, the positive sign must be chosen for φ' in (3.17) on this branch. Thus

$$x(\varphi) = \sqrt{\frac{P_E}{P}}\int_0^{\varphi}\left\{(\alpha^2-t^2) + \frac{\varepsilon^2}{(1-P)^3}\left[\frac{\alpha^2}{(1-\alpha)(1+\alpha/2)} - \frac{t^2}{(1-t)(1+t/2)}\right]\right\}^{-\frac{1}{2}}dt,$$

$$0 \le \varphi \le \alpha\,. \qquad (3.18a)$$

Also

$$x(\varphi) = \sqrt{\frac{P_E}{P}}\int_0^{\varphi/\alpha}\left[1 + \frac{\varepsilon^2}{(1-P)^3}\,\frac{1-(\alpha t/2)/(1+t)}{(1-\alpha)(1+\alpha/2)(1-\alpha t)(1+\alpha t/2)}\right]^{-\frac{1}{2}}\frac{dt}{\sqrt{1-t^2}}\,,$$

$$0 \le \varphi \le \alpha\,. \qquad (3.18b)$$

For the other branch we choose the negative sign for φ' and make it satisfy the

far end boundary condition. In this way we find that $\varphi(x)$ is even with respect to the midspan. We can now confine our discussion to the first branch only, replacing the boundary condition (3.4d) by

$$\varphi(\frac{\pi}{2}) = \alpha \tag{3.19}$$

which, when applied to (3.18b), comes to

$$\sqrt{\frac{P_E}{P}}\int_0^1 [1 + \frac{\varepsilon^2}{(1-P)^3}\frac{1-(\alpha t/2)/(1+t)}{(1-\alpha)(1+\alpha/2)(1-\alpha t)(1+\alpha t/2)}]^{-\frac{1}{2}}\frac{dt}{\sqrt{1-t^2}} = \frac{\pi}{2} \tag{3.20}$$

and as is usual in this kind of problems, (3.20) constitutes the exact *post-buckling equilibrium path* relation for the globally-perfect column. (3.18b) provides its post-buckling deflection shape.

3.5.1 Asymptotics of the Exact Solution: Closed form evaluation of (3.18b) and (3.20) is likely to be possible (in terms of elliptic integrals) but not very useful. On the other hand, asymptotics can characterize the solution quite satisfactorily, and point at the behavior approximate solutions should imitate.

First, the asymptotic behavior of (3.18b) and (3.20) as $\alpha \to 0$ (i.e. small deflection) is sought. We obtain to the first order in α [4]

$$x(\varphi) \sim \arcsin\frac{\varphi}{\alpha} + \frac{\alpha}{2}(1-\frac{P}{P_E})[(\frac{2}{\pi}\arcsin\frac{\varphi}{\alpha} - 1) + (1+\frac{\varphi}{2\alpha})\sqrt{\frac{1-\varphi/\alpha}{1+\varphi/\alpha}}], \tag{3.21a}$$

$$(P_E - P)(1-P)^3 - \varepsilon^2 P(1+\frac{2}{\pi}\alpha) \sim 0\,. \tag{3.21b}$$

It is seen that initially the deflection is sinusoidal. For small φ/α the bracket in (3.21a) can be shown to approach 0.1366 φ/α. Hence, as α increases from zero, the deflection shape tends slightly towards the triangular. The load-deflection relation (3.21b), together with others, will be investigated in Section 3.8.

4. In obtaining (3.21a) use is made of (3.21b). Note also that $\varphi/\alpha \leq 1$ as $\alpha \to 0$.

We now let α approach 1 close enough so that $\varepsilon^2/(1-\alpha) >> 1$. [5] We see from (3.17) that either $\varphi \sim \alpha$ and $\varphi' \sim 0$ or, neglecting quantities of order 1 and smaller:

$$\varphi' \sim \sqrt{\frac{2}{3P_E(1-P)^3}\frac{\varepsilon^2 P}{1-\alpha}}$$

which is independent of φ. It appears, therefore, that the limiting deflection shape as $\alpha \to 1$ is triangular. When applying the boundary condition (3.19) we get

$$x(\varphi) \sim (\pi/2)\varphi/\alpha\,, \tag{3.22a}$$

$$P_E(1-P)^3 - \varepsilon^2 P\frac{\pi^2/6}{1-\alpha} \sim 0\,. \tag{3.22b}$$

Note, however, that if φ' is to be finite P must tend to zero and therefore $a \to \infty$. We have thus arrived again at the $a \to \infty$ local mode of Figure 3-2, this time through the limit $a \to \infty$ for any ε, in agreement with the conclusion in Section 3.2.2. Here it is (3.19) that determines x_{lb} to be $\pi/2$.

If quantities of order 1 are retained, a quite laborious expansion gives, first, uniformly valid but too lengthy expressions for $x(\varphi)$ and the load-deflection relation. By breaking the φ-region into subregions, further simplifications can be made. The results are:

$$x(\varphi) \sim \frac{\pi}{2} - \sqrt{\frac{6P_E(1-P)^3}{\varepsilon^2 P}}(1-\alpha)\sqrt{\alpha-\varphi}, \quad \alpha-\varphi << 1-\varphi\,; \tag{3.23a}$$

$$x(\varphi) \sim \sqrt{\frac{3P_E(1-P)^3(1-\alpha)}{2\varepsilon^2 P}}\left\{\left[1 + \frac{1-\alpha}{2}\left(\frac{5}{3} - \frac{3(1-P)^3}{2\varepsilon^2}\right)\right]\varphi + \right.$$

$$\left. +(1-\alpha)\left[\frac{(1-P)^3}{4\varepsilon^2}\varphi^3 + \ln\frac{(1+\varphi/2)^2}{\sqrt{1-\varphi}} - \frac{3}{2}\varphi\right]\right\}, \quad 1-\varphi >> 1-\alpha\,; \tag{3.23b}$$

$$\left(P_E - \frac{\pi^2}{6}P\right)(1-P)^3 - \varepsilon^2 P\left\{\frac{\pi^2}{6}\left[\frac{1}{1-\alpha} + \ln(1-\alpha) + \left(\frac{7}{3} + \ln\frac{4}{81}\right)\right]\right\} \sim 0\,. \tag{3.23c}$$

Note that (3.23a) may be inverted to give

5. Eqn. (3.9b) may thereby be violated. However, what we are looking for now is the nature of the solution of (3.4) regardless of its strict physical validity.

$$\varphi(x) \sim \alpha - \frac{\varepsilon^2 P}{6P_E(1-P)^3}\frac{1}{(1-\alpha)^2}\left(\frac{\pi}{2}-x\right)^2; \quad \alpha-\varphi << 1-\varphi \qquad (3.23d)$$

which shows how the midspan curvature behaves as $\alpha \to 1$, and which could have been deduced directly from (3.4b). In (3.23b), the first term carries all the linearity and the second term is positive and has a positive 2nd derivative, whence we learn the behavior for low to moderate φ. In order to get purely geometrical expressions P has to be eliminated in favor of α using (3.23c).

To conclude, for $\varepsilon > 0$ the deflection shape changes gradually with α from the global mode at $\alpha=0$ to the triangular local mode at $\alpha=1$. Figure 3-6 depicts this behavior.

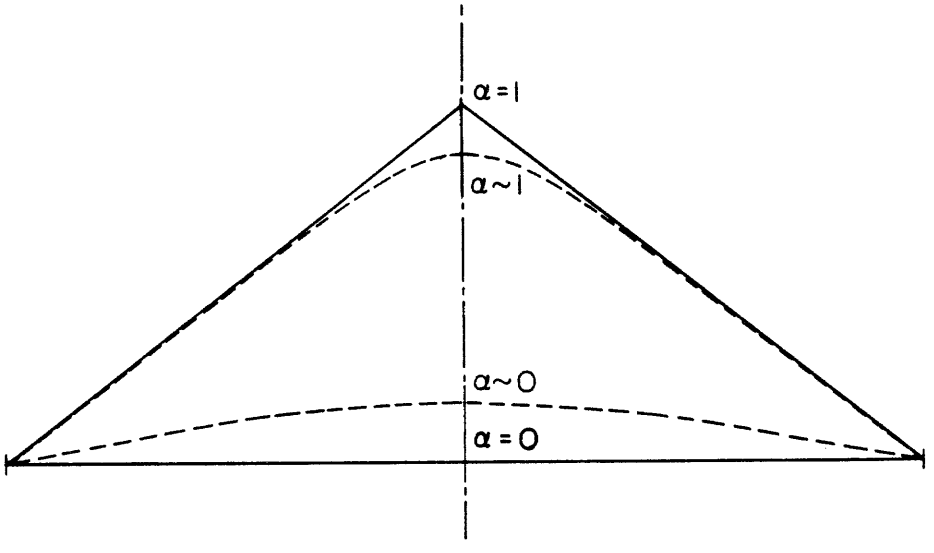

Figure 3-6. Post-buckling deflection shape as function of α (qualitative).

3.6 Approximate Load-Deflection Relation for the Globally-Perfect Column

Though one may feel content with the asymptotics of the exact solution as regards the deflection shape, one wishes to know the load-deflection relation for all $0 \leq \alpha \leq 1$. Numerical evaluation of eqn.(3.20) is not very convenient, and

moreover, we might not have an equivalent of (3.20) for the general, globally-imperfect case. Therefore a simplified, approximate load-deflection relation is desired, tested against the known exact asymptotic behavior.

In order to achieve this goal the following steps will be taken: (1) The general form of the sought load-deflecion relation is determined by using the Ritz-Galerkin procedure. It is found to conform with (3.21b) and (3.22b) except for having a more general α-dependence. (2) The asymptotic behavior as $\alpha \to 0$ and as $\alpha \to 1$ of the result is then compared with (3.21b) and (3.22b) respectively and is found not altogether satisfactory. (3) A method is devised in which two exact representations of the load-deflection relation - one which is known completely (eqn. 3.20) but does not posses the required form and another, which has that form but contains unknown functions - are compared, thereby identifying the required approximate α-dependence. This, in turn, is found to satisfy exactly the asymptotic α-wise behavior.

Following [34] the Ritz-Galerkin procedure is applied to either (3.4b) or (3.17). In both cases an assumed solution $\varphi = \alpha \sin x$ is substituted, the equation is then multiplied through by the same $\sin x$ as a weight function and integrated over $[0, \pi]$. The approximate load-deflection relation thus obtained is of the form

$$(P_E - P)(1 - P)^3 + \varepsilon^2 P f(\alpha) = 0 \tag{3.24}$$

where, if (3.4b) is used

$$f(\alpha) = f_1(\alpha) \equiv \frac{2}{3\pi\alpha} \int_0^{\pi} \left[\frac{\sin t}{(1-\alpha \sin t)^2} - \frac{\sin t}{1+(\alpha/2)\sin t)^2} \right] dt \tag{3.25}$$

or, if (3.17) is used [6]

$$f(\alpha) = f_2(\alpha) \equiv \frac{2}{(1-\alpha)(1+\alpha/2)} \int_0^{1} \frac{1-(\alpha t/2)/(1+t)}{(1-\alpha t)(1+\alpha t/2)} t\, dt \tag{3.26}$$

6. In deriving (3.26) care must be taken to average the error of φ' rather than that of φ'^2. Neglecting the square of the error with respect to $\alpha^2 \cos^2 x$ is also needed.

(both of which are easily evaluated in closed form). Unfortunately, when compared with (3.21b) and (3.22b), none of these has a completely satisfactory asymptotic behavior,

$\alpha \to 0$	$\alpha \to 1$
$f_1(\alpha) \sim 1 + (2/\pi)\alpha$	$f_1(\alpha) \sim (4/3)(1-\alpha)^{-3/2}$
$f_2(\alpha) \sim 1 + (4/3 - \ln 2)\alpha$	$f_2(\alpha) \sim -(2/3)\dfrac{\ln(1-\alpha)}{1-\alpha}$
desired: $1 + (2/\pi)\alpha$	desired: $(\pi^2/6)/(1-\alpha)$,

and therefore both of them are abandoned. Instead, we look for an appropriate $f(\alpha)$ along the following lines. First we ask what is the most general exact load-deflection relation that conforms with (3.24). To answer this we again integrate (3.4b) multiplied by $2\varphi'/P_E$, but this time we take a definite integral over $[0, \pi/2]$, invoking the boundary conditions (3.4c) and $\varphi'(\pi/2)=0$. Defining $\vartheta_0 \equiv \varphi'(0)$ we can write

$$(P_E - \frac{\alpha^2}{\vartheta_0^2(\alpha,\varepsilon,P_E)}P)(1-P)^3 - \varepsilon^2 P \frac{\alpha^2/\vartheta_0^2(\alpha,\varepsilon,P_E)}{(1-\alpha)(1+\alpha/2)} = 0 \qquad (3.27)$$

which is the form sought. The end-slope ϑ_0, which is anticipated to be a function of α, ε, and P_E, is an unknown function. If ϑ_0 could be somehow determined this would have provided us with an exact $f(\alpha)$. We shall see, however, that this cannot be done. Nevertheless, we can reduce the number of arguments of ϑ_0 as follows. Define

$$K \equiv \frac{\varepsilon^2}{(1-P)^3}, \qquad H \equiv \frac{P_E}{P},$$

and rewrite (3.27) in the form

$$\frac{\alpha^2}{\vartheta_0^2(\alpha,\varepsilon,P_E)}\left(1 + \frac{K}{(1-\alpha)(1+\alpha/2)}\right) = H. \qquad (3.28)$$

Now take (3.20), which is also an exact expression of the *same* load-deflection

relation, and write it in terms of K and H

$$\left\{\frac{2}{\pi}\int_0^1 \left[\,1 + K\frac{1-(\alpha t/2)/(1+t)}{(1-\alpha)(1+\alpha/2)(1-\alpha t)(1+\alpha t/2)}\right]^{-\frac{1}{2}} \frac{dt}{\sqrt{1-t^2}}\right\}^{-2} = H\,. \qquad (3.29)$$

Since the right-hand sides of (3.28) and (3.29) are identical so must be the left-hand sides, and we see immediately that ϑ_0 cannot be a function of P_E or H; it must be a function of α and K only

$$\vartheta_0 = \vartheta_0(\alpha, K)\,.$$

It is now clear that identifying ϑ_0 from (3.28) and (3.29) will yield a dependence on P (through K) which is not desirable in (3.27) and which only prior knowledge of $\alpha(P)$ (i.e. the load-deflection relation itself) can eliminate. Instead we use the following trick. Based upon the Ritz-Galerkin form (3.24) and also the asymptotic results (3.21b), (3.22b), and (3.23c) we *postulate* a desired *approximate* load-deflection relation of the form

$$[P_E - g(\alpha)P](1-P)^3 - \varepsilon^2 P f(\alpha) = 0. \qquad (3.30)$$

In other words, since those asymptotic results indicate that in their respective limits the functions f and g in (3.30) are independent of P, P_E, or ε, we are suppressing any possible dependence on these variables throughout the α-range. We do not even require that f and g be related in the manner implied by (3.27). Instead, we *identify* (3.30) with (3.27) and this forces a certain K-wise behavior on ϑ_0, namely

$$\frac{\alpha^2}{\vartheta_0^2} = \frac{(1-\alpha)(1+\alpha/2)}{(1-\alpha)(1+\alpha/2)+K}[g(\alpha) + Kf(\alpha)]\,.$$

Assuming that this holds approximately for $0 \le \alpha \le 1$ we can now substitute it into (3.28) and equate (3.28) with (3.29):

$$g(\alpha) + Kf(\alpha) = \left\{ \frac{2}{\pi} \int_0^1 \left[1 + K \frac{1-(\alpha t/2)/(1+t)}{(1-\alpha)(1+\alpha/2)(1-\alpha t)(1+\alpha t/2)} \right]^{-\frac{1}{2}} \frac{dt}{\sqrt{1-t^2}} \right\}^{-2}.$$

The crucial point consists of requiring now that this equation be an identity, i.e., be satisfied for *any* K. Taking first K=0 and then $K \to \infty$ we can identify $g(\alpha)$ and $f(\alpha)$ as follows

$$g(\alpha) = 1 \tag{3.31a}$$

$$f(\alpha) = \frac{\pi^2/4}{(1-\alpha)(1+\alpha/2)} \left(\int_0^1 \sqrt{\frac{(1-\alpha t)(1+\alpha t/2)}{(1-t)(1+[1-\alpha/2]t)}}\, dt \right)^{-2}. \tag{3.31b}$$

Indeed, it is not difficult to show that (3.31b) satisfies the required asymptotic behavior for $\alpha \to 0$ as well as for $\alpha \to 1$. Therefore, in accordance with (3.30) and (3.31a) we determine the ***working equilibrium path relation*** of the globally-perfect ideal column to be

$$(P_E - P)(1-P)^3 - \varepsilon^2 P f(\alpha) = 0 \tag{3.32}$$

where $f(\alpha)$ is given by (3.31b). Note that (3.32) differs from (3.23c) in the first term. However, we know already that as $\alpha \to 1$ P is of order $1-\alpha$, therefore so must be order of the difference.

The functions $f(\alpha)$ and $f_1(\alpha)$ are shown in Figure 3-7.

3.7 Load-Deflection Relation - The Doubly-imperfect Case

In the general, globally- and locally-imperfect case, $\varphi_o \neq 0$ and we cannot solve (3.4b) exactly. Thus, as outlined in the previous section, we assume a fixed-shape deflection, $\varphi = \alpha \sin x$, and employ the Ritz-Galerkin averaging method [34]. By eqns. (3.15) and (3.3a) we have

$$w_o = e \sin x, \qquad \varphi_o = \frac{2eP}{1-P} \sin x,$$

and carrying out the averaging procedure on (3.4b) the following load-deflection

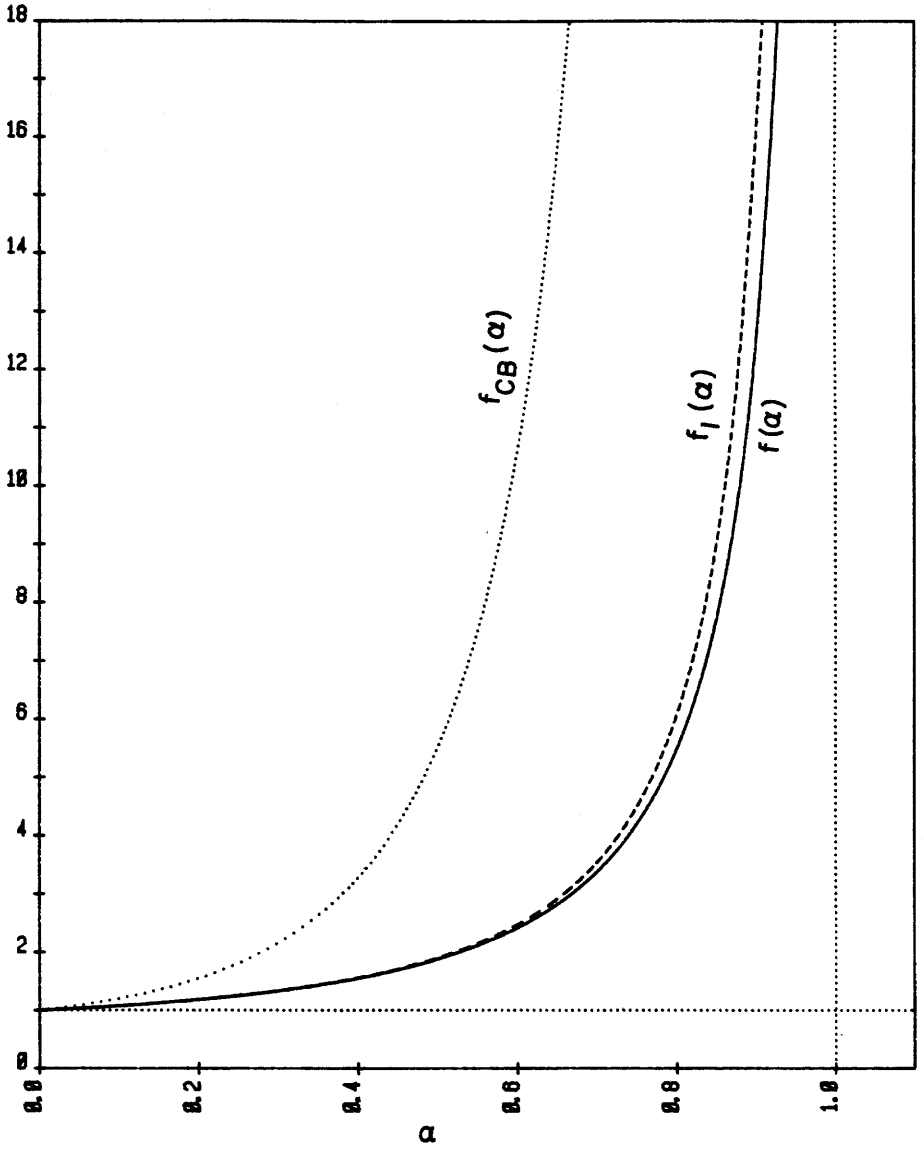

Figure 3-7. The functions $f(\alpha)$, $f_1(\alpha)$ and $f_{CB}(\alpha)$.

relation is obtained:

$$(P_E-P)(1-P)^3 - 2eP_EP(1-P)^2(1/\alpha) - \varepsilon^2 P f_1(\alpha) = 0 .$$

However, noting that this must reduce to (3.32) when $e \to 0$, we replace $f_1(\alpha)$ by $f(\alpha)$ [7] and adopt the following equation:

$$(P_E-P)(1-P)^3 - 2eP_EP(1-P)^2(1/\alpha) - \varepsilon^2 P f(\alpha) = 0 \qquad (3.33)$$

where $f(\alpha)$ is given by (3.31b).

3.8 Behavior in the a-P Plane of the Ideal Column

In this section we will discuss those aspects of the column behavior which are represented by its equilibrium path (3.33).

3.8.1 The Perfect Column: Letting in (3.33) $e=0$, $\varepsilon \to 0$ we can solve it immediately to get two equilibrium paths

$$P = P_E, \quad 0 \le a \le a_{max} ;$$
$$P = 1 , \quad 0 \le a \le a_{max} .$$

But since ε is zero and $f(1) \to \infty$ a third possibility exists: [8]

$$\alpha = 1 ; \quad 0 \le a \le a_{max}$$

where $a_{max}=a(1)$ is the limit of validity of the present theory according to (2.13j). The first of these is recognized as the $a>0$ branch of the global line for $e=0$, (Figure 3-4) whereas the last is the LBL, shown in Section 3.2.2 to be indeed an equilibrium path for $\varepsilon=0$. These equilibrium paths are shown in Figure 3-8 for 3 P_E cases. Also shown in this figure are the first and the second bifurcation points corresponding to the three P_E cases. In the first the column bifurcates

7. It can be shown that this operation is equivalent to letting the imperfection shape w_o resemble the deflection shape w for all $o< \alpha< 1$, i.e., $w_o(x)=(e/a)w(x)$.
8. To show this replace $f(\alpha)$ in (3.33) by its asymptotic value $(\pi^2/6)/(1-\alpha)$, solve for α and then let $\varepsilon = 0$.

from the " trivial mode" to the global mode, and in the second, from the global mode to the local mode. The actual behavior is supposed to follow the lowest-possible path, which can be shown to correspond to the least total potential energy.

3.8.2 Local Imperfection Only: Upon letting e=0, the load-deflection relation (3.33) reduces back to the form (3.32). Numerical solutions are shown graphically in Figures 3-9 for three P_E cases. [9] The situation is now that discussed in Section 3.5 and the equilibrium paths obtained are post-buckling lines. They depart from the fundamental path a=0 in the first bifurcation point, the value of which is the global buckling load, eqn. (3.13b).

3.8.3 Global Imperfection Only: For this case $\varepsilon \to 0$ and (3.33), using (3.3b), reduces to the Euler column relation (3.16b). The equilibrium paths are now the global lines of Section 3.4 and Figure 3-4. A family of them is shown in Figure 3-10. Upon their crossing of the LBL at the second bifurcation point bifurcation from global mode to local mode is triggered.

3.8.4 The General Case: Typical equilibrium paths of the general, doubly-imperfect column, are shown in Figures 3-11 for three P_E cases. Also shown in these figures are the LBL, global lines (ε=0), post-buckling lines (e=0) and the corresponding bifurcation points. It is seen that the general paths are bounded by both the global lines and the post-buckling lines, the later are, in turn, bounded by the LBL. Thus, the general paths have maxima and the column failure is by snap-buckling (also called *'limit point instability'.)*

The value of P at the maximum is the ultimate load-carrying capacity of the

9. The graphs in Figures 3-9 and 3-11 through 3-13 were produced using $f_1(\alpha)$ rather than the more exact $f(\alpha)$.

column and is denoted by P_m. P_m is found by intersecting the locus of maxima $dP=0$ with the path itself. Implicitly

$$e = \frac{(1-P_m)(P_E-P_m)}{2P_E P_m} \frac{\alpha^2 f'(\alpha)}{[\alpha f(\alpha)]'}, \tag{3.34a}$$

$$\varepsilon^2 = (P_E/P_m-1)(1-P_m)^3 / [\alpha f(\alpha)]' . \tag{3.34b}$$

On the other hand we have the nominal (perfect-column) load-carrying capacity P_p,

$$P_p \equiv \begin{cases} P_E, & P_E < 1; \\ 1, & P_E \geq 1; \end{cases} \tag{3.35}$$

so one can plot on an ε-e plane, for different values of the design parameter P_E, the amount of ε and e required to knock the column performance down to a certain fraction of the nominal load, say one half. A plot like this is given in Figure 3-12. It provides information on the column imperfection sensitivity in the finite, as opposed to the asymptotic, sense. It is seen that the nearer P_E is to 1 the less is the imperfection required to cause a prescribed performance degradation.

3.9 Comparison with Crawford and Benton

Recall from Section 3.3 the use that was made by Thompson and Hunt [20] of the tangent modulus in conjunction with Shanley's buckling formula to derive the global buckling load. In their paper [33] Crawford and Benton extended the use of this method to solve the complete problem. In doing so they had to assume that the tangent modulus remains spanwise uniform also in the bent state, in spite of the then non-uniform distribution of internal forces. Another questionable feature of their approach is the adoption of an imperfect Euler column load-deflection relation of the type (3.16b) -- P_E serving as a variable dependent on the tangent moduli -- as a basis for their general load-deflection

relation. We are now in a position to ascertain the extent of the error resulting from these assumptions.

It can be shown that eqs. (21) and (22) of [33] reduce, in our notation, to the form (3.33), but that instead of f(α) there appears

$$f_{CB}(\alpha) \equiv \frac{2/3}{(1-\alpha)^3} + \frac{1/3}{(1+\alpha/2)^3} \tag{3.36}$$

which has a significantly different behavior from ours. $f_{CB}(\alpha)$ is shown, for comparison, in Figure 3-7 (Section 3.6). A comparison of resulting paths is given in Figure 3-13, where the path e=0.2 corresponds to Figure 4 of [33]. It is seen that the method of Crawford and Benton significantly underestimates the column performance.[10]

10. Recall that Figure 3-13 was plotted using $f_1(\alpha)$ rather than the more exact $f(\alpha)$. Judging from Figure 3-7 this underestimation is even higher than seems from Figure 3-13.

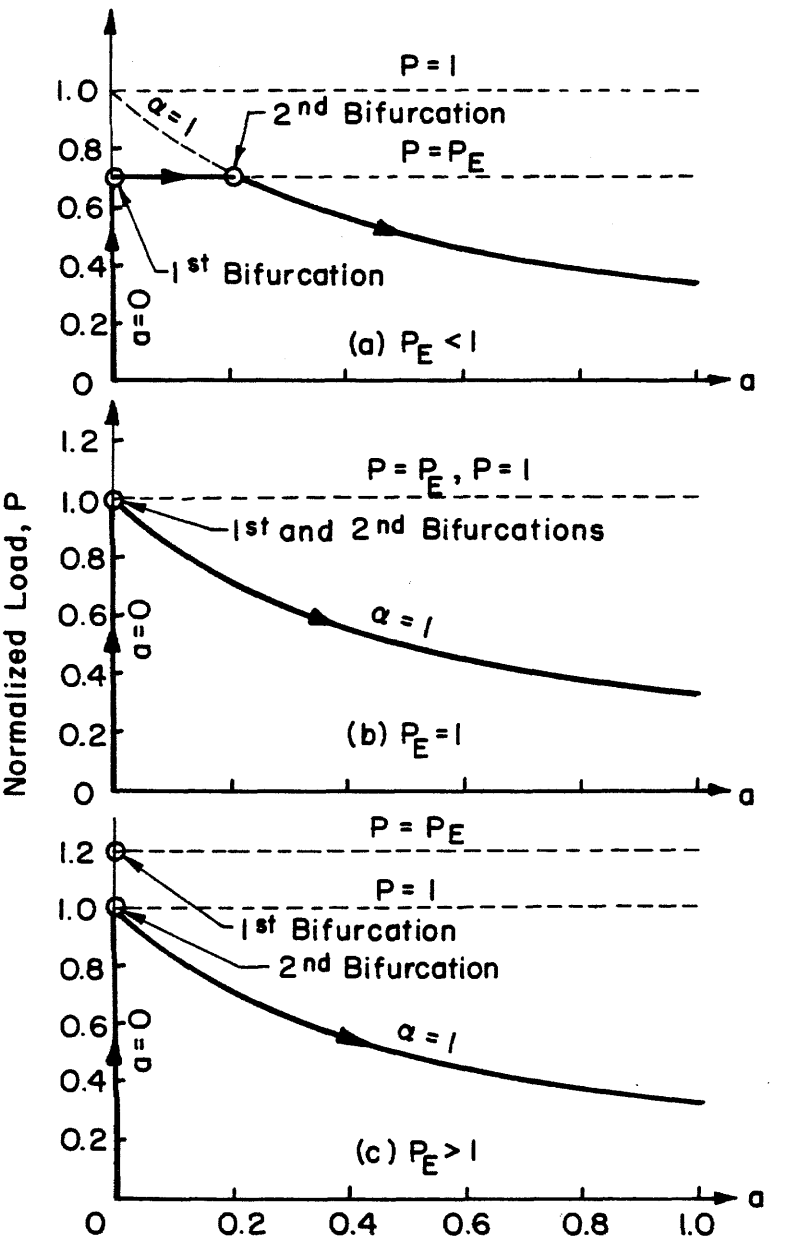

Figure 3-8. Equilibrium paths of the perfect column ($e = 0, \varepsilon \to 0$).

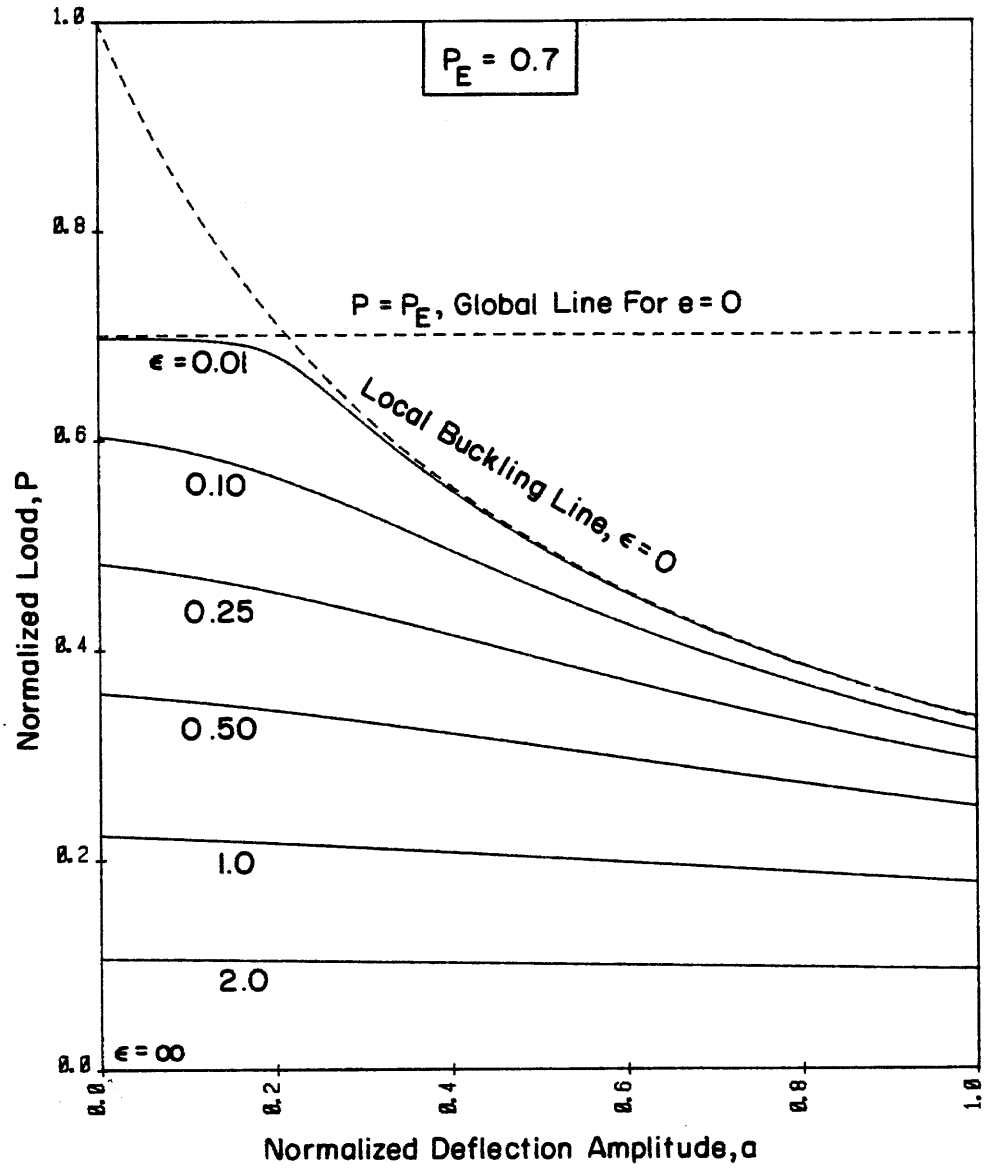

Figure 3-9a. Post-buckling behavior of the globally-perfect column. (I) $P_E < 1$.

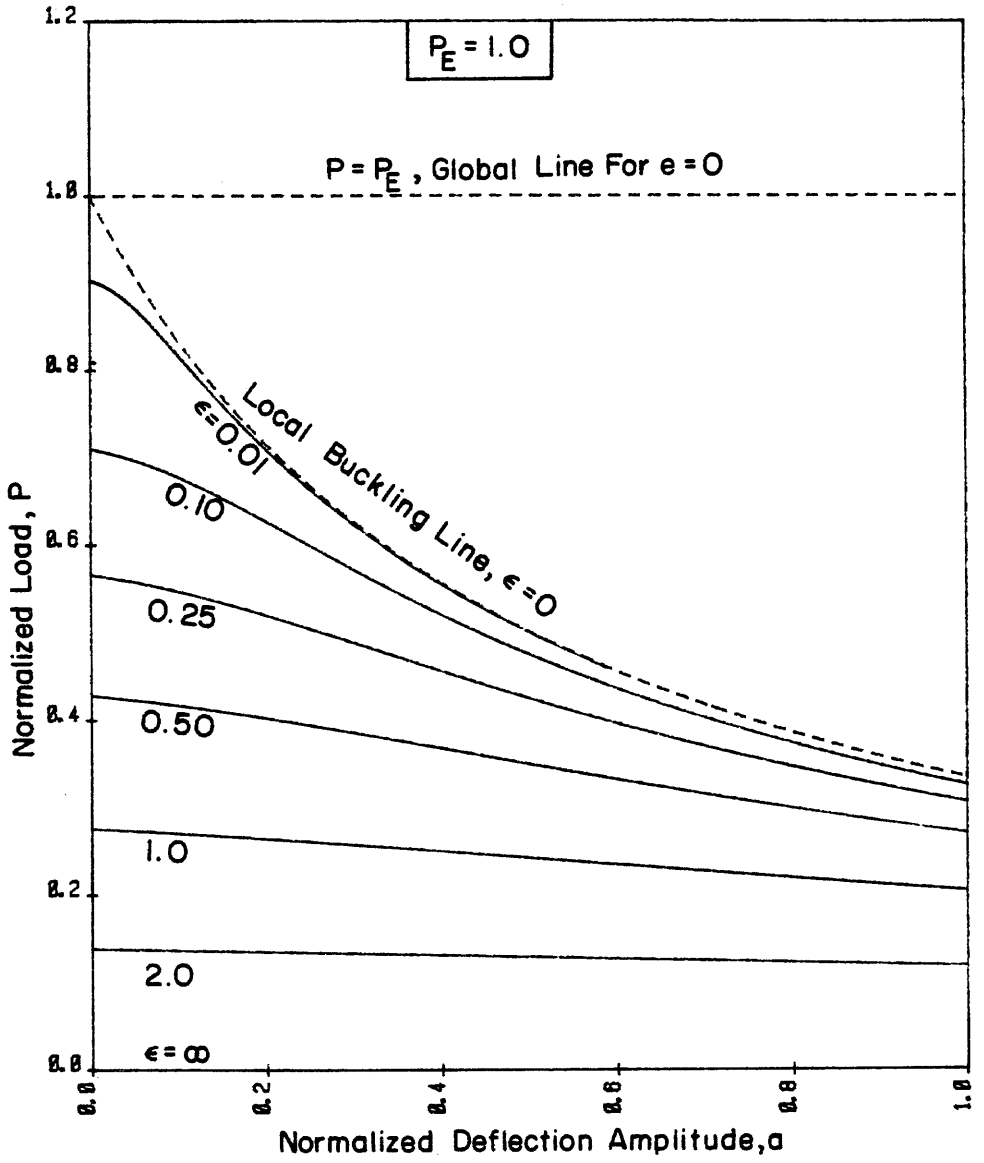

Figure 3-9b. Post-buckling behavior of the globally-perfect column. (II) $P_E = 1$.

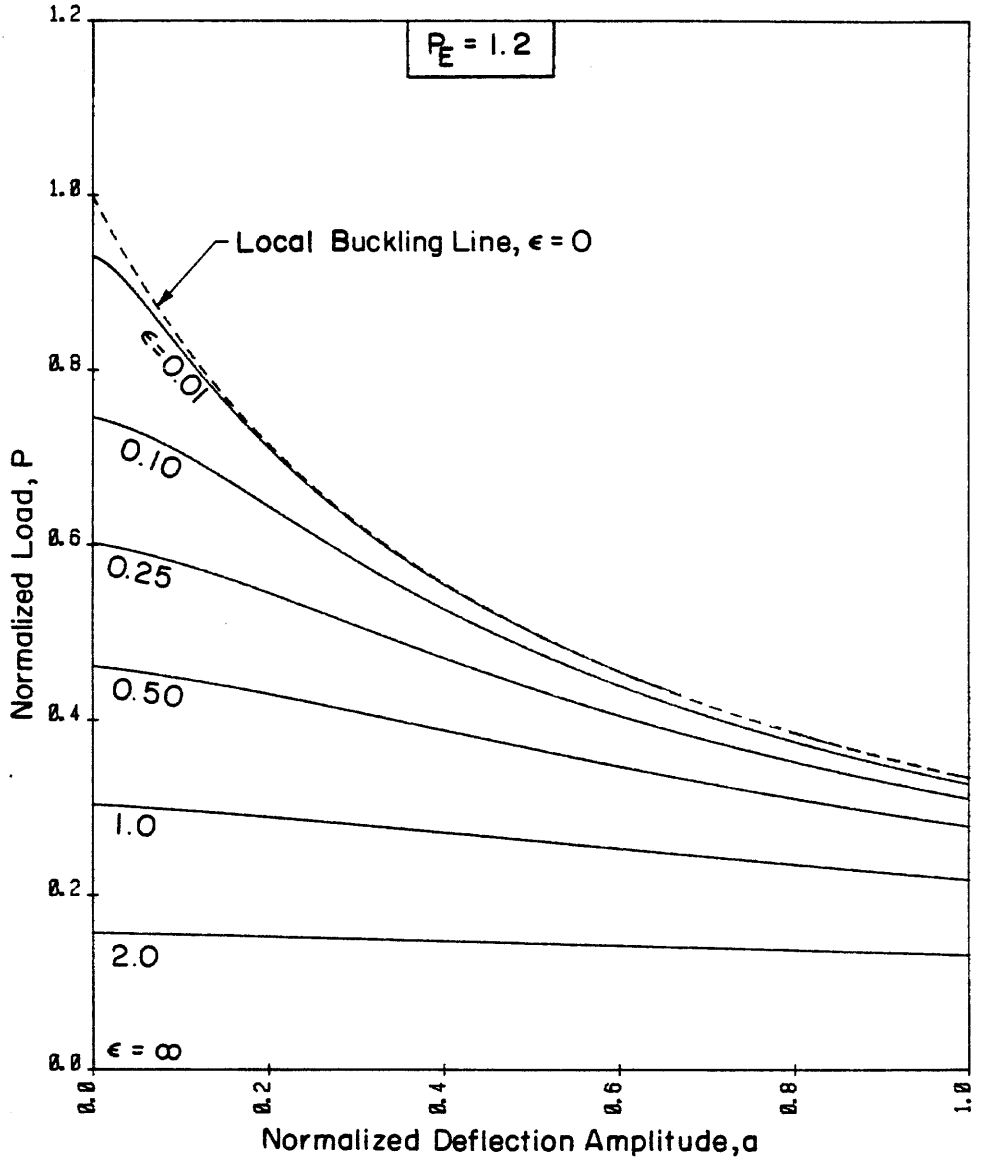

Figure 3-9c. Post-buckling behavior of the globally-perfect column. (III) $P_E > 1$.

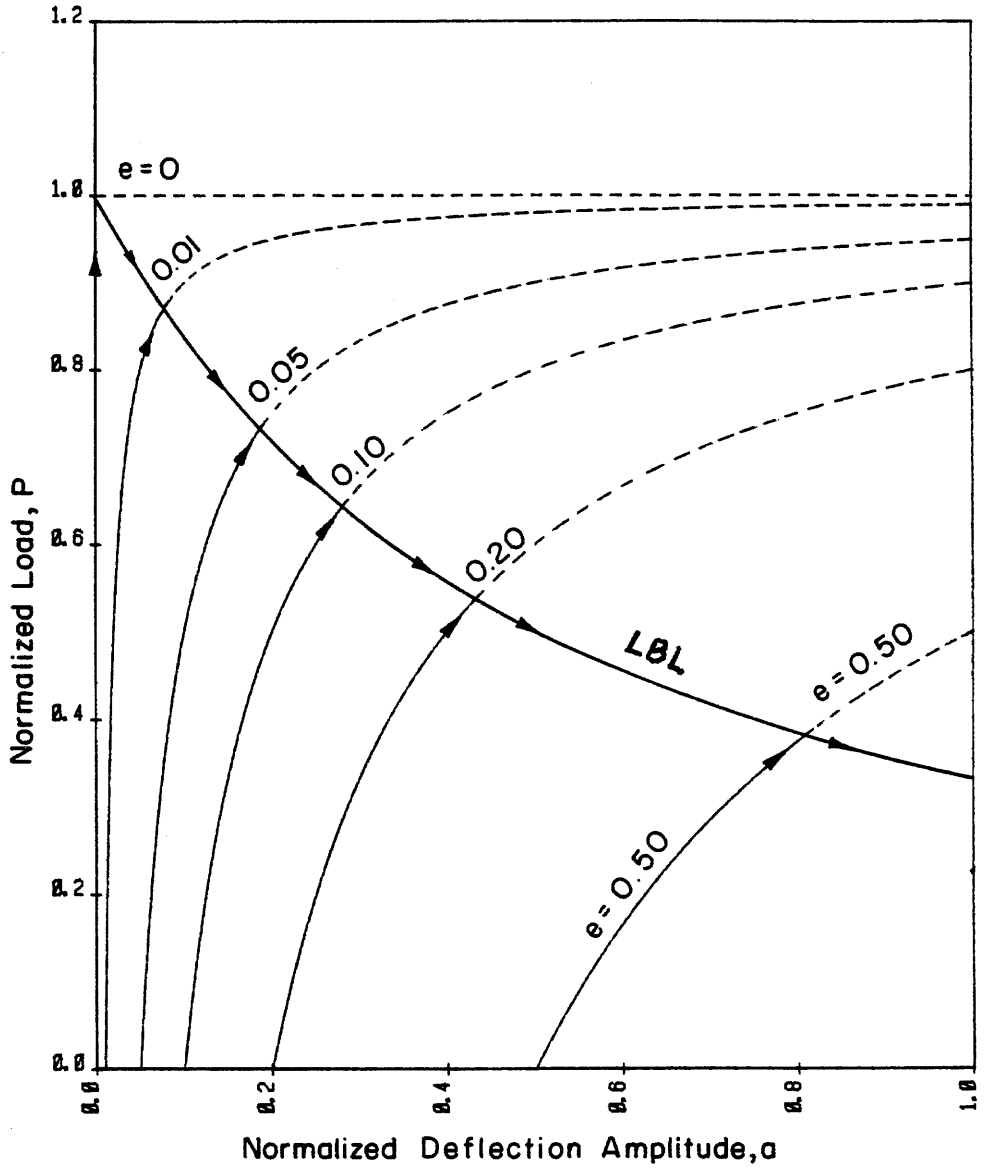

Figure 3-10. Equilibrium paths of the locally-perfect column; $\varepsilon \to 0$, $P_E = 1$, varying e.

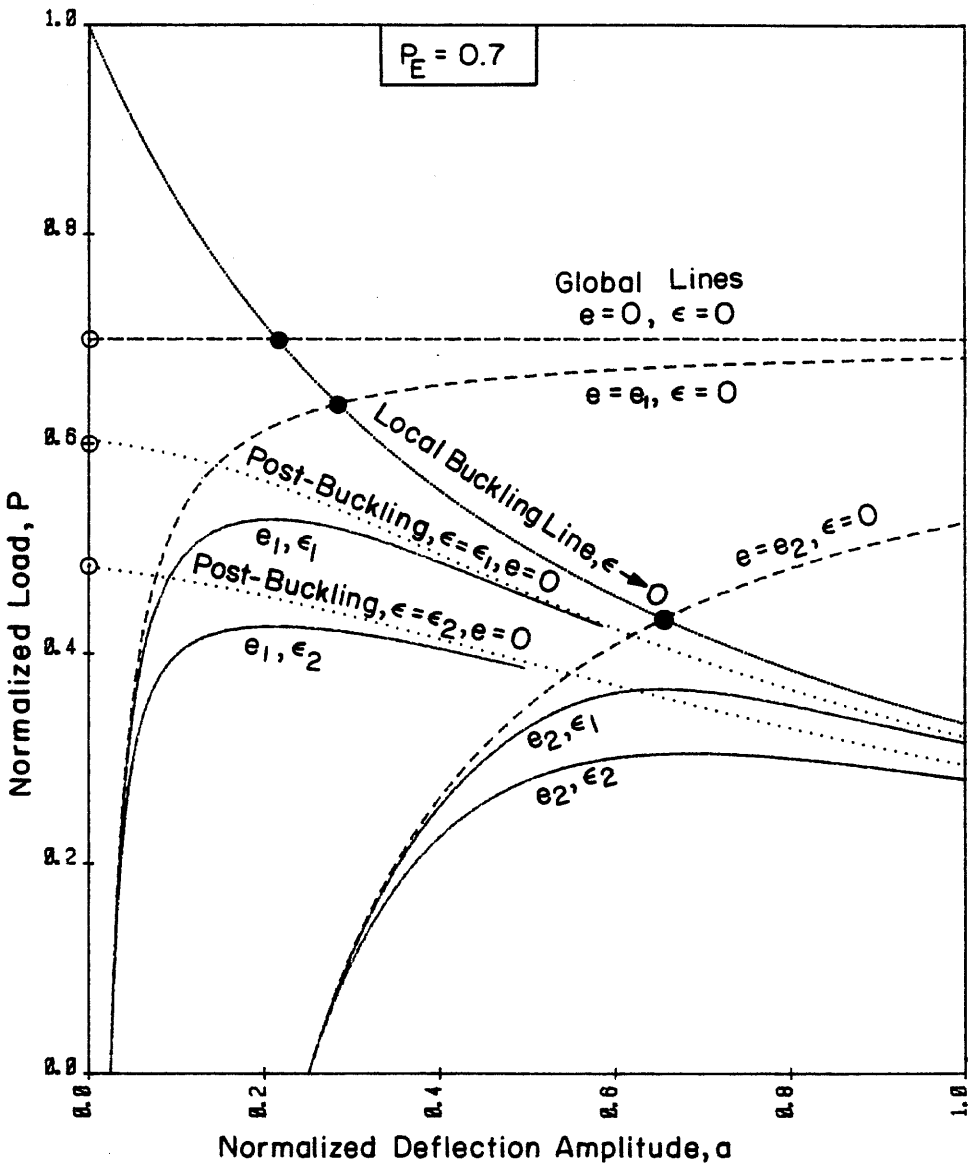

Figure 3-11a. Typical equilibrium paths of the doubly-imperfect ideal column for $P_E < 1$.
$\varepsilon_1 = 0.10$; $\varepsilon_2 = 0.25$; $e_1 = 0.025$, $e_2 = 0.25$.
○ First Bifurcation, ● Second Bifurcation.

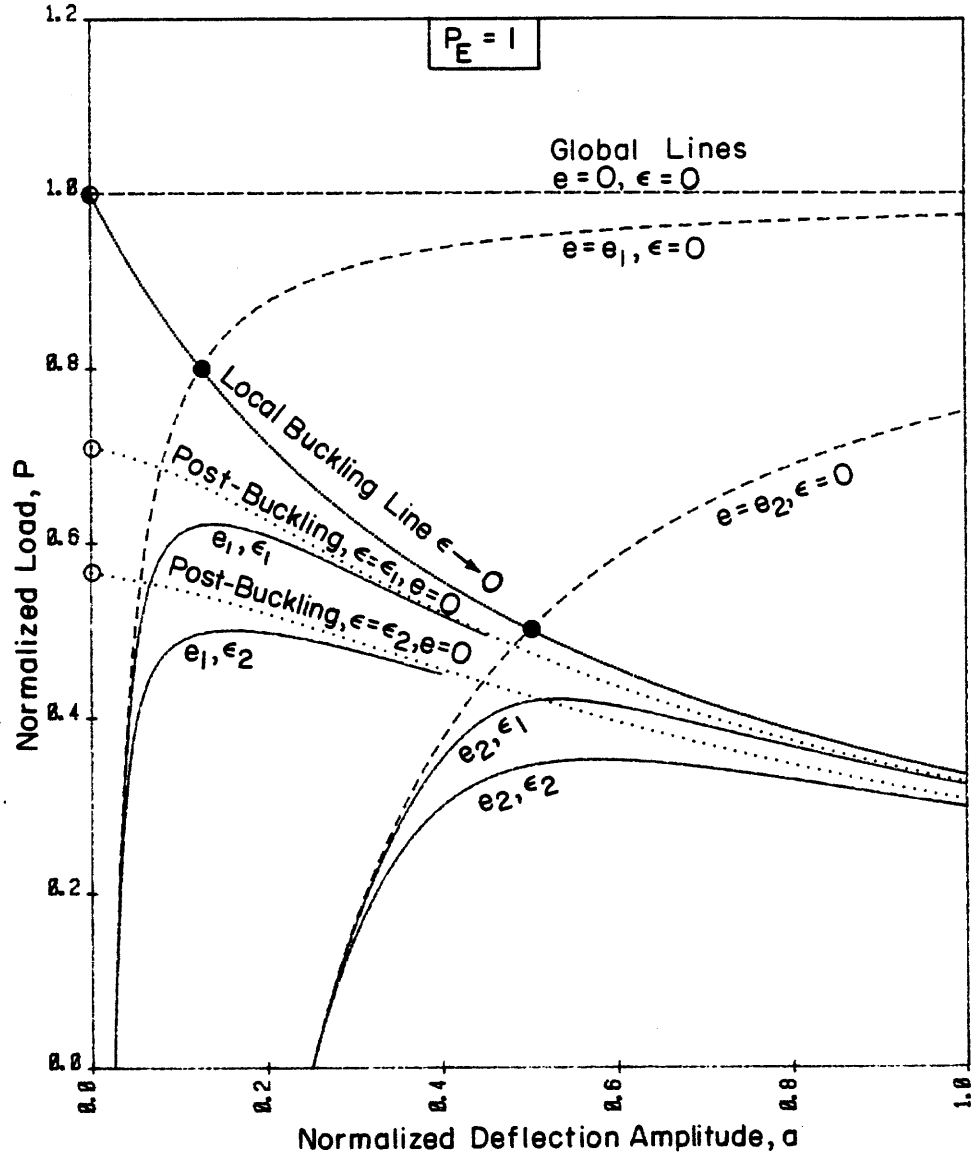

Figure 3-11b. Typical equilibrium paths of the doubly-imperfect ideal column for $P_E = 1$.
$\varepsilon_1 = 0.10$, $\varepsilon_2 = 0.25$; $e_1 = 0.025$, $e_2 = 0.25$.
○ First Bifurcation, ● Second Bifurcation.

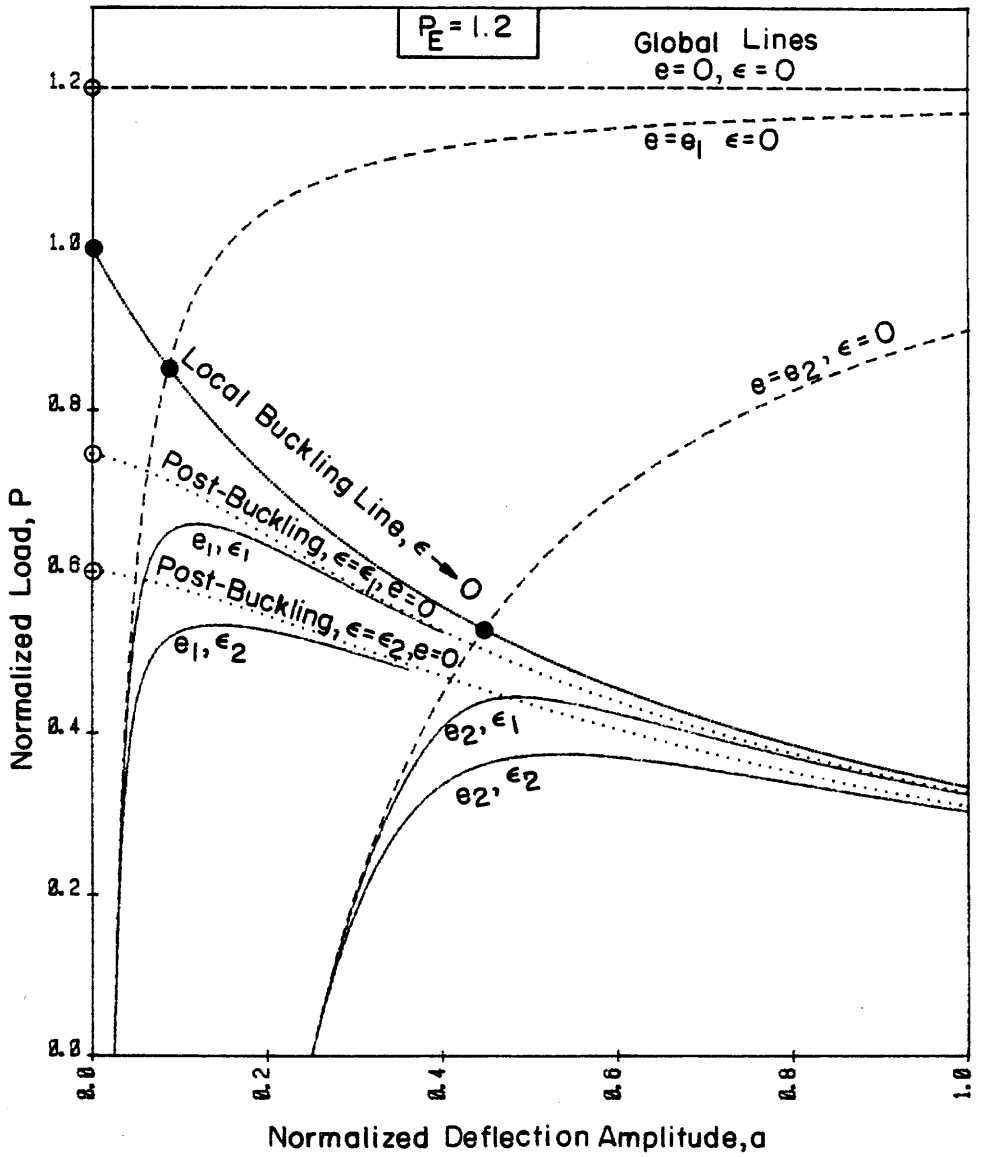

Figure 3-11c. Typical equilibrium paths of the doubly-imperfect ideal column for $P_E > 1$.
$\varepsilon_1 = 0.10$, $\varepsilon_2 = 0.25$; $e_1 = 0.025$, $e_2 = 0.25$.
○ First Bifurcation, ● Second Bifurcation.

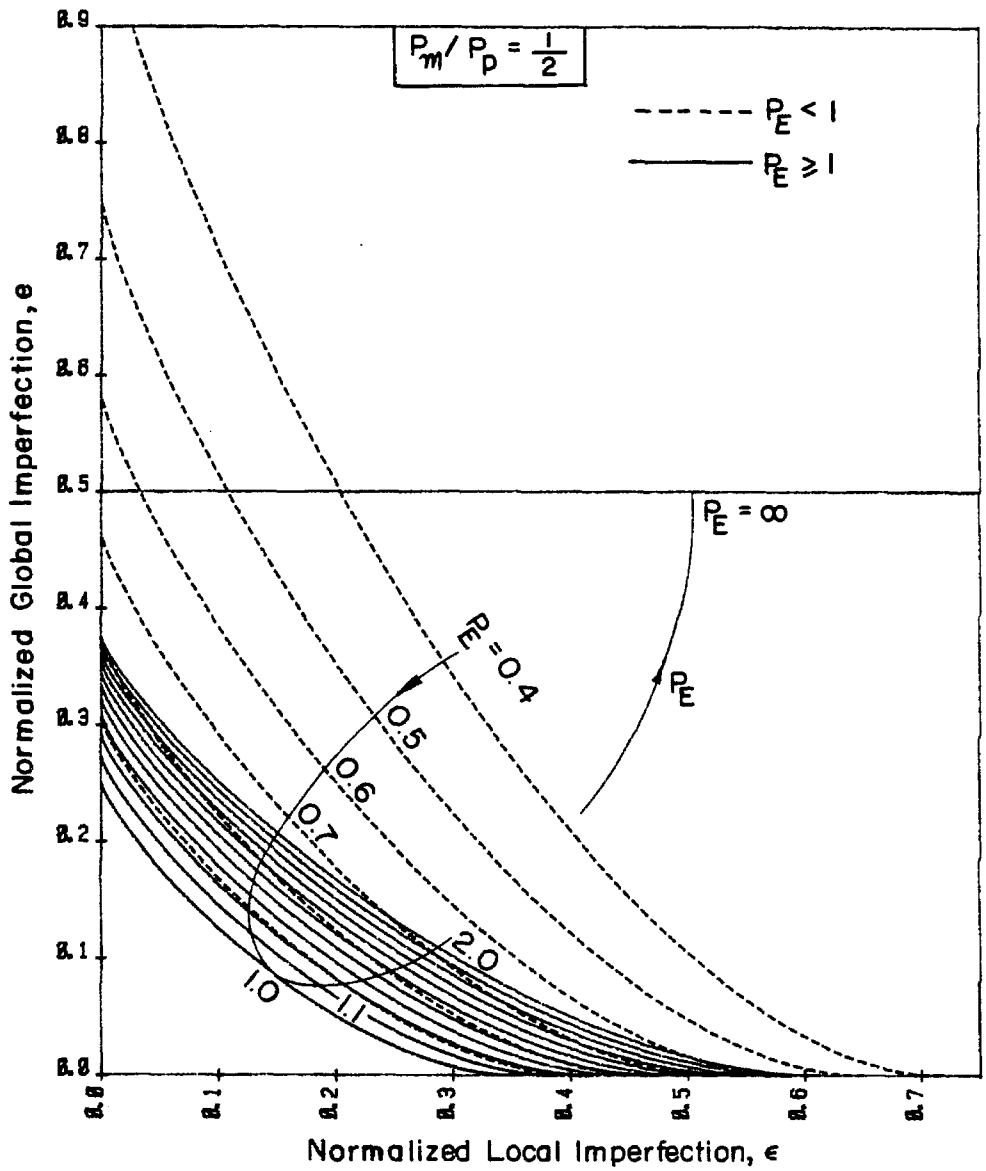

Figure 3-12. Overall imperfection-sensitivity chart. Combinations of local and global imperfections that reduce the normalized ultimate load-carrying capacity P_m to half the normalized nominal load P_p. ($P_p = P_E$ for $P_E < 1$ and 1 for $P_E \geq 1$.)

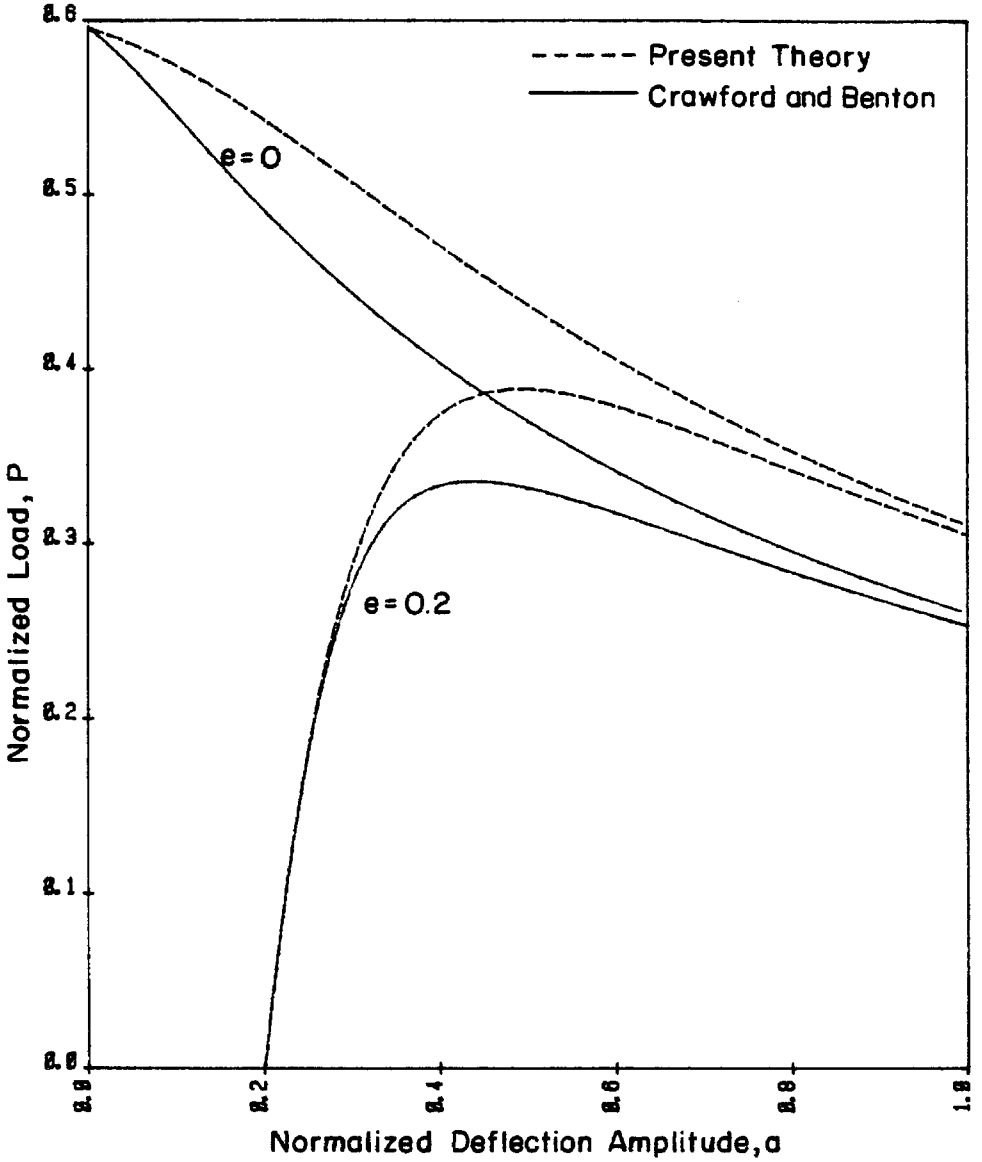

Figure 3-13. Comparison of results with Crawford and Benton [33]. Typical post-buckling (e = 0) and equilibrium (e = 0.2) paths. $\varepsilon = 0.3/\sqrt{2}$, $P_E = 1$.

4. THE UNDEFLECTED AND SLIGHTLY DEFLECTED GENERAL COLUMN

We now leave the ideal column and return to the general problem. In this chapter we focus on the behavior of the column when it is deflected -- imperfection deflections included -- only slightly or not at all. Higher deflection domains will be dealt with in subsequent chapters. The problems we address here are the prebuckling behavior, diagonal slackening and local buckling in the absence of deflection, global buckling and initial post buckling and small global imperfection sensitivity. The approach to the slightly-deflected cases will be one of perturbations applied directly to the displacement differential equations.

Whenever use of displacement differential equations is required, region I system will be used. Consequently, results such as the global buckling load will lack validity if the slackening load turns out to be lower than that result. This is no handicap because in that case slackening and not buckling is the failure mode. Practically, one has to calculate the buckling load as if there were no slackening, and the slackening load as if there were no buckling, and then decide as to what actually happens by comparing the loads and choosing the lower one. Except for local buckling we do not intend to study post-slackening phenomena in this chapter; these are left to Chapter 7.

4.1 The Globally-Perfect Prebuckling Solution

It is easily verified that in the absence of global imperfections

$$u' = u'^{(o)} = \text{const.}, \quad \vartheta = \gamma = w = 0,$$

is a valid solution of eqns. (2.37) satisfying the boundary conditions (2.44). For obvious reasons this solution will be referred to as the *prebuckling solution*. The value of $u'^{(o)}$ can be obtained from (2.37b,e,f). For this purpose, as well as for others, it is convenient to define the *mean longeron force*, $\bar{p}$, as follows

$$\bar{p} \equiv (p_{11} + 2p_{22})/3. \tag{4.1}$$

When calculated from (2.37e,f) $\bar{p}$ is found to be

$$\bar{p} = P + p_o + 4\kappa P_E(u' - u_o'). \tag{4.2}$$

It is interesting that $\bar{p}$ is independent of any displacement but u'. Thus it can serve, and wherever convenient will serve, as a u' replacement-unknown. In the prebuckled configuration $p_{11} = p_{22} = \bar{p}(\text{prebuckling}) \equiv \bar{p}^{(o)}$ and with the help of (4.2) we can summarize the prebuckling solution as follows:

$$\vartheta^{(o)} = \gamma^{(o)} = w^{(o)} = 0, \tag{4.3a}$$

$$(1 + 2\kappa)(\bar{p}^{(o)} - p_o) - P + \kappa\varepsilon^2 \left[\frac{1}{(1 - \bar{p}^{(o)})^2} - \frac{1}{(1 - p_o)^2} \right] = 0, \tag{4.3b}$$

$$u'^{(o)} = -\frac{1}{4\kappa P_E}(P - \bar{p}^{(o)} + p_o). \tag{4.3c}$$

Equation (4.3b) has to be solved (usually numerically) for $\bar{p}^{(o)}$ and then $u'^{(o)}$ can be determined from (4.3c). Whenever deflection vanishes $\bar{p} = \bar{p}^{(o)}$. In such cases we will omit, for notational convenience, the order index (o) from $\bar{p}^{(o)}$ trusting that no confusion will arise.

The $\bar{p}$–P plane turns out to be a highly useful instrument for the description of occurrences in the undeflected column. The prebuckling solution can be represented as a line in this plane, corresponding to eqn. (4.3b). This line is shown in Figure 4-1 and is referred to as the 'equilibrium line'. In Figure 4-1 we note the following features:

1. The equilibrium relation, eqn.(4.3b), is represented by the indicated partially heavy, partially dashed-heavy line. This line originates at $(p_o, 0)$ and goes to infinity as $\bar{p} \to 1$. As $\varepsilon \to 0$ it approaches dashed-line segments '1' and '2'. These segments intersect at the 'P* point', (1,P*), where

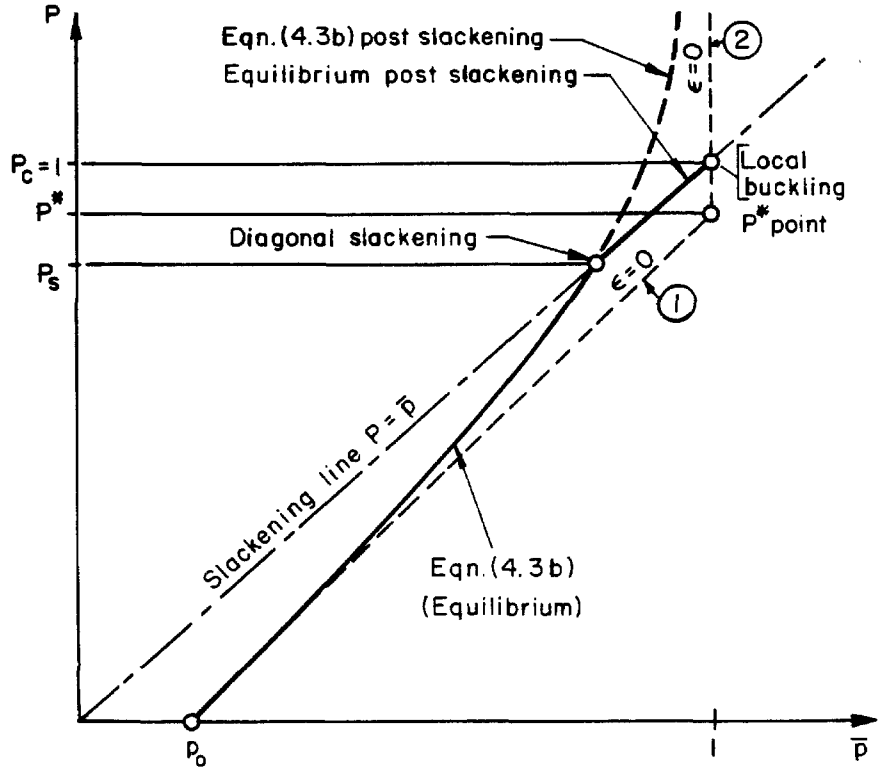

Figure 4-1. The undeflected column in the $\bar{p}$–P plane (qualitative).

$$P^* \equiv (1+2\kappa)(1-p_o). \tag{4.4a}$$

2. The locus $P = \bar{p}$ -- where the external load and the internal longeron force become equal -- clearly corresponds to the vanishing of the diagonal forces, i.e., to diagonal slackening. It is referred to in Figure 4-1 as the 'slackening line'. Any point in the $\bar{p}$–P plane located above this line implies the diagonals are in compression, and therefore is a physically invalid point.

3. The line representing eqn. (4.3b) crosses the slackening line at the 'diagonal slackening point', the value of P at which is P_s. Clearly, diagonal slackening constitutes, under the present circumstances, a mode of failure of the column. P_s is analyzed in detail in Section 4.2, yet an immediate result evident from Figure 4-1 is that $P_s \leq 1$.

4. Eqn. (4.3b), derived for taut diagonals, breaks down upon slackening of these diagonals. Clearly, the post-slackening relation between $\bar{p}$ and P is simply $P=\bar{p}$. Thus the dashed-heavy portion of the corresponding line in Figure 4-1 no longer represents equilibrium and must be replaced by the heavy segment *lying on the slackening line.*

5. Local buckling must lie on the intersection of equilibrium and $\bar{p}=1$. One sees immediately, on the basis of the foregoing discussion, that ***regardless of*** ε the value of P at local buckling (denoted formerly by P_c) is 1, ***same as in the ideal column.*** From (3) and (5) it follows immediately that ***slackening precedes local buckling:***

$$P_s \leq P_c(a=0)=1\ . \tag{4.4b}$$

6. For $\varepsilon=0$ the intersection representing slackening is between the slackening line and either of dashed-line segments '1' or '2', depending on whether $P^*>1$ or not. Thus, for the perfect column

$$P_s = \min(1,\ 1+\frac{1-P^*}{2\kappa})\ . \tag{4.4c}$$

7. If $\varepsilon=0$ the intersection between segment '2' and $\bar{p}=1$, representing local buckling, becomes indeterminate. It follows from (5), however, that by taking ε to zero through a limit process we must find

$$P_c=1 \tag{4.4d}$$

for the perfect column as well. Indeed, a point on segment '2' between P^* and $P=1$ represents a ***stable*** equilibrium because any increase in P can be absorbed by unloading the diagonals; no increase in $\bar{p}$ beyond 1 is required.

The post-slackening situation described in Figure 4-1, namely $P=\bar{p}$, is strictly correct only inasmuch as the column, now lacking any shear resistance, is somehow prevented from undergoing shear or out-of-plane deformations. As

shown later (Chapter 7) the actual post-slackening deformation includes twist. It turns out, however, that *to* $o(h)$ *accuracy* the relation $P=\bar{p}$ still holds. Therefore, Figure 4-1 and all the results derived from it describe the actual post-slackening situation accurately-enough.

4.2 Slackening of the Undeflected Column

In the last section we already derived some qualitative (eqn. (4.4b)) and perfect-column (eqn. 4.4c) slackening results. We now turn to the complete title problem. The slackening point is obtained, according to Figure 4-1, from intersecting eqn. (4.3b) with the slackening condition $P=\bar{p}$:

$$\frac{\varepsilon^2/2}{(1-P_s)^2}-(1-P_s)=C_s \tag{4.5}$$

where C_s, the *slackening parameter* is given by

$$C_s \equiv C_s^o + \frac{\varepsilon^2/2}{(1-p_o)^2} \tag{4.6a}$$

$$C_s^o \equiv (1+2\kappa)\frac{p_o}{2\kappa}-1=\frac{1-P^*}{2\kappa} \tag{4.6b}$$

and P^* is given by (4.4a).

By multiplying (4.5) through by $(1-P_s)^2$ and then letting $\varepsilon=0$ the solution (4.4c) is obtained. If $\varepsilon>0$ yet very small it is still possible to obtain an easy closed-form solution of (4.5), using a perturbation procedure around (4.4c). In this way we get

$$P_s\sim 1-\sqrt{\frac{\kappa}{1-P^*}}\varepsilon, \qquad 0<(1-P^*)/2\kappa=O(1); \tag{4.7a}$$

$$P_s\sim 1-2^{-1/\beta}\varepsilon^{2/\beta}, \qquad |1-P^*|/2\kappa=o(\varepsilon); \tag{4.7b}$$

$$P_s\sim 1-\frac{P^*-1}{2\kappa}-\left(\frac{2\kappa}{P^*-1}\right)^2\frac{\varepsilon^2}{2}, \qquad 0<(P^*-1)/2\kappa=O(1). \tag{4.7c}$$

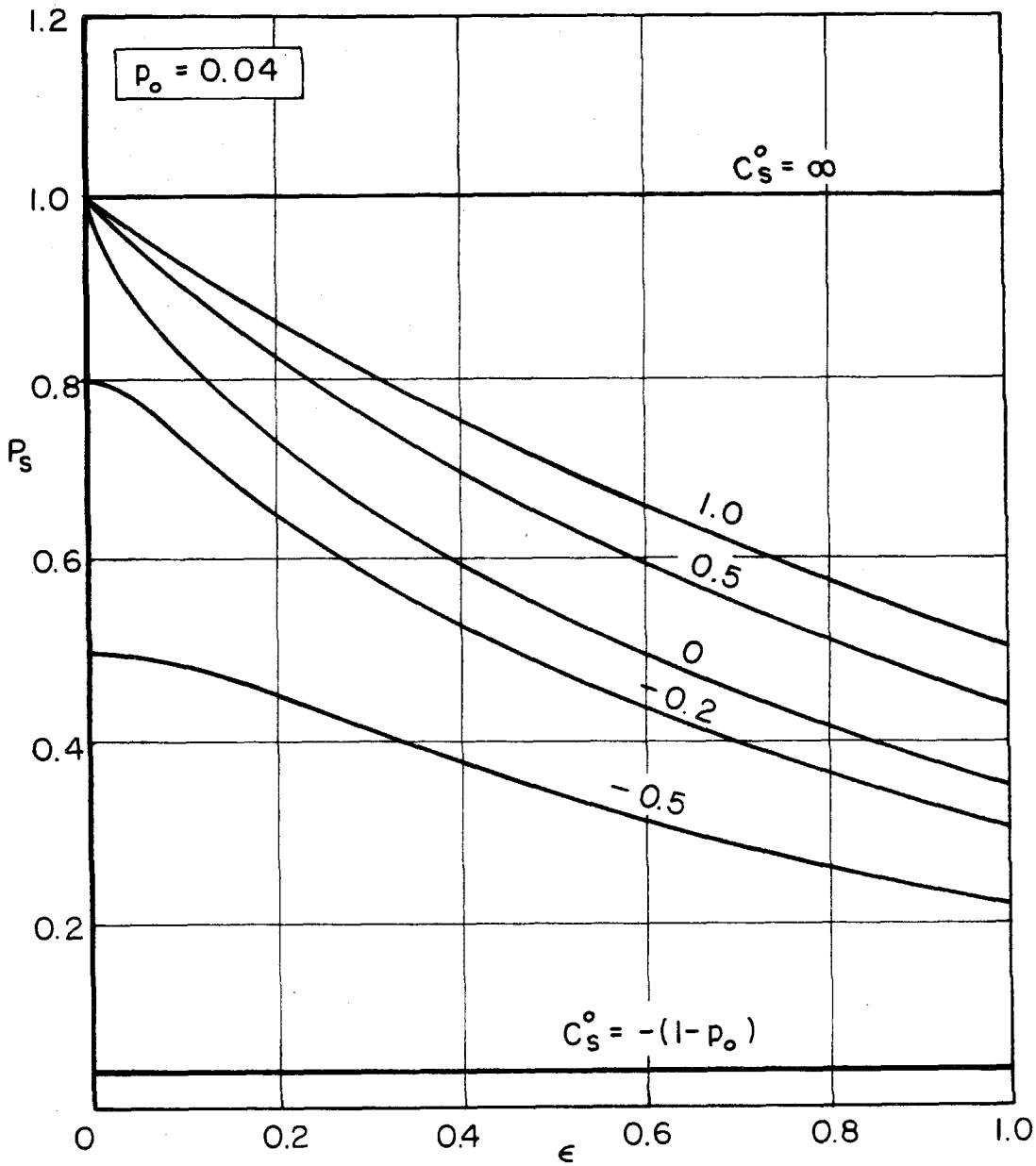

Figure 4-2. The slackening load as function of ε and C_s^o.

These are the *slackening imperfection-sensitivity power-laws*. They are seen to be less severe than those of the ideal-column global buckling, eqns (3.14). Note the increased sensitivity as $P^* \to 1$. This is of special interest since $P^* = 1$ will turn out (Section 4.4) to be an *optimal* choice. Here too, optimization is accompanied by increased imperfection sensitivity.

Numerical results of P_s for a range of ε and $C_s^o = (1 - P^*)/2\kappa$ are shown graphically in Figure 4-2. In this graph p_o is held constant $= 0.04$ and only ε and κ change, the latter from o to ∞. The general similarity to Figure 3-3a is striking indeed.

4.3 Perturbation Equations for the Globally-Perfect Case

We now use a perturbation scheme to find a solution different from (4.3), yet in its immediate vicinity, which satisfies equations (2.37) and boundary conditions (2.44). The condition for its existence will provide us with the first bifurcation point. We are interested also in the initial post-buckling behavior and this dictates that second order terms be retained in the perturbation series. Since the solution (4.3) is characterized by a zero transverse deflection we will choose a, the deflection amplitude, as the measure of deviation of the perturbed solution from the prebuckling one. We thus write the sought solution as perturbation series, asymptotic as $a \to 0$

$$\left.\begin{aligned} u' &\sim u'^{(o)}(a) + u'^{(1)}(a) + u'^{(2)}(a), \\ \vartheta &\sim \vartheta^{(o)}(a) + \vartheta^{(1)}(a) + \vartheta^{(2)}(a), \\ \gamma &\sim \gamma^{(o)}(a) + \gamma^{(1)}(a) + \gamma^{(2)}(a), \\ w &\sim w^{(o)}(a) + w^{(1)}(a) + w^{(2)}(a), \\ \bar{p} &\sim \bar{p}^{(o)}(a) + \bar{p}^{(1)}(a) + \bar{p}^{(2)}(a), \end{aligned}\right\} \qquad (4.8a\text{-}e)$$

where the bracketed superscripts indicate the order of a term in the sense (e.g)

$$w^{(n)}(\alpha a) = \alpha^n w^{(n)}(a).$$

The zeroth order terms in (4.8 a-e) are those given by equations (4.3). We now proceed to derive the higher order equations. First we note

$$\left.\begin{aligned} p_{11} &\sim \bar{p}^{(o)} + p_{11}^{(1)} + p_{11}^{(2)}, \\ p_{22} &\sim \bar{p}^{(o)} + p_{22}^{(1)} + p_{22}^{(2)}. \end{aligned}\right\} \qquad (4.8f,g)$$

Substituting equations (4.8) into (2.37a-d), expanding the non-linear terms in the latter in Taylor series around their zeroth-order values and retaining terms up to second order we obtain

$$P_E\left(1+\frac{\kappa}{2}\right)(\vartheta'^{(1)} + \vartheta'^{(2)}) + P(w'^{(1)} + w'^{(2)}) + \frac{\varepsilon^2/3}{(1-\bar{p}^{(o)})^3}[(p_{11}^{(1)} - p_{22}^{(1)}) + (p_{11}^{(2)} - p_{22}^{(2)})]$$

$$+ \frac{\varepsilon^2/4}{(1-\bar{p}^{(o)})^4}(p_{11}^{(1)\,2} - p_{22}^{(1)\,2}) = 0, \qquad (4.9a)$$

$$2P_E(1+2\kappa)(u'^{(1)} + u'^{(2)}) + \frac{\varepsilon^2/3}{(1-\bar{p}^{(o)})^3}[(p_{11}^{(1)} + 2p_{22}^{(1)}) + (p_{11}^{(2)} + 2p_{22}^{(2)})]$$

$$+ \frac{\varepsilon^2/2}{(1-\bar{p}^{(o)})^4}(p_{11}^{(1)\,2} + 2p_{22}^{(1)\,2}) = 0, \qquad (4.9b)$$

$$4\kappa P_E(\gamma^{(1)} + \gamma^{(2)}) - \nu P(w'^{(1)} + w'^{(2)}) = 0, \qquad (4.9c)$$

$$(\vartheta^{(1)} + \vartheta^{(2)}) + \frac{2}{3}\lambda(\gamma^{(1)} + \gamma^{(2)}) - (w'^{(1)} + w'^{(2)}) = 0. \qquad (4.9d)$$

In deriving equations (4.9) we have used the fact that the zeroth order terms satisfy equations (4.3) in order to eliminate them from the system.

Upon departing from the prebuckling solution at the first bifurcation point $P=P_b$, P is expected to vary. At the same time $\bar{p}^{(o)}$, dependent on P through (4.3b), will vary too. We thus express them both[1] by perturbation series around their bifurcation-point values.

$$\left.\begin{aligned} P &\sim P_b + P^{(1)}, \\ \bar{p}^{(o)} &\sim \bar{p}_b + \bar{p}^{(01)}. \end{aligned}\right\} \qquad (4.10a,b)$$

By perturbing (4.3b) we obtain

$$(1+2\kappa)(\bar{p}_b - p_o) - P_b + \kappa\varepsilon^2\left[\frac{1}{(1-\bar{p}_b)^2} - \frac{1}{(1-p_o)^2}\right] = 0, \qquad (4.11a)$$

$$\bar{p}^{(01)} = \frac{P^{(1)}}{1+2\kappa\left(1+\dfrac{\varepsilon^2}{(1-\bar{p}_b)^3}\right)}. \qquad (4.11b)$$

The first is an implicit expression for the longeron force at buckling whereas the second allows us to write (retaining only needed orders)

$$\frac{1}{(1-\bar{p}^{(o)})^3} \sim \frac{1}{(1-\bar{p}_b)^3} + \frac{3P^{(1)}}{(1+2\kappa)(1-\bar{p}_b)^4 + 2\kappa\varepsilon^2(1-\bar{p}_b)}, \qquad (4.12a)$$

$$\frac{1}{(1-\bar{p}^{(o)})^4} \sim \frac{1}{(1-\bar{p}_b)^4}. \qquad (4.12b)$$

We need also expressions for $p_{mm}^{(j)}$. These we obtain from (2.37e,f) after substituting in them from (4.8a) and (4.10) and forming expressions of homogeneous order

1. The necessity of perturbing $\bar{p}^{(o)}$ along with P can be understood if one imagines replacing it in equations (4.9a,b) by a P-dependent expression obtainable, in principle, from (4.3b).

$$\left.\begin{aligned}
p_{11}^{(1)} &= 2P_b\ w^{(1)} + 4\kappa P_E u'^{(1)} + \kappa P_E \vartheta'^{(1)},\\
p_{22}^{(1)} &= -P_b\ w^{(1)} - 4\kappa P_E u'^{(1)} - \frac{\kappa}{2} P_E \vartheta'^{(1)},\\
p_{11}^{(2)} &= 2P^{(1)}w^{(1)} + 2P_b w^{(2)} + 4\kappa P_E u'^{(2)} + \kappa P_E \vartheta'^{(2)},\\
p_{22}^{(2)} &= -P^{(1)}w^{(1)} - P_b w^{(2)} + 4\kappa P_E u'^{(2)} - \frac{\kappa}{2} P_E \vartheta'^{(2)}.
\end{aligned}\right\} \qquad (4.13a\text{-}d)$$

Substituting equations (4.12) and (4.13) into (4.9) and requiring that the latter be satisfied regardless of a we obtain two systems of linear differential equations, one for each perturbation order, the unknowns of which are the perturbation displacements:

FIRST-ORDER EQUATIONS:

$$\left.\begin{aligned}
&P_E[\,1 + \frac{\kappa}{2}(1 + \frac{\varepsilon^2}{(1-\bar{p}_b)^3})\,]\vartheta'^{(1)} + P_b(1 + \frac{\varepsilon^2}{(1-\bar{p}_b)^3})w^{(1)} = 0,\\
&u'^{(1)} = 0,\\
&4\kappa P_E \gamma^{(1)} - \lambda P_b w'^{(1)} = 0,\\
&\vartheta^{(1)} + \frac{2}{3}\lambda\gamma^{(1)} - w'^{(1)} = 0.
\end{aligned}\right\} \qquad (4.14a\text{-}d)$$

SECOND-ORDER EQUATIONS:[2]

$$P_E[\,1 + \frac{\kappa}{2}(1 + \frac{\varepsilon^2}{(1-\bar{p}_b)^3})\,]\vartheta'^{(2)} + P_b(1 + \frac{\varepsilon^2}{(1-\bar{p}_b)^3})w^{(2)} =$$

$$-(1 + \frac{\varepsilon^2}{(1-\bar{p}_b)^3})\,w^{(1)}p^{(1)} + \qquad (4.15a)$$

$$-\frac{3\varepsilon^2}{(1-\bar{p}_b)^4}\Big[\frac{P^{(1)}}{1 + 2\kappa(1 + \frac{\varepsilon^2}{(1-\bar{p}_b)^3})}(P_b w^{(1)} + \frac{\kappa}{2}P_E\vartheta'^{(1)}) + \frac{1}{2}(P_b w^{(1)} + \frac{\kappa}{2}P_E\vartheta'^{(1)})^2\Big],$$

2. Here $u'^{(1)}$ is omitted according to (4.14b).

$$2P_E[\,1+2\kappa(1+\frac{\varepsilon^2}{(1-\bar{p}_b)^3})]\,u'^{(2)} = -\frac{3\varepsilon^2}{(1-\bar{p}_b)^4}(P_b w^{(1)} + \frac{\kappa}{2}P_E \vartheta'^{(1)})^2, \tag{4.15b}$$

$$4\kappa P_E \gamma^{(2)} - \lambda P_b w'^{(2)} = \lambda P^{(1)} w'^{(1)}, \tag{4.15c}$$

$$\vartheta^{(2)} + \frac{2}{3}\lambda\gamma^{(2)} - w'^{(2)} = 0. \tag{4.15d}$$

As usual in perturbation methods one first solves (4.14) for the first-order perturbations and then uses the results in (4.15) to solve for the second-order ones. The boundary conditions (2.44) should be satisfied by all orders. Note the frequent occurrence of the combination $1+\varepsilon^2/(1-\bar{p}_b)^3$ which, by (2.15b), is nothing but (E/E_t) evaluated at the bifurcation point.

4.4 First Bifurcation, Global Buckling

The behavior at the first bifurcation point is obtained from solving the first order equations (4.14) subject to the boundary conditions (2.44). The system (4.14) can easily be decoupled, resulting in

$$P_E[\,1+\frac{\kappa}{2}(1+\frac{\varepsilon^2}{(1-\bar{p}_b)^3})\,](1-\nu\frac{P_b}{P_E})w''^{(1)} + P_b(1+\frac{\varepsilon^2}{(1-\bar{p}_b)^3})w^{(1)} = 0, \tag{4.16a}$$

$$\vartheta^{(1)} = (1-\nu\frac{P_b}{P_E})\,w'^{(1)}, \tag{4.16b}$$

$$\gamma^{(1)} = \frac{\lambda}{4\kappa}\frac{P_b}{P_E}w'^{(1)} = \frac{3}{2}(\frac{\nu}{\lambda})\frac{P_b}{P_E}w'^{(1)}, \tag{4.16c}$$

where ν is the shear compliance parameter defined by (2.41c).

Only if the coefficients of (4.16a) are equal is a half-wave non-trivial solution possible. This condition gives us the ***global buckling load*** P_b:

$$P_b = \frac{P_E[\,1+\frac{\kappa}{2}(1+\frac{\varepsilon^2}{(1-\bar{p}_b)^3})\,]}{\nu+(1+\frac{\lambda^2}{12})(1+\frac{\varepsilon^2}{(1-\bar{p}_b)^3})} = \frac{P_E[\,1+\frac{\kappa}{2}(1+\frac{\varepsilon^2}{(1-\bar{p}_b)^3})\,]}{\nu+(1+\frac{\varepsilon^2}{(1-\bar{p}_b)^3})}. \tag{4.17}$$

Eqn. (4.17) satisfied, the fundamental initial global buckling mode is seen immediately to be

$$u'^{(1)} = 0, \tag{4.18a}$$

$$w^{(1)} = a \sin x, \tag{4.18b}$$

$$\vartheta^{(1)} = a\left(1 - \nu \frac{P_b}{P_E}\right) \cos x, \tag{4.18c}$$

$$\gamma^{(1)} = a \frac{\lambda}{4\kappa}\left(\frac{P_b}{P_E}\right) \cos x, \quad \left(\frac{\lambda}{4\kappa} \equiv \frac{3}{2}\frac{\nu}{\lambda}\right). \tag{4.18d}$$

Before we proceed any further the following should be noted:

1. By (4.18a) no change occurs upon buckling in the axial compression u'.

2. The deflection constituent of the global mode, eqn. (4.18b), is seen to be identical with that of the ideal column, eqn. (3.13a).

3. In contrast to the ideal case the present global mode is seen to contain some shear deformation, eqn. (4.18d). Its magnitude relative to ϑ and w' is $(2/3)\lambda\gamma = (\nu P_b/P_E)w'$, an $o(h)$ quantity.[3] Taking $\nu = 0$ removes this shear deformation. Recall the role of ν, discussed in Section 3.1, as a shear compliance parameter.

4. Eqn. (4.17) is the counterpart of the ideal case eqn. (3.13b). It reduces to the latter upon setting $\nu = 0$, $\kappa = 0$, $\bar{p}_b = P_b$.

5. At global buckling the quantity $1 + \varepsilon^2/(1-\bar{p}_b)^3$ is of $o(1)$. This can be seen by isolating it from (4.17):

3. Recall that γ was normalized so as to be of $o(1)$. Hence, for purposes of comparison with ϑ and w', the quantity $(2/3)\lambda\gamma$, rather than γ itself, should be used. See, e.g., eqn. (2.37d).

$$1+\frac{\varepsilon^2}{(1-\bar{p}_b)^3}=\frac{P_E-\nu P_b}{P_b-(\kappa/2)P_E}. \tag{4.19}$$

It follows that $(\varepsilon^2/2)/(1-\bar{p}_b)^2$ must also be of $o(1)$, thus satisfying (2.16).

For obtaining P_b values eqn. (4.17) must be solved in conjunction with (4.11a). E.g., the right hand sides of (4.17) and (4.11a) are compared to obtain an equation for $\bar{p}_b$; the root is then substituted into either. Because of the algebraic complexity involved in this a numerical approach is, in general, a necessity.

The $\bar{p}$–P plane is highly useful also for the description of global buckling. Eqn. (4.17) -- subscript b omitted -- is represented by a line in this plane along which the bifurcation condition is met. We will call it the ***bifurcation line***. Its intersection with the *equilibrium line* (4.3b) satisfies (4.17) as well as (4.11a) and thus represents global buckling. Figure 4-3 contains the features that appeared already in Figure 4-1 plus those added for global buckling representation.

From examining eqn. (4.17), the corresponding bifurcation line and its interaction with the equilibrium line we learn the following:

1. The bifurcation condition is represented by the indicated heavy line. Regardless of ε this line has a minimum at $(1, (\kappa/2)P_E)$. As $\varepsilon \to 0$ it approaches the dashed-line segments numbered '3' and '4'. Dashed-line '3' intercepts the P axis at $P = P_E^*$, where

$$P_E^* \equiv \frac{1+\kappa/2}{1+\nu+\lambda^2/12}P_E = \frac{1+\kappa/2}{1+\nu}P_E. \tag{4.20a}$$

2. For $\varepsilon = 0$ and $P_E^* < P^*$ the intersection representing global buckling is between dashed-line segments '1' and '3'. Clearly then $P_b = P_E^*$. On the other hand, if $P_E^* > P^*$, we have an intersection between segments '3' and '2', (an overlap between '2' and '4') and another intersection between '4' and '1'. A closer look (see Section 4.4.1) reveals the correct intersection is the latter, i.e.

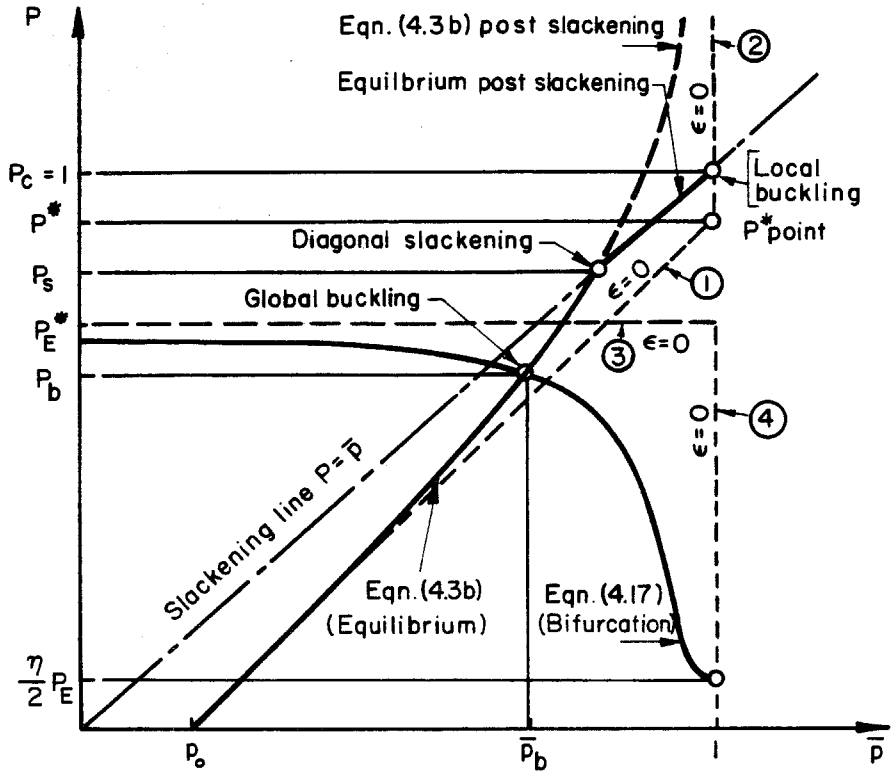

Figure 4-3. Global buckling added to the $\bar{p}$–P plane (qualitative).

$P_b = P^*$. This can also be inferred from the corresponding ideal column results. The actual buckling load must be taken as the lowest:

$$P_b = \min(P_E^*, P^*). \tag{4.20b}$$

Eqn. (4.20b) unfolds a situation which is perfectly analogous to that of the ideal case (see Section 3.8.1) provided P_E^* and P^* are regarded as replacements for P_E and $P = 1$ respectively. P_E^* is seen to be the global (Euler) buckling load of the perfect (non-ideal) column. The analogy of P^* to '1' is somewhat more complicated: in the ideal case $P = 1$ is P_c(perfect), a degeneracy which is resolved in the non-ideal case. It is only in its capacity as a potential P_b that '1' is replaced by

P^*. We have seen (eqn. (4.4b)) that P_c is unchanged in going from the ideal case to the general one.

From eqns (4.20a) and (4.4a) it is seen that P_E^* and P^* differ from their ideal values by two $o(h)$ influences of opposing nature each. Both are increased due to the increase in column cross section stiffeness brought about by the diagonals. P_E^* is decreased by the shear compliance, represented by ν, whereas P^* is decreased because of p_o.

Another conclusion we can draw from (4.20b) and (4.4c) is that as long as P^* is chosen less than 1 the perfect column buckles globally before it slackens.

If slackening is considered, from an engineering standpoint, as a mode of failure (we shall see in Chapter 7 that post slackening loads are higher than P_s) we can summarize the maximum strength of the ***perfect, non-ideal*** column as follows (see (4.4c) and (4.20b)):

$$P_m = \min\left(P_E^*,\ P^*,\ 1+\frac{1-P^*}{2\kappa},\ 1\right). \tag{4.20c}$$

It is important to realize that the choice of P^*, as well as that of P_E^*, may directly translate to column strength. From (4.20c) it is seen that -- imperfection-sensitivity considerations aside -- the optimal value of P^* is 1. Recall (eqns. (4.7)) that this optimization produces a maximal slackening imperfection-sensitivity.

4.4.1 Global Buckling Load -- Local Imperfection Sensitivity: So far we have discussed only cases of $\varepsilon = 0$. For $\varepsilon \neq 0$ equating (4.17) and (4.11a) results in a 6th-order polynomial equation for $(1-\bar{p}_b)$, requiring a numerical treatment. This is done in Section 4.4.2. If, however, ε is vanishingly small, a perturbation solution of this polynomial equation is possible. The root $(1-\bar{p}_b)$ can then be substituted in either (4.17) or (4.11a) to give the following asymptotic local-imperfection-sensitivity power laws:

$$P_b \sim P_E^* - \left[\frac{1+2\kappa}{P^*-P_E^*}\right]^3 P_E^* - (\kappa/2)\frac{P_E}{1+\nu}\varepsilon^2, \qquad 0<(P^*-P_E^*)=o(1); \quad (4.21a)$$

$$P_b \sim P^* - \left[\frac{P^*-(\kappa/2)P_E}{(1+2\kappa)(1+\nu)}\right]^{\frac{1}{4}}(1+2\kappa)\varepsilon^{\frac{1}{2}}, \qquad |P^*-P_E^*|=o(\varepsilon); \quad (4.21b)$$

$$P_b \sim P^* - \left[\frac{P^*-(\kappa/2)P_E}{(P_E^*-P^*)(1+\nu)}\right]^{\frac{1}{3}}\left(1+2\kappa-\frac{\kappa(1+\nu)(P_E^*-P^*)}{P^*-(\kappa/2)P_E}\right)\varepsilon^{\frac{2}{3}}, \quad 0<(P_E^*-P^*)=o(1). \quad (4.21c)$$

These are the non-ideal counterparts of eqns. (3.14) and reduce to the latter upon letting $\nu=\kappa=0$, $P^*=1$, $P_E^*=P_E$. The powers of ε are seen to be the same as in the ideal case. The answer to the question whether the imperfection sensitivity in the general case is stronger or weaker is not clear-cut; it depends on the relative magnitudes of ν, κ, and p_o.

4.4.2 Global Buckling Load -- Numerical Results: Since it turns out that the global buckling load results do not differ radically from those of the ideal case the quantity of interest here is the relative change, $[P_b(\text{ideal})-P_b]/P_b(\text{ideal})$. Some numerical solutions expressed in this quantity of the system (4.17), (4.11a) are presented graphically in Figure 4-4.[4] The central design point (around which parameter variations are taken) in this figure is a 40-bay column ($\lambda=\pi/40$) with $P_E=1$, $\varepsilon=0.125$, $\nu=0.05$, $\kappa=0.02$ and $p_o=0.04$ ($P^* \cong 1$). The following are to be noted:

1. For reasonable values of ε and ν the deviation from the ideal case is of the order of a few percent. Hence the general behavior of the global buckling load with respect to changes in P_E and ε is still qualitatively that depicted in Figures 3-3.

2. At moderate ε values ($\varepsilon \cong 0.1$) and for low values of P_E the shear effect is seen to be dominant in the deviation from the ideal case. As the number of bays decreases (it takes 20 bays to make $\nu = 0.2$ while keeping κ the same)

4. It is in principle possible to obtain closed-form expression for this quantity treating κ, ν, and p_o as $o(h)$ perturbations around the ideal column. The expression thus obtained is, however, too complicated to be useful.

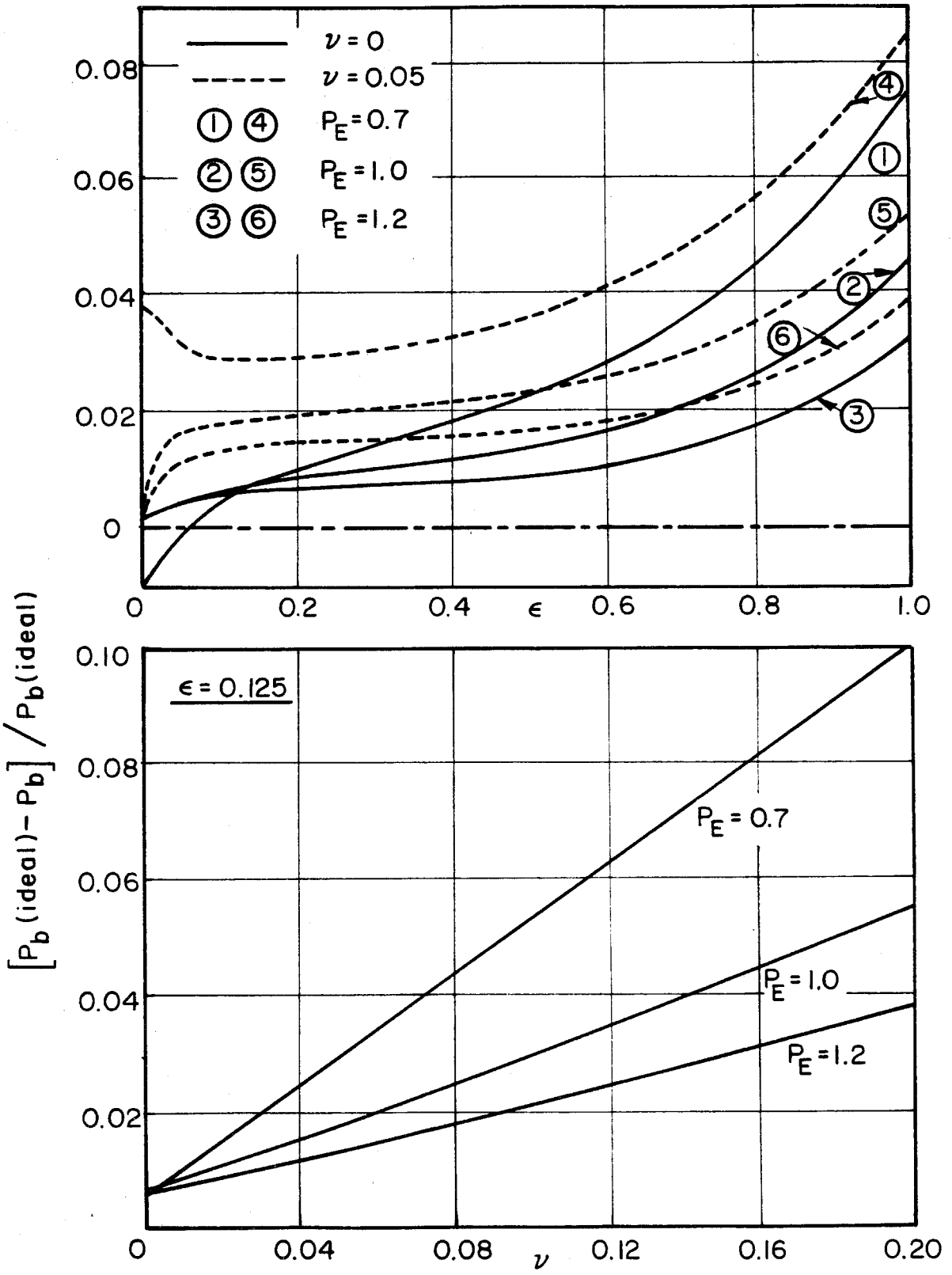

Figure 4-4. Effect of finite shear rigidity and coupling web on the global buckling load (κ=0.02, p_o=0.04.)

the deviation due to shear becomes by far the more important -- about 10% for $P_E = 0.7$.

3. The coupling-web effect is the deviation from the ideal case when the shear effect is inhibited, i.e., for $\nu = 0$. For moderate ε's it is in the vicinity of and not larger than 1%. It is striking that this effect can be negative. The reason is that for $P_E^* < P^*$ and small ε the only influence comes from the change in P_E^* and if $\nu = 0$ this change is always an increase.

4. By reducing κ and p_o in such a way that P^* remains constant it is possible to reduce further the coupling-web effect. This, however, will be accompanied by an increase in $\nu = \lambda^2/6\kappa$ and thereby, as expected, by a more shear-affected buckling load.

It should be noted that by taking here $P^* = 1$ an important source of deviation has been eliminated, thereby making the above picture too optimistic. For the P^* effect see the paragraph following eqn. (4.20c).

4.5 Initial Post-Buckling

The initial post-buckling behavior is obtained from solution of the second-order perturbation equations (4.15) subject to boundary conditions (2.44). The 1st order perturbations appearing in (4.15) are taken from the solution (4.18) and use is made of the fact that at $P = P_b$ the two coefficients of (4.16a) are equal. Again the system can easily be decoupled and neglecting $\lambda^2/12$ compared to 1 we obtain for bending

$$(1+\frac{\varepsilon^2}{(1-\bar{p}_b)^3})P_b(w''^{(2)}+w^{(2)}) =$$

$$-aP^{(1)}[\nu+(1+\frac{\varepsilon^2}{(1-\bar{p}_b)^3})+\frac{3\varepsilon^2/(1-\bar{p}_b)^4}{1+2\kappa(1+\frac{\varepsilon^2}{(1-\bar{p}_b)^3})}(P_b-\frac{\kappa}{2}P_E)]\sin x +$$

$$-a^2[\frac{(3/2)\varepsilon^2}{(1-\bar{p}_b)^4}(P_b-\frac{\kappa}{2}P_E)^2]\sin^2 x. \qquad (4.22)$$

Together with the boundary conditions this constitutes an eigenvalue problem for $P^{(1)}$, the solution of which is

$$P^{(1)} = -a\,\frac{\frac{4}{\pi}\frac{\varepsilon^2}{(1-\bar{p}_b)^4}(P_b-\frac{\kappa}{2}P_E)^2}{\nu+(1+\frac{\varepsilon^2}{(1-\bar{p}_b)^3})+\frac{3\varepsilon^2/(1-\bar{p}_b)^4}{1+2\kappa(1+\frac{\varepsilon^2}{(1-\bar{p}_b)^3})}(P_b-\frac{\kappa}{2}P_E)},^{5} \qquad (4.23a)$$

$$w^{(2)} = -a^2\,\frac{\frac{\varepsilon^2}{(1-\bar{p}_b)^4}(P_b-\frac{\kappa}{2}P_E)^2}{P_b(1+\frac{\varepsilon^2}{(1-\bar{p}_b)^3})}[\frac{2}{\pi}x\cos x+\frac{1}{2}(1-\cos x)^2]. \qquad (4.23b)$$

These are the counterparts of the ideal column eqns. (3.21) and, with some work, can be shown to agree with the latter upon setting $P_b=\bar{p}_b$, $\kappa=\nu=0$.

The shapes of the first two terms in the asymptotic expansion of $w(x)$ as $a\to 0$, namely, $w^{(1)}/\max(w^{(1)})$ and $w^{(2)}/\max(w^{(2)})$ are depicted in Figure 4-5. Since $w^{(1)}$ and $w^{(2)}$ differ in sign it is seen that $w^{(1)}+w^{(2)}$ is a more 'pointed' function than $w^{(1)}$ alone, in agreement with the general picture of Figure 3-6.

4.6 Global-Imperfection Sensitivity Near First Bifurcation

Having obtained the second order perturbation equation (4.22) it is now an easy matter to find how the behavior near the first bifurcation point is affected by introducing a slight amount of global imperfection resembling in all except

5. The limit $\varepsilon\to 0$ of this result is not valid. See remark (1) in Section 6.1.4.

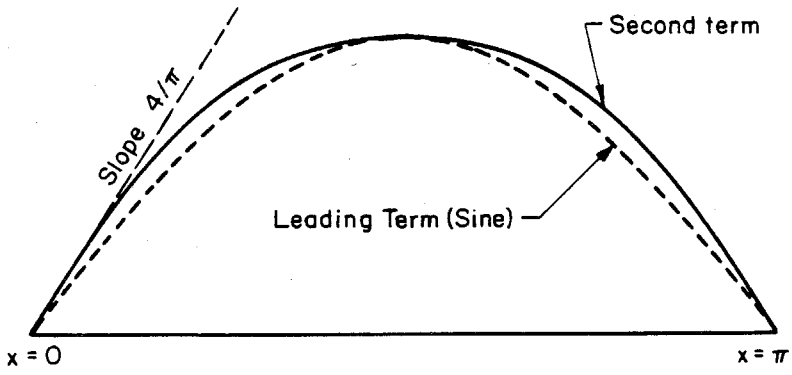

Figure 4-5. Shape of the first two terms in the expansion of w(x).

the amplitude the initial global buckling mode (4.18):

$$u_o' = 0\,, \tag{4.24a}$$

$$w_o = e \sin x\,, \tag{4.24b}$$

$$\vartheta_o = e(1 - \nu \frac{P_b}{P_E}) \cos x\,, \tag{4.24c}$$

$$\gamma_o = e \frac{\lambda}{4\kappa} (\frac{P_b}{P_E}) \cos x\,. \tag{4.24d}$$

The imperfection parameter e is taken to be small -- small as necessary to make the derivation valid. (See, e.g., Budiansky [35].) It turns out that we must take e to be comparable to $||a||^2$, where $||a||$ is some norm of the a-range-of-interest, $||a||$ = a(P=maximum), say.

Upon introducing the above imperfection, terms $P_E(1+\kappa/2)\vartheta_o'$ and $4\kappa P_E \gamma_o$ will appear on the right hand sides of (4.9a) and (4.9c) respectively. Also, terms $-\kappa P_E \vartheta_o'$ and $-\kappa P_E \vartheta_o'/2$ will have to be added to the internal forces p_{11} and p_{22} respectively. [See equations (2.37)]. Now because the new terms are by

assumption of $o(\|a\|^2)$, the operation of grouping terms into expressions of homogeneous order will place them in the second-order expressions, with the result that the first-order equations (4.14) will remain unchanged. The second-order equations, on the other hand, will be modified and the right hand side of (4.22) will include an additional imperfection term

$$P_E[\,1+\frac{\kappa}{2}(1+\frac{\varepsilon^2}{(1-\bar{p}_b)^3})\,](\vartheta_o'+\frac{2}{3}\lambda\gamma_o) = -eP_E[\,1+\frac{\kappa}{2}(1+\frac{\varepsilon^2}{(1-\bar{p}_b)^3})\,]\sin x\,.$$

Instead of (4.23a) the eigenvalue problem will now result in

$$P^{(1)} = -\frac{a\frac{4}{\pi}\frac{\varepsilon^2}{(1-\bar{p}_b)^4}(P_b-\frac{\kappa}{2}P_E)^2+\frac{e}{a}P_E[\,1+\frac{\kappa}{2}(1+\frac{\varepsilon^2}{(1-\bar{p}_b)^3})\,]}{\nu+(1+\frac{\varepsilon^2}{(1-\bar{p}_b)^3})+\frac{3\varepsilon^2/(1-\bar{p}_b)^4}{1+2\kappa(1+\frac{\varepsilon^2}{(1-\bar{p}_b)^3})}(P_b-\frac{\kappa}{2}P_E)}. \qquad (4.25)$$

This is the *imperfect, asymptotic as* $e\to 0$ *and* $a=o(\sqrt{e})$, load-deflection relation. Evidently it is of homogeneous order and it has a maximum. Using substitutions from (4.19) and (4.20a) the location of this maximum can be written in the form

$$a(\max) = \frac{\sqrt{\pi\, e P_b(P_E^*-\frac{\kappa}{2}P_E)(1-\bar{p}_b)/(P_E^*-P_b)}}{2(P_b-\frac{\kappa}{2}P_E)}. \qquad (4.26)$$

From this it is seen that if either $(1-\bar{p}_b)=o(e)$ or $(P_E^*-P_b)=o(e)$ the location of the maximum is outside the region of validity. In the first case it is too small and e/a belongs in the first-order system; in the second case it is too large and a higher order post-buckling expansion is required. Both cases occur when ε is small and are distinguished by whether $P_E^*\geq P^*$ (first) or $P_E^* < P^*$ (second). Since proper expansions for these cases are not attempted here the validity of the results is accordingly restricted.

The value of the total load at the maximum is the strength P_m of the imperfect column. Again using substitutions from (4.19) and (4.20a) we obtain

$$P_m = P_b - \frac{4}{\sqrt{\pi}} \cdot \frac{\sqrt{e\,P_b(P_E^* - \frac{\kappa}{2}P_E)(P_E^* - P_b)/(1-\bar{p}_b)}}{1 + (P_E^* - P_b)\left[\frac{1}{P_b - \frac{\kappa}{2}P_E} + \frac{3}{(1-\bar{p}_b)\left[1 + 2\kappa\left(1 + \frac{\varepsilon^2}{(1-\bar{p}_b)^3}\right)\right]}\right]} \qquad (4.27)$$

It is important to note that this result by no means corresponds to eqns. (3.16) of the ideal column.[6] Besides ε being zero there, the bifurcation point itself is a different one.

4.7 Finite-Difference Derivation of the Buckling Load

In Section 2.8 it was mentioned that the magnitude of the de-discretization error is expected to be of $o(\lambda^2)$. Here we show that this is true for the linearized first order column equations (4.14). The approach is to solve the boundary-eigen-value problem using exact finite difference calculus and to compare the results with those of Section 4.4.

For notational simplicity we omit the order superscripts and define constants A,B,C such that eqns. (4.14a) and (4.16b) take the form

$$A\vartheta_i' + Bw_i = 0; \qquad (4.28a)$$

$$\vartheta_i - Cw_i' = 0; \qquad i = 1,2,\cdots N; \qquad (4.28b)$$

where the subscript i indicates that the corresponding variables are to be treated as sequences of i -- the bay number -- rather than functions of x, and N is the number of bays in the column. We also restore the finite-difference definitions of variable values and derivatives from normalized versions of (2.1) and (2.2)

6. An ideal counterpart of (4.27) was not presented. It is easy to obtain that by subjecting (3.33) with $\alpha \to 0$ to a perturbation treatment. The result then agrees with (4.24) for $\bar{p}_b = P_b$, $P_E^* = P_E$ and $\kappa = 0$, and the restriction on ε stands out clearly.

$$\vartheta_i = \frac{1}{2}(\vartheta_i^b + \vartheta_{i-1}^b), \qquad \vartheta_i' = \frac{1}{\lambda}(\vartheta_i^b - \vartheta_{i-1}^b), \tag{4.29a,b}$$

$$w_i = \frac{1}{2}(w_i^b + w_{i-1}^b), \qquad w_i' = \frac{1}{\lambda}(w_i^b - w_{i-1}^b). \tag{4.29c,d}$$

By algebraic manipulation of (4.28) and (4.29) which involves also shifting of the subscript i it is possible to obtain a decoupled finite-difference equation for w_i^b

$$(1+K)\,w_{i+1}^b - 2(1-K)\,w_i^b + (1+K)\,w_{i-1}^b = 0; \quad i = 1,2,\cdots N-1; \tag{4.30}$$

where $K \equiv \lambda^2 B/4AC$. Statement of the problem is completed by specifying the boundary conditions (2.40a,b)

$$w_o^b = 0, \qquad w_N^b = 0. \tag{4.31a,b}$$

Guided by the differential solution we try and find that

$$w_i^b = a \sin \lambda i \tag{4.32}$$

satisfies (4.31) (see (2.26)). It satisfies (4.30) too provided that

$$K = \lambda^2 \frac{B}{4AC} = \frac{1-\cos\lambda}{1+\cos\lambda}.$$

This is the characteristic equation. Substituting for A,B, and C their implied value from (4.14a) and (4.16b) we obtain the exact finite-difference buckling load

$$P_b = \left(\frac{2}{1+\cos\lambda}\right)^2 \left(\frac{\sin\lambda}{\lambda}\right)^2 \frac{P_E\left[1 + \frac{\kappa}{2}\left(1 + \frac{\varepsilon^2}{(1-\bar{p}_b)^3}\right)\right]}{\nu + \left(1 + \frac{\lambda^2}{12}\right)\left(1 + \frac{\varepsilon^2}{(1-\bar{p}_b)^3}\right)}. \tag{4.33}$$

Comparing this with (4.17) and noting that the coefficient in front is $\sim 1 + \lambda^2/6$ we see that the de-discretization error is indeed of second order. From (4.32) and (4.18b) we see also that no de-discretization deflection error exists at the batten points. At bay nodes, however, comparison has to be made between w_i, (eqn. 4.29c) and the deflection obtained from (4.18b), $a \sin\lambda(i - \frac{1}{2})$

$$\sin\lambda(i-\frac{1}{2})-w_i/a=[\sin\frac{\lambda}{2}-\frac{1}{2}\sin\lambda]\cos\lambda i-[\cos\frac{\lambda}{2}-\frac{1}{2}(1+\cos\lambda)]\sin\lambda i.$$

This is again an $o(\lambda^2)$ quantity.

4.8 The Prevalent Failure Mode

Another point of interest connected with the behavior of the undeflected column is the answer to the question which is the prevalent (i.e., occurring at a lower P) failure mode -- global buckling or slackening -- and what are the conditions that determine the answer. From (4.4b) we know already that local buckling is out of the race.

A comparison of (4.4c) and (4.20b) shows that for $\varepsilon=0$ a sufficient condition that $P_s > P_b$ is

$$(C_s^o > 0) \cup (P_E^* < 1+C_s^o) \Rightarrow P_s > P_b \qquad (4.34)$$

where C_s^o is defined in (4.6b). We now proceed to find how does $\varepsilon > 0$ influence this condition and whether or not it is also a necessary one.

For our purposes here it suffices to use a crude approximation of (4.17) for the buckling load. This will be an $o(h^o)$ [7] approximation in which, for the sake of later comparison with (4.34), P_E^* is written instead of P_E:

$$P_b=\frac{P_E^*}{1+\frac{\varepsilon^2}{(1-\bar{p}_b)^3}}. \qquad (4.35)$$

Considering the particularly simple position of P_E^* in (4.35) and the fact that it does not appear at all in (4.5) it is advantageous to pose the question of buckling vs. slackening as follows: Given ε and C_s^o, what is the value of P_E^* that brings about simultaneous buckling and slackening? Noting that this simultaneity implies $P_b=\bar{p}_b=P_s$ the answer is obtained directly from (4.35)

7. That (4.35) is an $o(h^o)$ approximation for any $\bar{p}_b < 1$ can be verified by using (4.19).

$$P_{ES} \equiv P_E^*(\text{which makes } P_b=\bar{p}_b=P_s) = P_s[\,1+\frac{\varepsilon^2}{(1-P_s)^3}\,] \qquad (4.36)$$

where P_s is the solution of (4.5). Since P_b invariably increases with P_E^* it is clear that

$$(P_E^* > P_{ES}) \Longleftrightarrow (P_b > P_s)\,. \qquad (4.37)$$

Numerical P_{ES} results generated from (4.36) and (4.5) are shown graphically in Figure 4–6 [8] for three slightly different C_s^o values around zero. Each line constitutes a ***boundary*** between an (ε, P_E^*) region where buckling prevails and another, in which slackening prevails.

It is seen from Figure 4-6 that if C_s^o is chosen ≥ 0 (i.e. $P^* \leq 1$) and P_E^* is not much larger than 1 than, except for impractically high ε's, failure would occur by buckling. Slackening failure for reasonable P_E^* and ε can only occur if C_s^o is chosen < 0.

Note the distinguished behavior as $\varepsilon \to 0$ of the case $C_s^o = 0$,[9] a behavior which is *not* approached as $C_s^0 \to 0$ from either side! Whereas the two solid lines are included in (4.34) the $C_s^o = 0$ line is not. To make (4.34) a necessary and sufficient condition we have to modify it as follows

$$(C_s^o > 0) \cup (P_E^* < 1+C_s^o) \cup [\,(C_s^o=0) \cap (P_E^* < \sim 3)\,] \Longleftrightarrow P_s > P_b \qquad (4.38)$$

where ~ 3 means that 3 is an $o(h^o)$ approximation of the correct value.

---

8. In construction of Figure 4-6 the quantity $(\varepsilon^2/2)/(1-p_o)^2$ was approximated by $\varepsilon^2/2$, in accordance with the $o(h^o)$ accuracy required here.
9. This behavior can also be seen from the fact that as $P^* = 1$ and $P_E^* = P_E \to 3$ the P_b and P_s asymptotic series (3.14c) and (4.7b) become identical in their first two terms.

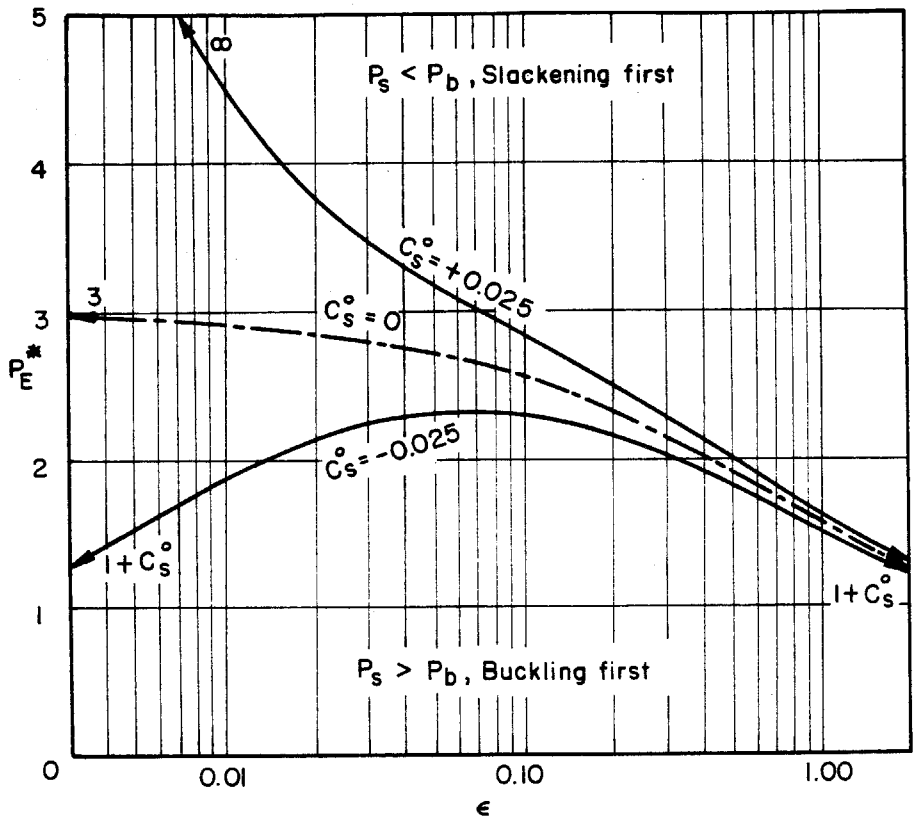

Figure 4-6. Buckling vs. slackening regions, $\sigma(h^\circ)$ approximation.

5. ANALYSIS OF DIAGONAL SLACKENING

Diagonal slackening in the undeflected column was treated already in Section 4.2. In this chapter we follow slackening phenomena into the a-P plane. The conditions which determine diagonal slackening and region transitions are given by equations (2.37g,h) and (2.38g,h). The displacement unknowns appearing in these equations are related to one another and to the load P through equilibrium. To find a definite a or a definite P for which a certain slackening phenomenon occurs one must usually possess a complete a-P-dependent solution, and its associated equlibrium path, which are algebraically docile. Since this is practically never the case we undertake a more modest task: to construct lines in the a-P plane - *slackening loci* - as universal as possible, which, when crossed by the appropriate equilibrium paths, signify the occurrence of their specific slackening phenomena. This direction will be pursued even though it is clear that the a-P plane is not always the most natural one for that purpose. Attention will be focused on the following problems: (1) Midspan bay slackening, (2) slackening at an end bay, (3) onset of slackening in post-buckling and (4) slackening of the back diagonals.

5.1 Midspan Bay Slackening

In this section we are looking for a locus in the a-P plane along which the diagonals of the bay located at the midspan (or the bays next to the midspan batten) becomes slack. Since we expect the parity of the number of bays to be of little consequence we choose for simplicity the case in which the midspan coincides with a bay node. At this bay we clearly have

$$w = a\,, \qquad w' = \vartheta = \gamma = \bar{\vartheta} = \bar{\gamma} = 0\,. \tag{5.1}$$

It is the fact that a appears here explicitly which makes the a-P plane particu-

larly suitable for the description of this locus. The slackening condition is now obtained from either (2.37g,h) or (2.38g,h)

$$\bar{u}' + \frac{1}{4}\bar{\vartheta}' = -\frac{p_o}{4\kappa P_E}. \tag{5.2}$$

The task is now to express $\bar{u}'$ and $\bar{\vartheta}'$ in (5.2) in terms of a and P using equilibrium, i.e., eqns (2.37a,b). This, however, is not easy to do exactly because these equations are coupled in a non-linear way through p_{11} and p_{22}. Fortunately, (5.2) itself removes the p_{11}-coupling (see eqn. (2.37e)) and an $o(h)$ approximation can be used to linearize the p_{22}-coupling. We obtain from (2.37e,f) using (5.2)

$$\frac{1}{(1-p_{11})^2} = \frac{1}{(1-P-2aP)^2}, \tag{5.3}$$

$$\frac{1}{(1-p_{22})^2} \cong \frac{1}{(1-P+aP)^2} - \frac{3\kappa P_E \bar{\vartheta}'}{(1-P+aP)^3}. \tag{5.4}$$

The approximation (5.4) is valid only inasmuch as $3\kappa P_E\bar{\vartheta}'/(1-P+aP) << 1$. By (5.2) $\bar{\vartheta}'$ is of $o(1)$ so this condition is satisfied for all large-enough a and for all P under the LBL. If, on the other hand, a is small and P is close to 1 the condition is still satisfied on account of $\bar{\vartheta}' \to 0$ as $a \to 0$. This can be tested later by verifying that the derived locus includes the case of slackening without deflection, eqn. (4.5).

Using eqns. (5.1), (5.3), and (5.4) in (2.37a,b) we can isolate $\bar{u}'$ and $\bar{\vartheta}'$ and then substitute in (5.2). In this way we obtain the *midspan slackening locus*

$$\frac{\varepsilon^2}{6}\left[\frac{1}{(1-P-2aP)^2} + \frac{2}{(1-P+aP)^2}\right] - (1-P) + \tag{5.5a}$$

$$+ \frac{1}{2}\left(aP + \frac{\varepsilon^2}{6}\left[\frac{1}{(1-P-2aP)^2} - \frac{1}{(1-P+aP)^2}\right]\right)\frac{1+2\kappa\left[1+\dfrac{\varepsilon^2}{(1-P+aP)^3}\right]}{1+\dfrac{\kappa}{2}\left[1+\dfrac{\varepsilon^2}{(1-P+aP)^3}\right]} = C_s$$

which indeed specializes to (4.5) upon setting a=0. C_s is the slackening parameter defined by eqns. (4.6). The $o(h^\circ)$ approximation of (5.5a) is

$$\frac{\varepsilon^2}{2}\left[\frac{1/2}{(1-P-2aP)^2}+\frac{1/2}{(1-P+aP)^2}\right]-(1-P)+\frac{1}{2}aP=C_s \qquad (5.5b)$$

provided that $\varepsilon^2/(1-P+aP)^3=o(1)$. From (5.5b) we can make the following observations:

1. Except through C_s the midspan slackening locus hardly depends on any of the parameters λ, p_o, and κ.

2. If $C_s=-1+\varepsilon^2/2$ (which implies $p_o=0$), the midspan slackening locus drops to P=0.

3. At the ideal LBL $1-P-2aP=0$ and if $\varepsilon\neq 0$ then C_s must be infinite. Hence for every $\varepsilon\neq 0$ and finite C_s the midspan slackening locus is below the ideal LBL.

4. If $\varepsilon=0$ eqn. (5.5b) becomes $(1-P-2aP)^2(1-P-\frac{1}{2}aP+C_s^\circ)=0$. The midspan slackening locus is the lowest root of this, namely

$$C_s^\circ \le -\frac{3}{4}: \qquad P=(1+C_s^\circ)/(1+\tfrac{a}{2}), \quad 0\le a<\infty; \qquad (5.6a)$$

$$-\frac{3}{4}< C_s^\circ < 0: \begin{cases} P=(1+C_s^\circ)/(1+\frac{a}{2}), & 0\le a < -C_s^\circ/(\frac{3}{2}+2C_s^\circ); \\ P=1/(1+2a), & a\ge -C_s^\circ/(\frac{3}{2}+2C_s^\circ); \end{cases} \qquad (5.6b)$$

$$C_s^\circ \ge 0: \qquad P=1/(1+2a), \qquad 0\le a<\infty. \qquad (5.6c)$$

A non-zero value of ε lowers the locus further below the line (5.6). Note that since $C_s^\circ\ge 0$ is a preferable design choice the locus will be dominated, in most practical cases, by the LBL.

5. Along the midspan slackening locus P is a monotonously decreasing function of a. The highest point in $[0,\infty]$ is at a=0 where $P=P_s$. The *initial* midspan slackening locus is independent of any parameter except through P_s and is given by

$$P \sim P_s(1-\frac{a}{2}), \qquad a \to 0 . \tag{5.7}$$

Equation (5.5b) and its graphical representation take a particularly agreeable form if we introduce the combined load-deflection variable α defined by (3.3b) and used extensively in the ideal column theory; for then (5.5b) becomes

$$\frac{\varepsilon^2/2}{(1-P)^2}\left[\frac{1/2}{(1-\alpha)^2}+\frac{1/2}{(1+\alpha/2)^2}\right]-(1-P)(1-\frac{\alpha}{4})=C_s \tag{5.8}$$

and the a–P region under consideration maps into the square $0\le\alpha\le 1$, $0\le P\le 1$. Figures 5-1 depict qualitatively midspan slackening loci in the a-P as well as the α–P plane. C_s^o was chosen there in the impractical range (5.6b) so that an interaction between the two roots may ensue.

5.2 Slackening at an End Bay

Another significant slackening locus is that which, when crossed by the equilibrium line pertaining to the same set of parameters, indicates the occurrence of slackening (or the arrival of a slackening front) at the bay closest to the column support. The transition is from region I to either region II or III depending on the sign of w' at the particular end under consideration (see eqn. (2.38g)). Because of the antisymmetry it suffices to look into only one case, w'> 0 say. The locus will therefore be based upon the limiting case of (2.37g)

$$\bar{u}'+\frac{1}{4}\bar{\vartheta}'-\bar{\gamma}=-\frac{p_o}{4\kappa P_E}. \tag{5.9}$$

At the end-bay we have, of course

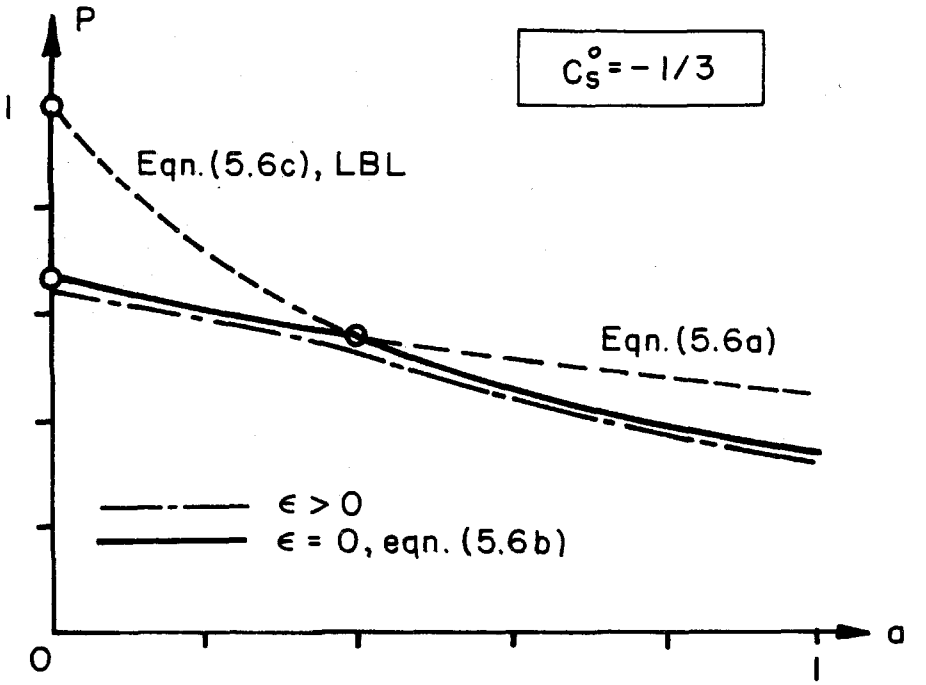

Figure 5-1a. Midspan slackening loci in the a-P plane.

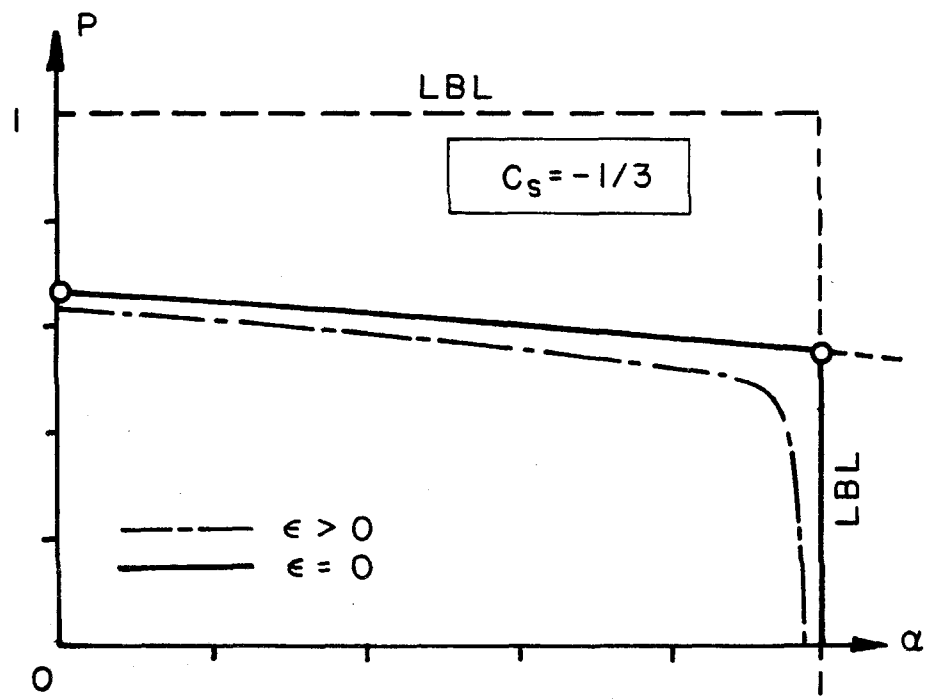

Figure 5-1b. Midspan slackening loci in the α–P plane.

$$w = \frac{\lambda}{2} w' \tag{5.10}$$

and using this as well as (5.9) and (2.37c,e,f) we obtain the following $o(h)$ approximations

$$\frac{1}{(1-p_{11})^2} \cong \frac{1}{(1-P)^2} + \frac{4\lambda P w'}{(1-P)^3}, \tag{5.11a}$$

$$\frac{1}{(1-p_{22})^2} \cong \frac{1}{(1-P)^2} + \frac{\lambda P w'}{(1-P)^3}. \tag{5.11b}$$

The approximations (5.11) are valid provided $\lambda P w'/(1-P) << 1$. This can be justified for all $a \geq 0$ using arguments similar to those which led to eqn. (5.4). Another assumption made in deriving (5.11b), verifyable from (2.37a), is that at an end bay $3\kappa P_E \bar{\vartheta}' = o(h^2)$ and thus negligible.

We can now use (5.10), (5.11) and (2.37a,b,c) to express $\bar{u}'$, $\bar{\vartheta}'$ and $\bar{\gamma}$ in terms of w'. By substituting them into (5.9) and again neglecting $\kappa\bar{\vartheta}'$ terms compared to $o(1)$ we obtain the *end-bay slackening condition* in the form

$$\frac{\varepsilon^2/2}{(1-P)^2} - (1-P) + \left[1 + \frac{5\kappa}{2}\left(1 + \frac{\varepsilon^2}{(1-P)^3}\right)\right] \frac{\lambda}{2\kappa} P w'(0) = C_s. \tag{5.12}$$

This also reduces to the P_s equation (4.5) upon setting $w'(0) = 0$.

It is seen that here, unlike in the midspan slackening case, the 'natural' plane to plot the locus is not that of a-P but the $w'(0)$–P plane. To map the locus into the a-P plane we have to have a relation between the deflection amplitude a and the end-slope $w'(0)$ for all $a \geq 0$. Since such a relation is not available in closed form we resort to rougher approximations and adopt for this purpose the ideal column relation (3.17) which, using (3.3a,b) and taking $w \cong 0$, gives

$$w'(0) \cong a\sqrt{\frac{P}{P_E}\left[1 + \frac{\varepsilon^2/(1-P)}{(1-P-2aP)(1-P+aP)}\right]}. \tag{5.13}$$

When doing this there is no point in retaining the $o(h)$ term in (5.12) so we

finally have

$$\frac{\varepsilon^2/2}{(1-P)^2} - (1-P) + \sqrt{\frac{P}{P_E}\left[1 + \frac{\varepsilon^2/(1-P)}{(1-P-2aP)(1-P+aP)}\right]}\,\frac{\lambda}{2\kappa}aP = C_s \qquad (5.14a)$$

or, in terms of α, eqn. (3.3b)

$$\frac{\varepsilon^2/2}{(1-P)^2} - (1-P)\left[1 - \frac{\lambda}{4\kappa}\sqrt{\frac{P}{P_E}\left(1 + \frac{\varepsilon^2/(1-P)^3}{(1-\alpha)(1+\alpha/2))}\right)}\,\alpha\right] = C_s\,. \qquad (5.14b)$$

Note that different loci can be obtained by using the ideal load-deflection relation (3.33) to replace P/P_E or $\varepsilon^2/(1-P)^3$ by some other expressions. It is important to understand in this context that *only the intersection* between the locus and the equilibrium path has a physical meaning, hence all loci which intersect a particular equilibrium path at the same point are equally valid. The most suitable one is, of course, the one dependent on the least structural and imperfection parameters, i.e., the one which is most universal.

To investigate the locus (5.14b) it is best to start with the case $\varepsilon = 0$. The locus equation then becomes

$$\sqrt{1-\alpha}\,(1-P)^3\left[1 - \frac{\lambda}{4\kappa}\sqrt{\frac{P}{P_E}}\,\alpha + \frac{C_s^\circ}{1-P}\right] = 0 \qquad (5.15)$$

and a graphical description of its behavior in the α–P plane is given in Figure 5-2a. The fixed branches α=1 and P=1 constitute the extreme limits to which the locus may be pushed. If $C_s^\circ < 0$, long stretches of the locus must occur below the LBL. On the other hand, if $C_s^\circ \geq 0$, there is always a possibility to push the locus out to the LBL itself. This is done by either increasing $4\kappa\sqrt{P_E}/\lambda$ beyond 1 or by increasing C_s° so that the point of minimum α belonging to the branch moves beyond $\alpha = 1$. (It is seen from the figure and from eqn. (4.6b) that for $4\kappa\sqrt{P_E}/\lambda = 1/3$ it is enough to choose P* slightly less than $1-\kappa$ in order to achieve this.) In the a-P plane, the minimum-α feature occurring in $C_s^\circ > 0$ loci means only that a line $aP/(1-P)$=const. intersects the locus twice.

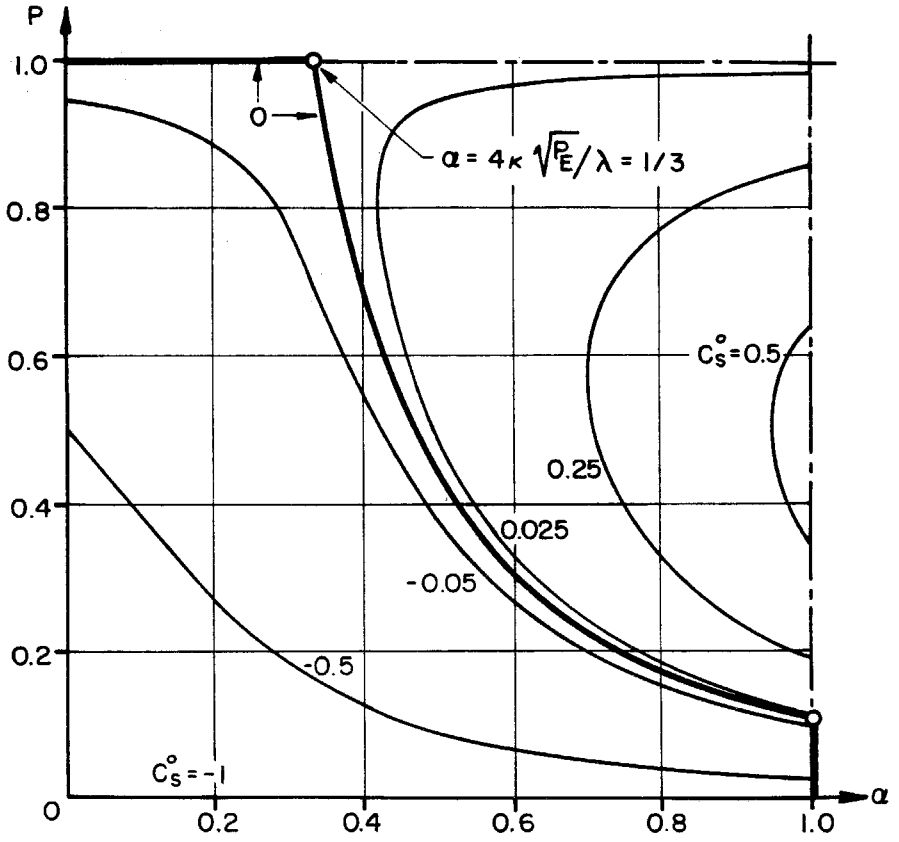

Figure 5-2a. End-slackening loci in the α–P plane for $\varepsilon = 0$.

Figure 5-2b shows what happens to the end-slackening loci upon increase of ε. The value of $4\kappa\sqrt{P_E}/\lambda$ there is 1/3, the same as in Figure 5-2a. We note the following:

1. The 'imperfection-sensitivity' of the loci is small for small C_s° and becomes very large as that parameter increases; especially so when α is small to moderate.

2. $\varepsilon > 0$ 'rounds the corners' off the intersections between the different $\varepsilon = 0$

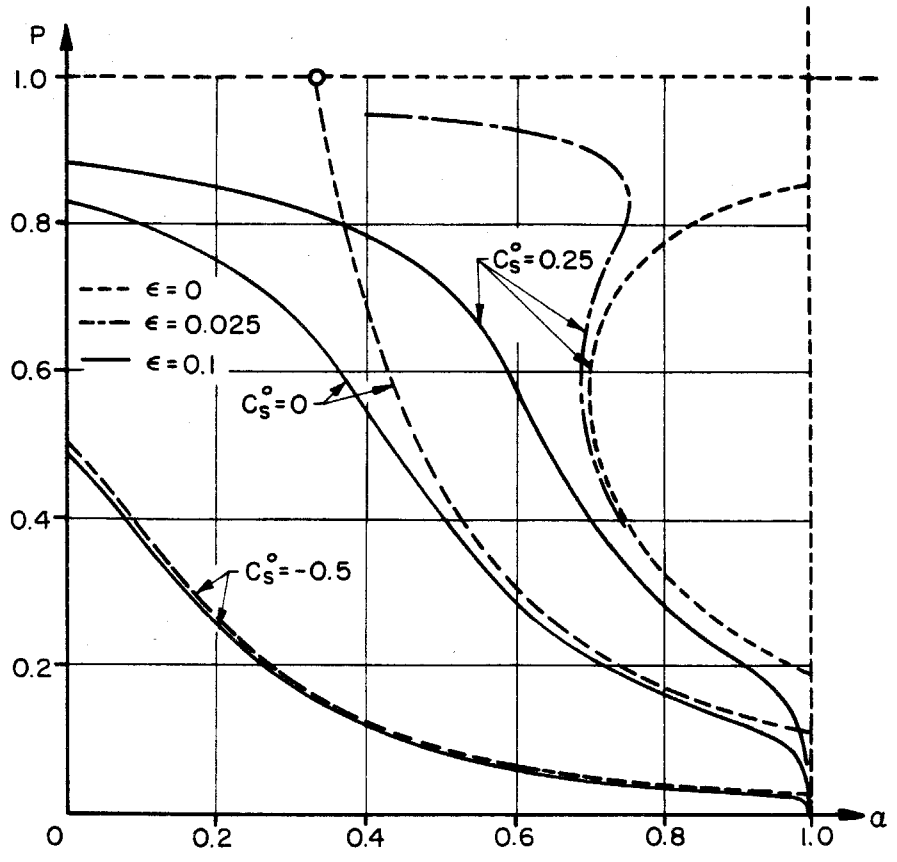

Figure 5-2b. Effect of ε on the end-slackening loci.

branches, thereby turning the locus into a continuous smooth curve. Note especially the effect as $\alpha \to 1$.

3. If $4\kappa\sqrt{P_E}/\lambda$ and C_s^o are not too large, and if ε is small enough, the locus may have a point of local maximum-α as well as a local minimum-α. Since for small ε the equilibrium path follows closely the P=1 (or $P=P_E$) and $\alpha=1$ branches it appears that there exists a possibility of the path crossing the locus twice. This means that, as the load drops, the slackened end-bay diagonals may become taut again.

Noting eqns (5.6) and comparing Figures 5-1b and 5-2a we find that in the $\varepsilon=0$ case end-slackening occurs *before* - at most simultaneously with - midspan slackening. Whether or not this is a rule applying also to $\varepsilon > 0$ cases depends on the relative 'imperfection sensitivity' of the midspan- and end-slackening loci. We will not attempt to answer this question here.

We conclude this study by remarking that the relation between a and w', eqn. (5.13), was originally derived for a globally-perfect column. It is believed, however, that within the accuracy required here this fact does not invalidate the results as far as application to not-too-globally-imperfect cases of $P^* < 1$ goes. The reason is that for such cases end-slackening occurs deep inside the a-P plane, long past the limit-load point, where the existence of an initial small deflection cannot influence the mode shape to an appreciable degree.

5.3 Onset of Slackening in Post-Buckling

A third slackening locus of interest - the *onset-of-slackening* locus - is that which, upon being crossed by the equilibrium path, signifies that in an otherwise all-region-I column, *somewhere* along the span, a bay slackens.

Unlike in the midspan and end cases, the spanwise location of this occurrence is itself an unknown, determined on the $w' > 0$ half-span by the condition (see eqns. (2.37g), (2.38g,h))

$$\bar{u}' + \frac{1}{4}\bar{\vartheta}' - \bar{\gamma} = \text{minimum} . \tag{5.16}$$

The onset locus is then determined by that minimum being equal to $-p_o/4\kappa P_E$.

It is clear that to conduct this study rigorously and in closed-form one must have closed-form solutions to $\bar{u}'$, $\bar{\vartheta}'$, and $\bar{\gamma}$ along the complete equilibrium path. Since in our work these are available only for the initial and final phases of post-buckling we must confine ourselves to deriving only the initial and final

stretches of the locus, and drawing whatever conclusions this situation affords.

We start with the case e=0 and small a - not necessarily infinitesimal. we still maintain those components of the buckling mode (4.18) which are P_b-independent, namely $u'^{(1)}=0$ and $w^{(1)}=a\sin x$. For $\vartheta^{(1)}$ and $\gamma^{(1)}$ we consult the more general relations (2.42c,d) and find that in (4.18c,d) P_b should be replaced by P. Adding the prebuckling solution (4.3) the quantities entering the slackening analysis are

$$\bar{u}' = -\frac{1}{4\kappa P_E}(P - \bar{p}^{(o)} + p_o)\,, \tag{5.17a}$$

$$\bar{\vartheta} = a\cos x\,, \tag{5.17b}$$

$$\bar{\gamma} = \frac{\lambda}{4\kappa}\left(\frac{P}{P_E}\right) a\cos x\,; \tag{5.17c}$$

where, consistent with the limited accuracy pursued so far in slackening analyses, the $o(h)$ term was omitted from (5.17b).

The spanwise location of the slackening onset is now found by substituting (5.17) into (5.16) and locating the minimum. This gives

$$x_{sP} = \tan^{-1}\left(\frac{\kappa}{\lambda}\cdot\frac{P_E}{P}\right). \tag{5.18}$$

It is interesting to note that if onset of slackening occurs at small enough a it occurs neither at the midspan nor at the supports, but somewhere between.

Substituting (5.18) back into (5.16) and requiring that that minimum be equal to $-p_o/4\kappa P_E$ (eqn. (2.37g)) we obtain an equation for the initial slackening-onset locus for the globally-perfect column:

$$(P - \bar{p}^{(o)}) + a\sqrt{(\kappa P_E)^2 + (\lambda P)^2} = 0. \tag{5.19}$$

The internal prebuckling force $\bar{p}^{(o)}$ is a function of P through the relation (4.3b).

Since for a=0 $\bar{p}^{(o)} \to P$ and $P \to P_s$ it is clear that the locus (5.19) starts at (a=0, P=P_s). To find the initial slope we expand both P and $\bar{p}^{(o)}$ in perturbation series around P_s and substitute into (4.3). The zeroth order solution is then the P_s equation (4.5) and for the 1st order we obtain

$$(P_s - P) \sim (P_s - \bar{p}^{(o)})\left[\, 1 + 2\kappa\left(1 + \frac{\varepsilon^2}{(1-P_s)^3}\right)\right] . \tag{5.20}$$

We can now express $P-\bar{p}^{(o)}$ in terms of P_s-P and substitute into (5.19). Taking only $o(a)$ and $o(h^o)$ quantities the latter becomes

$$P \sim P_s\left[\, 1 - \frac{a/2}{1 + \dfrac{\varepsilon^2}{(1-P_s)^3}} \sqrt{\left(\frac{P_E}{P_s}\right)^2 + \left(\frac{\lambda}{\kappa}\right)^2}\,\right] . \tag{5.21}$$

Now again one has to bear in mind that (5.21) is meaningful only inasmuch as the locus represented by it happens to be crossed, *within its range of validity* (namely $a \to 0$), by the equilibrium path corresponding to the same set of parameters. This implies that P_b of such a case must be very close to P_s. Within $o(h^o)$ accuracy we can thus use (4.35) to write

$$1 + \frac{\varepsilon^2}{(1-P_s)^3} \sim \frac{P_E}{P_s} . \tag{5.22}$$

If we now substitute this into (5.21) and also replace in (5.18) P by P_s we can summarize the *initial slackening-onset locus and spanwise location* as follows:

$$P \sim P_s\left[\, 1 - \frac{a}{2}\sqrt{1 + \left(\frac{\lambda}{\kappa}\right)^2 \left(\frac{P_s}{P_E}\right)^2}\,\right] , \tag{5.23a}$$

$$x_s = \tan^{-1}\left[\left(\frac{\kappa}{\lambda}\right)\left(\frac{P_E}{P_s}\right)\right] . \tag{5.23b}$$

It is interesting to compare (5.23a) with the initial midspan slackening and end-bay slackening loci. If the onset happens to occur at small a and at the midspan then (5.23b) tells us that $(\kappa/\lambda)(P_E/P_s) \to \infty$. Substituting this into (5.23a) eqn.

(5.7) is immediately recovered. Similarly, an end-bay onset is characterized by $(\kappa/\lambda)(P_E/P_s) \to 0$, which makes (5.23a) reduce to

$$P \sim P_s\left[1 - \frac{a}{2}\left(\frac{\lambda}{\kappa}\right)\left(\frac{P_s}{P_E}\right)\right]. \tag{5.24}$$

It can be shown that upon expanding (5.14a) around ($a=0$, $P=P_s$) and using (5.22) this should indeed be the result.

We conclude by observing from (5.23), (5.7), and (5.24) that as a column having positive but small $P_s - P_b$ proceeds along its post-buckling path the first locus to be encountered is indeed that of the onset. Whether the next one is the midspan locus or the end bay locus depends on whether $(\lambda/\kappa)(P_s/P_E)$ is less or more than 1 respectively. The situation is depicted qualitatively in Figure 5-3. (For explanation of the back-diagonals line see Section 5.4.)

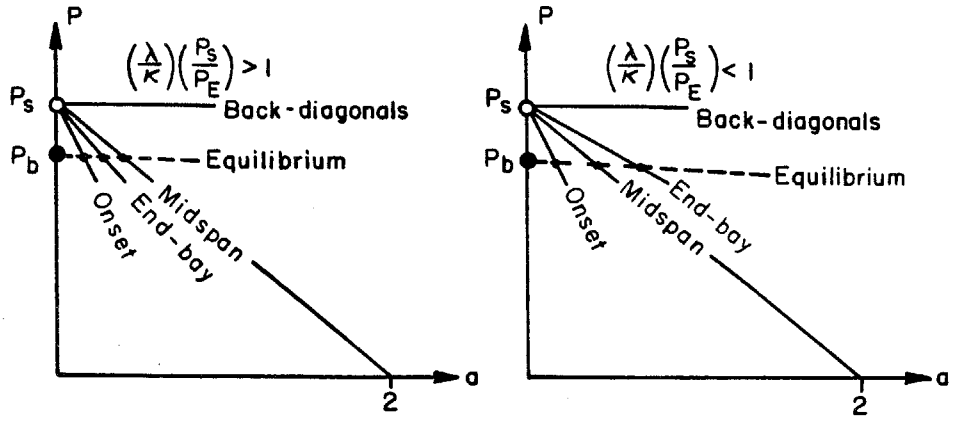

Figure 5-3. Sequence of slackening occurrences, $0 < (P_s - P_b) << 1$.

Consider now the case $e \neq 0$, small a. If slackening occurs on the ascending leg of the equilibrium path it must be that $P_s < P_b$. This is a case of no practical interest. If it occurs past the limit point and a is still small it means that e is

much smaller than a. In the latter case, just as the equilibrium path differ little from the post-buckling path so, we expect, does the $e \neq 0$ locus differ from the e=0 locus. In summary, it is expected that the results (5.23) are approximately correct also for the case $e \neq 0$ provided $e << a(\text{onset})$ and $0 < (P_s - P_b) << 1$.

We now examine the behavior of the slackening-onset locus as $a \to \infty$. We shall see (Chapter 6) that at this limit, regardless of any structural or imperfection parameters, the triangular local mode of the ideal column is valid and the triangle sides consist of region I bays:

$$x = \frac{\pi}{2}: \quad \bar{u}' = \bar{\vartheta}' \to -\infty, \quad \bar{\gamma} = 0, \quad w = a;$$

$$x < \frac{\pi}{2}: \quad \bar{u}' = \bar{\vartheta}' = 0, \quad \bar{\gamma} = 0, \quad w = \frac{2a}{\pi}x.$$

It is clear, therefore, that the spanwise location where eqn. (5.16) is satisfied is the midspan. It is clear also that unless $p_o/4\kappa P_E \to \infty$ the midspan bay is long past slackening. Hence we can choose the far portion of the onset locus to approach the locus of midspan slackening. Then only equilibrium paths belonging to very large values of $p_o/4\kappa P_E \to \infty$ will cross this portion.

5.4 Slackening of the Back Diagonals

Slackening of diagonals 23 and 32 - the back diagonals - causes the column to loose its shear rigidity with respect to deflections perpendicular to the x-z plane. As a result such deflections must ensue. Since in our theory only in-plane deflections are considered, its validity might break down upon intersection of the equilibrium path with the locus signifying slackening of back diagonals. Herein lies the importance of finding this locus.

The condition under which the back diagonals are *taut* is derived from the fifth of (2.31) in conjunction with (2.34b)

$$\bar{u}' - \frac{1}{2}\bar{\vartheta}' \geq -\frac{P_o}{4\kappa P_E} . \tag{5.25}$$

The first question to be asked is the following: what is the state of diagonals 21 of a bay (located on the $w' \geq 0$ halfspan) upon slackening of the back diagonals of the same bay? The answer to this is obtained by substituting into (2.37g) the equality limit of (5.25). We obtain for taut diagonal 21

$$-\frac{3}{4}|\bar{\vartheta}'| - \bar{\gamma} \geq 0$$

where we have introduced the fact -- obvious from (2.37a) -- that $\bar{\vartheta}' \leq 0$ everywhere (assuming $w \geq 0$ everywhere). Now in $w' \geq 0$ stretches of region I the last inequality is obviously violated. Moreover, at the midspan, where $\bar{\gamma}=0$, it is violated strongly because $|\bar{\vartheta}'|$ is maximum and at the end-bay, where $|\bar{\vartheta}'| \cong 0$, because $\bar{\gamma}$ is maximum. We therefore conclude

slackening of the back diagonals may only occur in bays which are deep inside regions II/III. (5.26)

The next question is *where* along the span do back diagonals slacken first. Fortunately, unlike in some previous cases, we do not have to have complete solutions in order to obtain an answer; it suffices to express the left hand side of (5.25) in terms of w and w' using region II/III displacement equations (2.38). With the help of (2.38c) the following combination of (2.38a,b) can be written

$$\bar{u}' - \frac{1}{2}\bar{\vartheta}' = \frac{-1}{2P_E(1-\kappa/2)}\{\kappa P_E(3\bar{u}' + \frac{8}{3}\bar{\gamma}) + [1 - (w + \frac{\lambda}{2}w')]P + \frac{\varepsilon^2/2}{(1-p_{22})^2} - \frac{\varepsilon^2/2}{(1-p_o)^2}\} \tag{5.27a}$$

where, again using (2.38c)

$$p_{22} = [1 - (w + \frac{3}{2}\lambda w')]P + \kappa P_E(6\bar{u}' + 4\bar{\gamma}) + \frac{3}{2}p_o . \tag{5.27b}$$

Now $\bar{u}'$ and $\bar{\gamma}$ are always maximum at the end bay whereas w there is minimum.

$w+(\lambda/2)w'$ and $w+(3/2)w'$ are nothing but w_i^b and w_{i+1}^b respectively. With this knowledge we can easily show from (5.27), on a term-by-term basis, that $\bar{u}'-(1/2)\bar{\vartheta}'$ is minimum at the end bay. It follows that

> if back diagonals slacken in a deflected column, the first do so are the end-bay back diagonals. (5.28)

Statements (5.26) and (5.28) together imply that back diagonals slackening can only occur substantially later than the arrival of the I/II transition point at the end bay.

To arrive at the back diagonals slackening locus we now take the following steps: (1) Eliminate $\bar{\gamma}$ from both of (5.27) using (2.38c); (2) substitute for w the end-bay deflection $(\lambda/2)w'$; (3) substitute for $u'-(1/2)\bar{\vartheta}'$ its slackening value $-p_o/4\kappa P_E$. Miraculously, these steps bring about the exact disappearance of *all* displacement unknowns from (5.27) and we are left with

$$\frac{\varepsilon^2/2}{(1-P)^2} + P = (1+2\kappa)\frac{p_o}{2\kappa} + \frac{\varepsilon^2/2}{(1-p_o)^2}$$

which, as an equation for P, is exactly identical to the P_s equation (4.5)! We therefore conclude that

> The exact back–diagonals slackening locus in the a–P plane is the straight and horizontal line $P = P_s$. (5.29)

The back diagonals slackening locus is added in Figure 5-3.

Since being above the line $P=P_s$ means the existence of slack back diagonals, which in turn implies out-of-plane instability, any pure-a-P equilibrium path segment that has that property is physically invalid. hence only equilibrium paths which belong to columns having $P_b \leq P_s$ are covered by the theory so far developed. These, however, by satisfying $P < P_b$ for all a, never encounter back diagonal slackening and continue to deflect in the x-z plane indefinitely.

5.5 Summary of Slackening Phenomena

Consider a globally-perfect column having $P_b < P_s$ as it deflects in post-buckling. First, as its equilibrium path crosses the slackening-onset locus, a region II bay will appear on the $w' \geq 0$ halfspan somewhere between $x=0$ and $x=\pi/2$. If P_b and P_s are fairly close the spanwise location of slackening-onset and its a-P locus are given by (5.18) and (5.19) respectively; if they are even closer, then (5.23a,b) become valid. As deflection continues region II spreads out gradually towards the end-bay on one side and towards the midspan bay on the other side. Depending on the value of $(\lambda/\kappa)(P_s/P_E)$, at least in the $(P_s-P_b) << 1$ case, one side or the other is reached first (see Figure 5-3). The arrival of the I/II transition point at the midspan bay is signified by the equilibrium path crossing the midspan slackening locus (5.5); its arrival at the end bay by the end-bay slackening locus (5.14). Further deflection leads, due to the drop in load, to reappearance of region I stretches, which eventually reclaim all but the locally-buckled midspan bay (see Chapter 6). If the initial diagonal preload is so high as to make slackening-onset occur far down the post-buckling path it will then occur at (or very close to) the midspan and remain confined to that area. Throughout the process described never and nowhere do back diagonals slacken.

6. SOLUTIONS AND EQUILIBRIUM PATHS OF THE DEFLECTED COLUMN

In Chapter 4 we investigated solutions and equilibrium paths in a narrow strip adjacent to the P axis in the a-P plane. The present chapter, on the other hand, is a collection of closed-form solutions and equilibrium paths elsewhere in the a-P plane. We can treat in closed-form only special cases. These will be the locally-perfect column and the three remaining boundaries of the a-P plane: the local mode and the LBL at the upper boundary and the two limits $a \to \infty$ and $P \to 0$. These results form a skeleton of the complete a-P behavior, with the help of which one can sketch a qualitative picture of general equilibrium paths. Since rigorous treatment of the latter can only be done using numerics, we attempt here to generate an engineering-oriented working formula for general columns equilibrium paths, which is based not on rigorous solutions but on interpolation between the known behavior on the boundaries.

6.1 The All-Region-I Locally-Perfect Column

In this section we discuss equations, solutions and equilibrium paths corresponding to locally-perfect columns. Recall that in the ideal case we had the following situation: The post-buckling path of a globally- and locally-perfect column was the LBL; the path of the only-locally-perfect column was the 'global line'; upon intersection of the two paths the 'second bifurcation' would occur, in which the solution bifurcated from the global to the local mode. Here we attempt to establish the modifications in this picture that follow from the fact that the column is no longer ideal. In doing so we ignore the possibility of slackening. This means that the results to be obtained are actual ones only inasmuch as they are predicted to occur below any slackening locus. We shall see in the following that this is not much of a restriction.

6.1.1 Locally-Perfect Equations; Subcritical, Critical, and Buckled Bays: Consider region I bending and compression displacement equations (2.37a,b). As $\varepsilon \to 0$ we have to consider two possibilities: either $p_{11} \neq 1$ and the potentially-singular terms $(\varepsilon^2/6)/(1-p_{11})^2$ vanish, or $p_{11} \to 1$ and they remain at least bounded. Mathematically we take account of this situation by multiplying the equations through by $(1-p_{11})^2$ and then letting $\varepsilon=0$. In this way, however, as $p_{11} \to 1$ the two equations degenerate into a single one. A second, independent equation can nevertheless be produced by *eliminating* the singular terms between the two original equations. Thus we obtain the region I, locally-perfect-column bending and compression equations in the form:

$$[(1 - P - 2wP) - 4\kappa P_E(\bar{u}' + \frac{1}{4}\bar{\vartheta}') - p_o]^2 [P_E(1 + \frac{\kappa}{2})\bar{\vartheta}' + wP] = 0 , \quad (6.1a)$$

$$P_E[2(1 + 2\kappa)\bar{u}' - (1 + \frac{\kappa}{2})\bar{\vartheta}'] + (1 - w)P = 0 , \quad (6.1b)$$

where the first factor in (6.1a) is just $(1-p_{11})^2$ taken from (2.37e). Now as long as $p_{11} < 1$ it is the second factor in (6.1a) which determines the behavior. If, on the other hand, $p_{11} = 1$, we still have a viable, linear, regular, complete system of equations in which the first factor in (6.1a) is the active one, and which leads to *different* behavior. Thus

$$\left.\begin{aligned} \bar{\vartheta}' &= -\frac{wP}{P_E(1+\kappa/2)} \\ \bar{u}' &= -\frac{P}{2P_E(1+2\kappa)} \end{aligned}\right\}, \quad p_{11} < 1 ; \quad (6.2a,b)$$

$$\left.\begin{aligned} \bar{\vartheta}' &= -\frac{1}{3\kappa P_E(1+\kappa)}\{[1 + (1 + 3\kappa)2w]P - P^*\} \\ \bar{u}' &= -\frac{1}{6\kappa P_E(1+\kappa)}\{[(1 + \frac{3}{2}\kappa) + 2w]P - \frac{1+\kappa/2}{1+2\kappa}\} \end{aligned}\right\}, \quad p_{11} = 1 . \quad (6.2c,d)$$

We see that as long as slackening does not occur the 'strains' $\bar{u}'$ and $\bar{\vartheta}'$ are well-

defined and bounded for any bay-deflection w. They might be large, though, of $o(1/h)$ if $p_{11}=1$, thereby violating the basis of the theory given in (2.21). Fortunately, it is only in an a-P domain where the numerators of (6.2c,d) are also small that interest in these equations arise.

The reason for the boundedness of the bay strains when $p_{11} = 1$ can be traced to the statical indeterminacy of the bay structure. As long as the diagonals are taut they lend some small bending stiffness to the bay. They become the sole source of bending stiffness (note the κ in the denominators of (6.2c,d)) when the 11 longeron-segment is no longer able to contribute anything, due to it having $p_{11} = 1$. Even then the bay is still capable of taking on load increases since the latter are lost to diagonal unloading; yet the diagonals cannot buckle the 11 longeron, because every shortening of that longeron is accompanied by diagonal unloading which in turn reduces the longeron load below 1, thereby restoring *all* of its stiffness (recall that $\varepsilon = 0$). To distinguish the bay state described above from that of a ***buckled bay***, in which 'strains' are infinite, we will refer to it as a *critical bay*. In constrast, a bay governed by eqns. (6.2a,b) will be called a *subcritical bay*.

6.1.2 The Subcritical Locally-Perfect Column: A column of which *all* the bays are subcritical is called here a ***subcritical column***. It is governed entirely by eqns. (6.2a,b) supplemented by (2.42c,d):

$$(P_E - \nu P)\left(1 + \frac{\kappa}{2}\right)w'' + Pw = P_E\left(1 + \frac{\kappa}{2}\right)w_o'' \tag{6.3a}$$

$$\bar{u}' = -\frac{P}{2P_E(1 + 2\kappa)} \tag{6.3b}$$

$$\bar{\vartheta} = \left(1 - \nu\frac{P}{P_E}\right)w' - w_o' \tag{6.3c}$$

$$\bar{\gamma} = \frac{\lambda}{4\kappa}\left(\frac{P}{P_E}\right) w' . \tag{6.3d}$$

Taking the global imperfection according to (4.24) the solution that satisfies the boundary conditions (2.44) is

$$w = a \sin x , \tag{6.4a}$$

$$u' = - \frac{P}{2P_E(1 + 2\kappa)} , \tag{6.4b}$$

$$\vartheta = \left[(1 - \nu \frac{P}{P_E})a - \nu \frac{P_b}{P_E} e \right] \cos x , \tag{6.4c}$$

$$\gamma = \frac{\lambda}{4\kappa P_E} (aP + eP_b) \cos x , \tag{6.4d}$$

provided that

$$a = \frac{e}{1 - P/P_E^*} , \tag{6.4e}$$

where P_E^* is given by (4.20a). Eqn (6.4e) gives the equilibrium path of the locally-perfect general column - its global line. It is seen to differ from that of the ideal column (3.16b) in P_E being replaced by its general-column equivalent P_E^*.

An analysis similar to that done in Section 5.3 and use of (6.4e) reveals that the subcritical locally-perfect column starts to slacken at the spanwise location

$$x_s = \tan^{-1} \frac{\kappa/\lambda}{1 + \kappa/2} \tag{6.5a}$$

and at a value of P which satisfies

$$e^2 \left[\left(\frac{\lambda}{\kappa}\right)^2 + \left(\frac{1}{1 + \kappa/2}\right)^2 \right] P^2 - \left[\frac{2(C_s + 1 - P)}{1 + 2\kappa} \left(1 - \frac{P}{P_E^*}\right) \right]^2 = 0 . \,^{1} \tag{6.5b}$$

Above this P the validity of eqns. (6.4) breaks down. This is, however, of no

1. Because of the assumption $p_{11} \neq 1$ made at the outset, eqn. (6.5b) does not reduce upon letting e = 0 to the complete P_s equation $(1 - P_s)^2 (C_s + 1 - P_s) = 0$. For the same reason it also misses the root present at local buckling, $P = P_c$, which is the dominant one if the other root is higher than P_c.

consequence if C_s is large enough, that is if

$$C_s \geq (1-P_c)\left[-1+\frac{1+2\kappa}{4}\sqrt{\left(\frac{\lambda}{\kappa}\right)^2+\left(\frac{1}{1+\kappa/2}\right)^2}\right], \tag{6.6}$$

for then the slackening load is above the second bifurcation load P_c given later in eqns. (6.19). It can be appreciated from (6.4) that even in most adverse cases C_s need not be excessively large in order to accomplish this; if $(1+\kappa/2)(\lambda/\kappa)=\sqrt{15}$ then $C_s=0$ more than suffices.

6.1.3 Onset of Criticality in a Locally-Perfect Column: We ask the following questions: (1) where along the span of an all-region-I, locally-perfect column is the bay located which is first to turn critical? (2) Where in the a-P plane is the locus which, when crossed by the corresponding equilibrium path, signifies that event?

The answer to the first question lies clearly in locating the spanwise maximum of p_{11}. Using (2.37e) this is formulated as

$$2wP + 4\kappa P_E(\bar{u}' + \frac{1}{4}\bar{\vartheta}') = \text{maximum} \tag{6.7}$$

which, using substitutions from (6.4), readily yields

$$x(\text{onset of criticality}) = \frac{\pi}{2}. \tag{6.8a}$$

Using this result in (6.4) and (4.24), substituting into (2.37e) and requiring that the resultant p_{11} equals 1 we obtain an expression for the desired *onset-of-criticality locus*

$$P = \frac{P^*}{1+2a\,\frac{1+2\kappa}{1+\kappa/2}}. \tag{6.8b}$$

This locus always originates at $P=P^*$. If $P^*\leq 1$ (i.e., $C_s^o \geq 0$) it stays below the LBL for all positive a. If $C_s^o \leq -3/4$ its entire length is obstructed by the LBL. Else, if

$-3/4 < C_s^o < 0$, its initial stretch is above the LBL but later on they cross. It is striking that the intersection is ***precisely*** the same as that of the locally-perfect midspan slackening locus (5.5a). Consequently, the a-P domain of criticality never interferes with that of midspan slackening. This situation is shown qualitatively in Figure 6-1.

We conclude by remarking that the forgoing discussion lends a new significance to the quantity P*. Besides being a potential global buckling load of the perfect column it appears here also in the role of a *critical load* of the same column. The vertical dashed-line segment in Figure 4-1 between the P* point and the local buckling point, which is a segment of the equilibrium line for $\varepsilon = 0$, pertains to an undeflected column state wherein all bays are critical. It is not accidental that the two roles of P* coincide: upon becoming all-critical the column looses almost all its bending rigidity and finds itself loaded far beyond its then-actual Euler load, $(\kappa/2)\,P_E$.

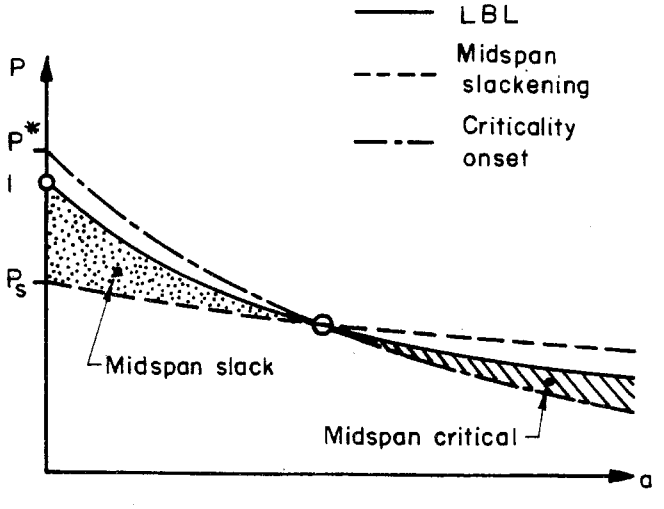

Figure 6-1. a-P domains of slack midspan and critical midspan for a locally-perfect column having $-3/4 < C_s^o < 0$.

6.1.4 The Critical Locally-Perfect Column: We now ask the following questions: (1) If an all-perfect column buckles globally at $P = P^*$ what is the nature of the post-buckling solution and equilibrium path? (2) What happens to a globally-imperfect column when its global line intersects the criticality-onset locus (6.8b)? An assertion that $P^* < 1$ is already implicit in the first question, since otherwise local buckling will precede global buckling. Similarly, in order that the phenomena discussed in the following be relevant the locus (6.8b) must occur *below* local buckling, wherever this may be.

Above the criticality-onset locus a locally-perfect column certainly comprises some critical bays, i.e., is critical. The problem therefore involves two different systems of differential equations, each valid in specific *criticality regions*. Once solutions are obtained they have to be matched at *transition points* separating these regions. Let x_c be the spanwise location of such a transition point. It is characterized as a point at which a *subcritical region* breaks down because of p_{11} reaching the value 1. Using (2.37e) for p_{11} and substituting in it $\bar{u}'$ and $\bar{\vartheta}'$ from (6.2 a,b)[2] one obtains an equation for x_c

$$w(x_c) = \frac{1}{2}\cdot\frac{1+\kappa/2}{1+2\kappa}\left(\frac{P^*}{P}-1\right); \qquad P = \frac{P^*}{1+2w(x_c)\dfrac{1+\kappa/2}{1+2\kappa}}. \tag{6.9a,b}$$

Transition is seen to occur at a certain *deflection*, which makes it clear that there exists at most one transition point per halfspan. Since w is symmetric about the midspan so must be the extent of the critical region. Moreover, comparing (6.9b) with (6.8b) one confirms that at criticality onset only the midspan is critical.

We can now pose the problem at hand using that symmetry and eqns (6.2). Only deflections are considered and $\bar{\vartheta}'$ is replaced with the help of (2.42c):

2. Note that (6.2c,d) cannot be used for this purpose, because they satisfy $p = 1$ identically.

$$(P_E-\nu P)w'' + \frac{1}{1+\kappa/2}Pw = P_E w_o'', \qquad 0< x< x_c; \tag{6.10a}$$

$$(P_E-\nu P)w'' + \frac{2(1+3\kappa)}{3\kappa(1+\kappa)}Pw = P_E w_o'' + \frac{P^*-P}{3\kappa(1+\kappa)}, \quad x_c< x< \frac{\pi}{2}; \tag{6.10b}$$

boundary conditions: $w(o)=0$, $w'(\pi/2)=0$; (6.10c)

matching conditions: $w(x_c^-)=w(x_c^+)$, $w'(x_c^-)=w'(x_c^+)$. (6.10d)

The differential equations (6.10a,b) are readily solved:

$$w = c_1 \sin\eta_1 x + E_1 \sin x, \qquad 0\le x< x_c; \tag{6.11a}$$

$$w = c_2 \cos\eta_2(\frac{\pi}{2}-x) + E_2 \sin x + D, \quad x_c< x\le \frac{\pi}{2}; \tag{6.11b}$$

where

$$\eta_1 \equiv \sqrt{\frac{P}{(1+\kappa/2)(P_E-\nu P)}}, \quad \eta_2 \equiv \sqrt{\frac{2(1+3\kappa)P}{3\kappa(1+\kappa)(P_E-\nu P)}}; \tag{6.11c,d}$$

$$E_1 \equiv \frac{e}{1-\dfrac{P}{P_E^*}}, \qquad E_2 \equiv \frac{e}{1-[\dfrac{2(1+3\kappa)}{3\kappa(1+\kappa)}+\nu]\dfrac{P}{P_E}}; \tag{6.11e,f}$$

$$D \equiv \frac{(P^*/P)-1}{2(1+3\kappa)}. \tag{6.11g}$$

These solutions already satisfy the boundary conditions (6.10c,d). There remains to determine the unknown coefficients c_1 and c_2 so as to satisfy the matching conditions (6.10e,f). This operation leads to

$$c_1 = \frac{w(x_c)-E_1\sin x_c}{\sin\eta_1 x_c}, \qquad c_2 = \frac{w(x_c)-D-E_2\sin x_c}{\cos\eta_2(\pi/2-x_c)}; \tag{6.12a,b}$$

where x_c is determined from the transcendental equation

$$\eta_1 (w(x_c) - E_1 \sin x_c) \operatorname{ctg} \eta_1 x_c +$$

$$- \eta_2 (w(x_c) - D - E_2 \sin x_c) \tan \eta_2 (\frac{\pi}{2} - x_c) +$$

$$+ (E_1 - E_2) \cos x_c = 0 \qquad (6.13)$$

and $w(x_c)$ is given by the right hand side of (6.9a).

Typical equilibrium paths for e=0 and e > 0, resulting from (6.11)-(6.13), are shown in Figure 6-2. Also shown in this figure are the ideal LBL and the onset of criticality locus. The upper section of the figure depicts two deflection shapes (over a halfspan) corresponding to the two marked points on the e = 0.3 path. The leftmost of these is just prior to onset of criticality whereas the remaining one has already a substantial critical region. Transition point motion due to change in a is given by the $w(x_c)$ dashed line. The following points are of interest:

1. The post-buckling equilibrium path originates from P* *tangent* to the criticality-onset locus. its initial slope is lower than that obtained from (4.23a) in the limit $\varepsilon \to 0$. Eqn. (4.23a) does not take criticality into account and therefore must be restricted to $\varepsilon \neq 0$.

2. The post-buckling equilibrium path approaches the ideal LBL. The rate of approach is very small compared to that of a locally-imperfect, but ideal column having the same global buckling load.

3. If e > 0 a 'bifurcation' is seen to occur at the point of intersection of the global line and the criticality onset locus. It indicates that upon onset of criticality the drop in overall bending resistance is large enough so as to prevent any further load increase. We will call this point the *critical* or *third bifurcation* point.

4. The critical bifurcation is similar to the ideal case second bifurcation, except that its bifurcated equilibrium path is e-dependent and no local

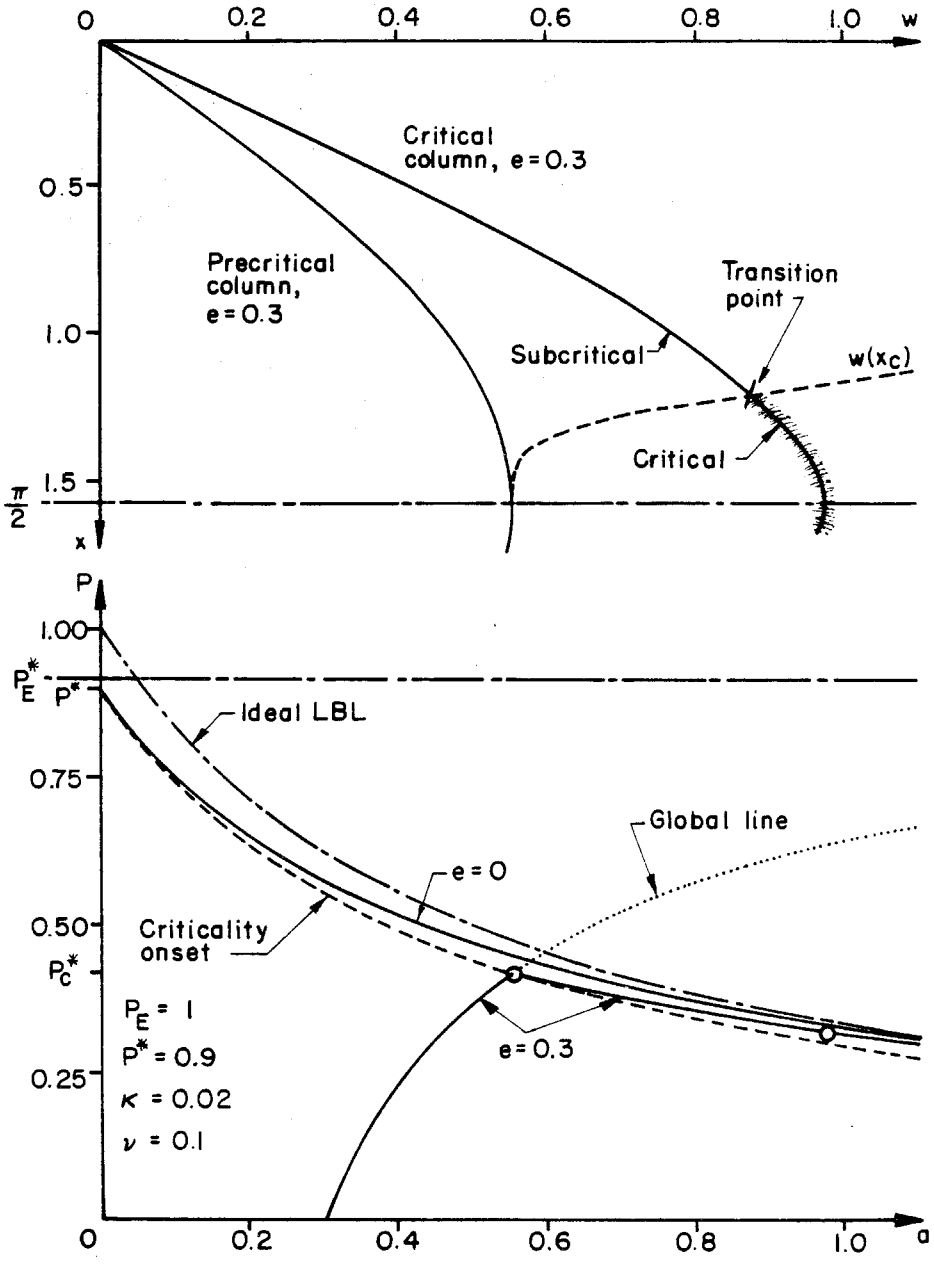

Figure 6-2. Typical equilibrium paths and deflection shapes of locally-perfect columns having $P^* < 1$, $P^* < P_E^*$.

buckling is involved. A critical region rather than a sharp break appears in the neighborhood of the midspan.

We will call the value of the load at critical bifurcation the *critical load*, P_c^*. Clearly, $P_c^* \to P_c$ upon reduction to the ideal column and $P_c^* \to P^*$ when $e \to 0$ (provided $P_E^* > P^*$). It is given by

$$P_c^* = \frac{1}{2}\left[P^* + P_E^*(1+2e^*) - |P^*-P_E^*| \sqrt{1 + 4e^* P_E^* \frac{P^* + (1+e^*)P_E^*}{(P^*-P_E^*)^2}} \right] \qquad (6.14)$$

where

$$e^* \equiv \frac{1+2\kappa}{1+\kappa/2} e \qquad (6.15)$$

and the analogy with (3.16c) is clear. The global imperfection sensitivities of P_c^* are readily obtained as

$$P_c^* \sim P_E^*\left(1 - \frac{2e^* P_E^*}{P^*-P_E^*}\right), \qquad 0 < (P^*-P_E^*)/P_E^* = O(e^0); \qquad (6.16a)$$

$$P_c^* \sim P^* - \sqrt{2e^*}, \qquad |P^*-P_E^*| = o(e); \qquad (6.16b)$$

$$P_c^* \sim P^* - 2e^* P_E^*/(P_E^*-P^*), \qquad 0 < (P_E^*-P^*)/P_E^* = O(e^0). \qquad (6.16c)$$

The critical load P_c^* is clearly an additional upper bound on the column strength, $P_m \leq P_c^*$.

6.2 Local Buckling of the Deflected Column

In the ideal case local buckling was defined as the condition that somewhere along the span there exists a single bay for which $p_{11} = 1$. The 'strains' $\bar{u}'$ and $\bar{\vartheta}'$ at this bay were than clearly indeterminate. In the general column the above definition is already taken by criticality, moreover, the infinite strains property does not coincide with that definition. To remedy this situation we redefine local buckling as *the occurrence, somewhere along the span, of a single bay having*

indeterminate strains. We now set forth to determine the conditions and consequences of that occurrence.

From either (2.37a,b) or (2.38a,b) it follows that a *necessary* condition for $\bar{u}'$ and $\bar{\vartheta}'$ to be indeterminate is that $p_{11} = 1$. In a manner similar to that of Section 3.2.2 we can show that $\bar{\vartheta}'$ in any slackening region adjacent to the buckled point must be bounded; it follows, using a formally once-integrated version of the applicable bending equation, that that boundedness is possible only if either $\varepsilon \to 0$ or $a \to \infty$. The indeterminacy of $\bar{\vartheta}'$ at the buckled point guarantees that the boundary conditions can be met regardless of the details of the solution elsewhere. Hence, as in the ideal case, the local mode is one which is characterized by a finite discontinuity in ϑ across the point of maximum deflection. Its existence in equilibrium requires, besides satisfying $p_{11} = 1$ at that point, also that $\varepsilon = 0$.

We have seen, however, in the last section, that these two conditions are not sufficient; they may lead to criticality rather than to local buckling. Moreover, eqns. (6.2c,d) imply that $\bar{u}'$ and $\bar{\vartheta}'$ in a region I critical bay are never indeterminate. Therefore, if local buckling is to occur at all, the bay which buckles must first be *slack*.

From the argument following eqns. (6.2c,d) it is clear that upon slackening a critical bay must collapse. Mathematically this is brought about by the replacement of the first factor in (6.1a) by its region II counterpart, $(1-P-2w^bP)^2$, (see eqn. (2.39)). Now there are no longer two equations for $\bar{u}'$ and $\bar{\vartheta}'$ but just one, (6.16), resulting in an indeterminate solution. Local buckling is thus clearly a post-slackening phenomenon. In the ideal column it becomes indistinguishable from criticality.

The a-P locus of local buckling is this given by the condition that *somewhere*

along the span a *slack* bay attains $p_{11} = 1$ and is the first[3] bay to do so. The governing equation for a region II slack bay is (2.39). We also write a similar equation, derived from (2.32a), for a somehow stabilized midspan bay having both side-diagonals - 12 as well as 21 - slack;[4]

$$\text{Region II bay:} \quad 1 - P - 2w^b P = 0 , \tag{6.17a}$$

$$\text{Midspan bay:} \quad 1 - P - 2w\,P = 0 . \tag{6.17b}$$

These equations show clearly that the bay to buckle first is the bay deflected most. If the point of maximum deflection happens to be occupied by a bay-node having the deflection $w = a$ then this bay must be a midspan bay to which eqn. (6.17b) applies. Else, if it is a batten which holds the maximum deflection 'a',[5] then an adjacent bay - the one on the $w' > 0$ side, say - is the one that buckles first; it is a region II bay for which $w^b = a$ and to which eqn. (6.17a) applies. Whichever is the case the local buckling locus obtained from (6.17) is one and the same:

$$P = \frac{1}{1+2a} \tag{6.18}$$

namely, the ideal LBL. From now on we will therefore drop the restrictive adjunct 'ideal' and refer to the locus (6.18) as *the* LBL.

We now recall from eqns. (5.6) that midspan slackening occurs below, at most in coincidence with, the locus (6.18). It is not difficult to show, using (6.2c,d) in (2.37g,h), that slackening of a critical bay occurs also precisely at the LBL. It is thus verified that a column satisfying (6.18) has indeed a slack midspan, and this, together with the fact discussed previously that the LBL is an $\varepsilon = 0$ equili-

3. "First" in the sense of "first among all other slack bays upon approaching that locus from below".
4. Unless 'somehow stabilized' such a bay will choose either region II or III, thereby shifting the point of maximum deflection to a nearby batten.
5. In our differential approximation the inconsistency in defining 'a' once as a batten deflection and once as a bay-node deflection is ignored.

brium path, render (6.18) a sufficient as well as a necessary local buckling condition.

If $P^* > 1$ at least part of the criticality-onset locus is above the LBL, thereby exposing it to intersections with active global lines. If this happens, then, just as in the ideal case, the second bifurcation is triggered. To obtain the corresponding local buckling load, P_c, and its associated imperfection sensitivities, all that we have to do is replace in (3.16c-f) P_E by P_E^* (compare (6.4e) with (3.16b)). We get

$$P_c = \frac{1}{2}[1+P_E^*(1+2e) - |1-P_E^*| \sqrt{1+\frac{4eP_E^*[1+(1+e)P_E^*]}{(1-P_E^*)^2}}]; \qquad (6.19a)$$

$$P_c \sim P_E^*(1-\frac{2eP_E^*}{1-P_E^*}), \qquad 0<(1-P_E^*)/P_E^* = O(e^0); \qquad (6.19b)$$

$$P_c \sim 1-\sqrt{2e}, \qquad |1-P_E^*| = o(e); \qquad (6.19c)$$

$$P_c \sim 1-2eP_E^*/(P_E^*-1), \qquad 0<(P_E^*-1)/P_E^* = O(e^0); \qquad (6.19d)$$

The *maximum strength of the locally-perfect column* can now be stated as follows:

$$P_m = \min(P_c, P_c^*) . \qquad (6.20)$$

This replaces (4.20c), which deals with an all-perfect column. Note that slackening is not considered a failure if the column is deflected.

6.3 Equilibrium Paths for Very Large Deflections

In this section we look into the nature of solutions and equilibrium paths as the deflection becomes large. Though formally the theory is not applicable for deflections larger than $o(1)$ it is nevertheless important to understand the behavior of the displacement equations at this limit. The case $\varepsilon = 0$ has been treated in Sections 6.1 and 6.2, so here we focus on the case $\varepsilon > 0$. This

excludes the possibility of critical solutions.

We start with the assumption, subject to later verification, that the column is all-region-I except, maybe, at the midspan itself. Since we take $a \to \infty$ all displacement unknowns should be normalized by a so as to keep them bounded. Region I bending equation (2.37a) then becomes

$$P_E(1+\frac{\kappa}{2})(\frac{\bar{\vartheta}}{a})' + (\frac{w}{a})P + \frac{\varepsilon^2}{6a}[\frac{1}{(1-p_{11})^2} - \frac{1}{(1-p_{22})^2}] = 0. \qquad (6.21)$$

Everywhere except at the midspan p_{11} is certainly less than 1 and therefore, as $a \to \infty$, the last term of (6.21) drops. Also, because the midspan is at most buckled, $P \leq 1/(1+2a) \sim 0$ as $a \to \infty$. We are left with only the first term and consequently

$$(\frac{\bar{\vartheta}}{a}) \sim \text{const.}, \qquad x \neq \pi/2. \qquad (6.22a)$$

Upon applying a similar procedure to the compression equation (2.37b) and also deriving the consequences of (6.22a) for $\bar{\gamma}$ and w' using the rest of (2.37) we obtain (taking $e/a \sim 0$)

$$(\frac{\bar{u}'}{a}) \sim 0, \quad (\frac{\bar{\gamma}}{a}) \sim \text{const.}, \quad (\frac{w'}{a}) \sim \text{const.}; \quad x \neq \pi/2. \qquad (6.22b,c,d)$$

It is seen that if the solution is to satisfy the boundary conditions and at the same time differ from trivial the midspan must be buckled and slack. This implies

$$P \sim \frac{1}{1+2a}. \qquad (6.23a)$$

Eqns. (6.22) can now be satisfied if the mode is the ***triangular local mode***, its 'legs' consisting of straight-line segments (Figure 3-2). Upon determining the constants in (6.22) we obtain

$$(\frac{w'}{a}) \sim (\frac{\vartheta}{a}) \sim \frac{2}{\pi}, \quad (\frac{u'}{a}) \sim (\frac{\gamma}{a}) \sim 0; \qquad x < \frac{\pi}{2} \qquad (6.23b\text{-}e)$$

and it is easily verified using (2.37g) that (6.23b-e) must belong to region I.

We thus conclude the following: regardless of any structural or imperfection parameter all equilibrium paths tend as $a \to \infty$ to the LBL. The column deflection shapes tend then to the triangular local mode with zero shear deformation. Except at the midspan, where the bay is slack and buckled, all column diagonals are taut.

This conclusion is in agreement with remark (3) following Figure 5-2b, which concerns the possibility of retightening of the end-bay diagonals. Based on it is the analysis in Section 5.3 of the behavior as $a \to \infty$ of the slackening-onset locus.

6.4 Initial Loading

If the column is locally as well as globally imperfect we can still treat in closed-form its behavior under a very low external load. This we call 'initial loading'.

The approach is one of perturbing the displacement unknowns and the load P around their P = 0 state. The governing equations are region I displacement equations (2.37). (It is assumed that the diagonals are taut at P = 0) and the P = 0 solution is just the global imperfection. Thus we write

$$\bar{u}' = u'^{(1)}, \quad \bar{\vartheta} = \vartheta^{(1)}, \quad \bar{\gamma} = \gamma^{(1)}, \quad w = w_o + w^{(1)}, \quad P = P^{(1)}. \qquad (6.24a\text{-}e)$$

Applying a standard perturbation scheme to eqns. (2.37a,b) one obtains the following first-order perturbation equations

$$P_E[\,1+\frac{\kappa}{2}(1+\frac{\varepsilon^2}{(1-p_o)^3})\,]\vartheta'^{(1)} + w_o(1+\frac{\varepsilon^2}{(1-p_o)^3})P^{(1)} = 0\,, \tag{6.25a}$$

$$2P_E[\,1+2\kappa(1+\frac{\varepsilon^2}{(1-p_o)^3})\,]u'^{(1)} + \quad (1+\frac{\varepsilon^2}{(1-p_o)^3})P^{(1)} = 0\,. \tag{6.25b}$$

The complete solution satisfying boundary conditions (2.44) and the (linear) rest of (2.37) and which corresponds to the global imperfection (4.24) is

$$u' = -\frac{1+\frac{\varepsilon^2}{(1-p_o)^3}}{2P_E[\,1+2\kappa(1+\frac{\varepsilon^2}{(1-p_o)^3})]}P\,, \tag{6.26a}$$

$$w = (1+\nu\frac{P}{P_E}+\frac{1+\frac{\varepsilon^2}{(1-p_o)^3}}{P_E[\,1+\frac{\kappa}{2}(1+\frac{\varepsilon^2}{(1-p_o)^3})]}P)e\sin x\,, \tag{6.26b}$$

$$\vartheta = (1-\nu\frac{P_b}{P_E}+\frac{1+\frac{\varepsilon^2}{(1-p_o)^3}}{P_E[\,1+\frac{\kappa}{2}(1+\frac{\varepsilon^2}{(1-p_o)^3})]}P)e\cos x\,, \tag{6.26c}$$

$$\gamma = \frac{\lambda}{4\kappa}\cdot\frac{P_b+P}{P_E}e\cos x\,. \tag{6.26d}$$

Letting in (6.26b) $x=\pi/2$ and neglecting $\lambda^2/12$ compared to 1 we find the initial loading segment of the equilibrium path to be

$$a = e\,(1+\frac{\nu+(1+\frac{\varepsilon^2}{(1-p_o)^3})}{P_E[\,1+\frac{\kappa}{2}(1+\frac{\varepsilon^2}{(1-p_o)^3})]}P)\,. \tag{6.26e}$$

For $e = 0$ eqns. (6.26) can be shown to reduce to the initial prebuckling solution (4.3). They reduce to the initial loading version of (6.4) for $\varepsilon = 0$ and to the initial loading version of (3.33) for the ideal column.

6.5 A Working Formula for the General Equilibrium Path

The results obtained so far, in this chapter as well as in Chapter 4, are probably most of what can be obtained in useful-closed-form. The greater complexity of the non-ideal column prevents us from deriving equilibrium paths expressions comparable to (3.33) that will hold throughout the a-P plane. Though there is a possibility to produce an $o(h)$-accuracy, totally-decoupled w-equation valid in most of the a-P plane prior to onset of slackening and criticality, an attempt to use it in deriving a universal equilibrium path is futile. Even a brute-force method like that of Ritz-Galerkin yields then an equivalent of the ideal column $f(\alpha)$-function which depends not only on α but also on P and most structural and imperfection parameters. It seems, therefore, that the heart of the a-P plane must be relinquished to the reign of computers.

There is, however, a third possibility that, though being devoid of any physics, may prove extremely useful in engineering calculations. This is the possibility of making a *learned interpolation* across the desolate plane between its results-inhabited boundaries. Whether or not products of such an operation are valuable can only be decided by comparison to their rigorous numerical conterparts.

The idea is to generate a nucleus of a load-deflection relation starting from the global buckling equations (4.17), (4.11a) and then generalizing it to include non-zero deflections. The ideal column equation (3.33) is used as a model for this generalization. Some $o(h)$ modifications are then introduced into that nucleus so as to make it satisfy certain special cases for which we have rigorous results. In this way we obtain the following system:

$$(P_E^*-P)(1-\bar{p}_r)^3 - 2eP_E^*P(1-\frac{\kappa}{2}\cdot\frac{P_E}{P_b})(1-\bar{p}_r)^2\frac{1}{\alpha_r} +$$

$$-\frac{\varepsilon^2}{1+\nu}(P-\frac{\kappa}{2}P_E)\,f(\alpha_r) = 0 \qquad (6.27a)$$

$$(P^*-P) - (1+2\kappa)[1-\bar{p}_r+\frac{\kappa}{2}(\frac{P_E}{P_b}-1)(1-P)\alpha_r] +$$

$$+\kappa\varepsilon^2[\frac{1}{(1-\bar{p}_r)^2}-\frac{1}{(1-p_o)^2}] = 0 \qquad (6.27b)$$

where

$$\alpha_r \equiv \frac{2aP}{1-\bar{p}_r}(1-\frac{\kappa}{2}\frac{P_E}{P_b}) \qquad (6.27c)$$

and the function f is the ideal one, (3.31b).

Before we discuss the reasons behind this choice a few notes regarding application are in order:

1. Eqns. (6.27) do not distinguish between criticality and local buckling, predicting failure to occur at the former only. Hence application should be limited to cases where $P^* \leq 1$. This restriction is also important from the point of view of slackening, which is ignored by (6.27). One has to be confident that slackening phenomena do not interfere within the region of interest, and the condition $P^* \leq 1$ - the practically more prevalent - usually guarantees this.

2. Eqns. (6.27) are expected to yield better results for not-too-large values of ε and e. This is because they are tailored to be almost accurate at the limits $\varepsilon \to 0$ and $e \to 0$.

3. Prior to application of (6.27) one must calculate P_b by solving (4.17) together with (4.11a). The equilibrium path is then constructed as follows: α_r is chosen in the range $0 \leq \alpha_r < 1$; $f(\alpha_r)$ is calculated from (3.31b); (6.27a,b)

are solved simultaneously for P and $\bar{p}_r$; a is calculated from (6.27c).

4. The value of $\bar{p}_r$ obtained in the above procedure, though reducing to $\bar{p}$ when a = 0, is just an auxiliary quantity and should not be interpreted physically.

Equations (6.27) were constructed to satisfy the following conditions and therein lies their usefulness:

1. Eqns. (6.27a,c) differ from their ideal counterparts (3.31b) and (3.3b) by terms of $o(h)$ only and reduce to the latter as $h \to 0$. Hence the general qualitative behavior depicted in Figures 3-11 is preserved.

2. For e = 0 the global buckling load and initial post buckling path generated by (6.27) are *precisely* those obtained from (4.17) × (4.11a) and (4.23a) respectively.

3. For $\varepsilon=0$ and $\alpha_r \neq 1$ eqn. (6.27a) reduces *precisely* to the correct global line (6.4e).

4. For $\varepsilon=0$ and $\alpha_r=1$ the equilibrium path becomes the onset of criticality locus (6.8b). Though we have seen (Figure 6-2) that this locus is not an equilibrium path, nevertheless, the maximum loads P_c^* are predicted correctly. If, however, part of that locus lies above the LBL an error may ensue since (6.27) do not recognize the fixed LBL.

5. For $P \to 0$ and $a \to e$ the following initial loading path is obtained:

$$a = e\left(1 + \frac{1+\nu+\frac{\varepsilon^2}{(1-p_o)^3}\left(1-\frac{2}{\pi}\cdot\frac{\kappa e P_E}{1-p_o}\right)}{P_E\left(1+\frac{\kappa}{2}\right)}P\right). \qquad (6.28)$$

Strictly, this differs by $o(h)$ from the correct result (6.26e). However, in practical engineering applications ε and e are small enough to render the error comparable to what we call $o(h^2)$.

On grounds of the foregoing properties it is believed that equilibrium paths generated by (6.27) will in general lie, everywhere in the interesting regions of the a-P plane, close to their exact numerical counterparts. In particular, (6.27) may be useful in predicting ultimate load-carrying capacities to a better accuracy than is possible using the ideal column model, a prediction that would otherwise involve very elaborate numerical schemes. The power of eqns. (6.27) is illustrated in Figure 6-3, in which comparison is made with exact numerical results. Shown is an expanded view of a near-peak equilibrium path segment belonging to a technologically feasible typical column: $P_E=1$, $\kappa=0.02$, $p_o=0.04$ ($P^* \simeq 1$), $\nu=0.02$ (64 bays), $\varepsilon=e=0.125$ ($l/1000$ and $L/1000$ respectively). The discrepancy between the exact results and those of eqns. (6.27) is seen to be minute indeed, having at the limit point the value of 0.15%! On the downward leg, since the two methods tend to slightly different asymptotes, the discrepancy is more pronounced. Note that from performance point of view the imperfections in this example are by no means small, knocking down the load-carrying capacity to less than 50% of the nominal value (1.00).

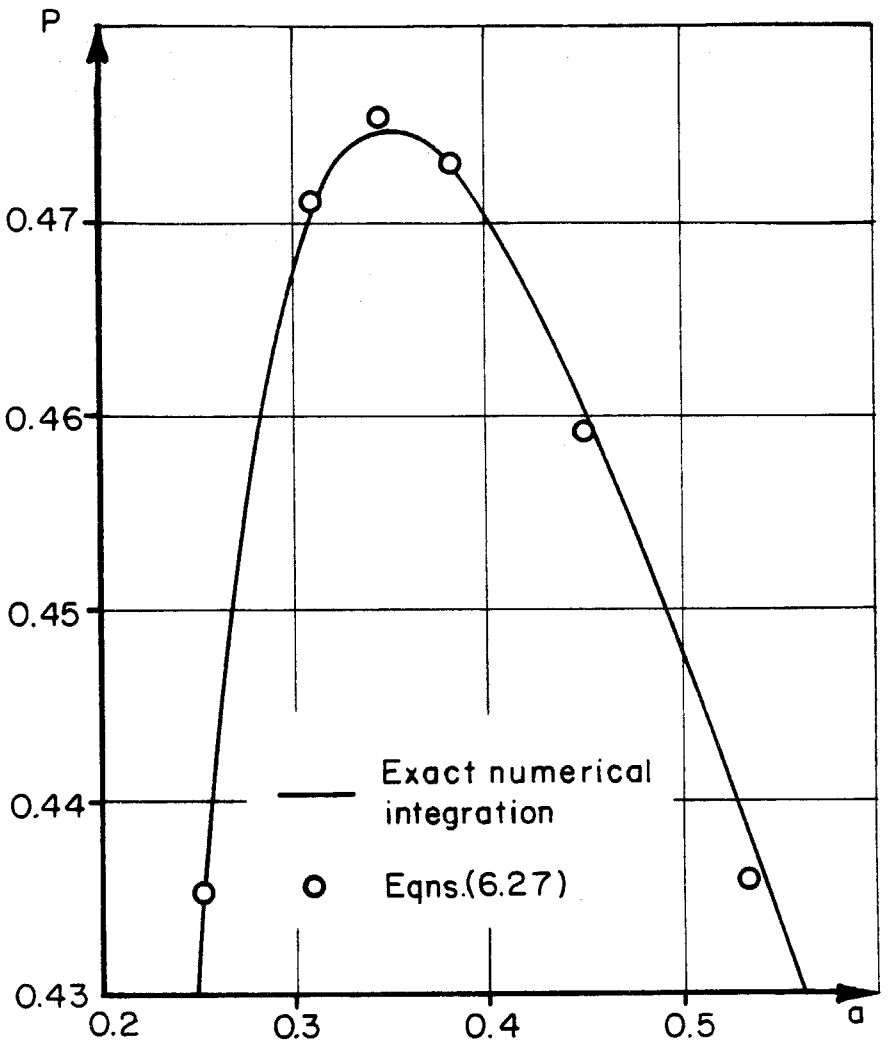

Figure 6-3. Comparison of equilibrium paths obtained using exact numerical integration of the displacement equations and using eqns. (6.27).

7. THE TORSIONAL POST-SLACKENING MODE

In Section 4.8 (Figure 4-6) we found conditions under which either global buckling or slackening is first to occur in a globally-perfect, undeflected column. All the results derived in Chapters 4, 5, and 6 were applicable only inasmuch as global buckling prevailed. It is therefore of interest to find out what happens if it is slackening which takes precedence, and what is the nature of the post-slackening behavior. This is the subject of the present chapter.

Consider a globally-perfect column and suppose for a moment that upon slackening the column deflects in a way still satisfying assumption (14) of Section 2.1, namely, all physical joint displacements occur in the x-z plane only. Then a careful analysis, not presented here, shows the following:

1. At $P = P_s$ there exist multitudes of deflection modes, each one of them consisting of a different number of waves of irregular length. These waves are formed by alternating region II and region III stretches. The boundary and inter-regional matching conditions do not suffice to determine either the number of waves or their individual length, resulting in the mentioned high multiplicity. Region I stretches are *not* possible.

2. Each one of these post-slackening modes is ***stable***, in the sense that it can take higher loads than $P = P_s$; their a-P equilibrium paths are ascending in the positive as well as in the negative a direction. The greater the modal wave number, the more stable is the mode. The least stable is, of course, the one-halfwave mode comprising two equal-length region II and region III stretches matched at the midspan batten. Even this mode has an ascending equilibrium path.

3. Recall from Section 5.4: an equilibrium point anywhere in the a-P plane above $P = P_s$ corresponds to a situation in which back-diagonals, at least

those of the end-bays, are slack. This has also been verified directly from the above-mentioned modal solution and it implies that in reality out-of-plane displacements must occur and that the assumption denying them no longer represents the correct situation.

Once the necessity in post-slackening behavior of out-of-plane displacements is recognized then symmetry considerations lead to a conviction that in a globally-perfect column these displacements must be purely torsional, i.e., rigid-body rotations of the battens around the column centroidal axis. Indeed, such differential batten rotations tighten 3 of the bay diagonals, say 12, 23 and 31, and slacken the others, 13, 32, and 21 (see Figure 7-1). We shall see that under these circumstances equilibrium is possible and moreover, that this equilibrium is stable. Thus, upon total slackening, a slight twist restores stability while maintaining equilibrium.

To analyze this situation eqns. (2.37) and (2.38) must be abandoned in favor of ones allowing rotation rather than deflection. Such equations are derived in this chapter and are applied to analyzing the post-slackening behavior. A study of the interaction between slackening and global buckling is not attempted since it involves a much more complicated system of equations allowing the battens all six degrees of freedom.

7.1 Analysis of the Twisted-Compressed Bay in Post Slackening

Consider a single bay constructed of 2 rigid battens, 3 longeron segments pinned to these battens, and 6 diagonals as shown in Figure 7-1. Joints and bay members are designated in the same way as in Section 2.2, Figure 2-4. Without loss of generality we choose the frame $\mathbf{i}, \mathbf{j}, \mathbf{k}$, such that $\mathbf{k}$ coincides with an axis of symmetry of batten i-1 and $\mathbf{i}$ points from batten i-1 to batten i. The battens are allowed an axial rigid-body translation $\mathbf{u}_i^b = u_i^b \mathbf{i}$ and a rigid-body rotation

$\boldsymbol{\psi}^b = \psi^b \mathbf{i}$, where u_i^b and ψ^b are again physical-dimensional quantities measured with respect to some fixed global coordinate system.

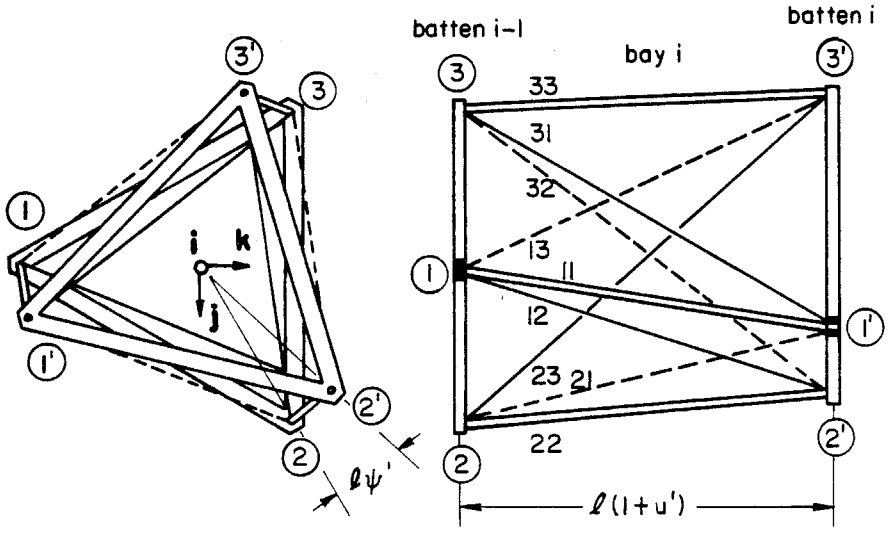

Figure 7-1. The twisted-compressed bay.

In a way similar to that of Section 2.2 we define the extensional and torsional 'bay-strains' of bay i as

$$u_i' = \frac{1}{l}(u_i^b - u_{i-1}^b) ; \qquad \psi_i' = \frac{1}{l}(\psi_i^b - \psi_{i-1}^b) . \tag{7.1a,b}$$

Let now the 'member-strains' be defined as in eqns. (2.3). To establish relations between member-strains and bay-strains we apply again the vectorial technique described in Section 2.2 while neglecting second order terms in u' and $R\psi'$ compared to 1. We obtain

$$\delta_{11} = \delta_{22} = \delta_{33} = -u' , \tag{7.2a}$$

$$\delta_{12} = \delta_{23} = \delta_{31} = \beta^2(u' + \frac{\sqrt{3}R}{2l}R\psi') , \tag{7.2b}$$

$$\delta_{21} = \delta_{32} = \delta_{13} = \beta^2(u' - \frac{\sqrt{3}R}{2l}R\psi') , \tag{7.2c}$$

where R and l are the column radius and bay length respectively (Figure 1-6) and β, the bay aspect ratio parameter, is defined by (2.5).

Suppose now that the column is on the verge of slackening: $P = P_s$, $\psi' = 0$, $p_{mn} = 0$ $(m \neq n)$. We see from eqns. (7.2b,c) that if $\psi' > 0$ is introduced diagonals 12, 23 and 31 will tighten whereas diagonals 21, 32, and 13 will slacken. If $\psi' < 0$ the opposite will happen. Therefore, in each bay, only three diagonals will remain active and we can ignore the other three. As far as an isolated bay is concerned we can assume without loss of generality that ψ' is always positive and accordingly that diagonals 13, 32, and 21 have been snipped away. That is why they appear in Figure 7-1 as dashed lines.

Next, we derive the bay equilibrium relations. This is done in a manner similar to that of Section 2.3, where with each ***deformed*** member we associate a force vector $\mathbf{p}_{mn} = p_{mn}(\mathbf{l}_{mn}/l_{mn})$, $(\mathbf{l}_{mn}/l_{mn})$ being a unit vector aligned with the deformed member. P_{mn} are member 'stresses' as in eqn. (2.7). Considering symmetry it suffices to require

$$\mathbf{p}_{mm} + \mathbf{p}_{mn} = -\frac{P}{3}\mathbf{i} , \tag{7.3a}$$

$$\mathbf{r}_m \times (\mathbf{p}_{mm} + \mathbf{p}_{mn}) = \mathbf{0} \tag{7.3b}$$

in order to satisfy equilibrium. Here $\mathbf{r}_m$ is the radius vector of the undisplaced joint m of batten i-1 (Figure 7-1). It is interesting to note that since no external torque exists the transverse components of the longeron force and its associated diagonal force must cancel each other exactly. The equilibrium relations finally obtained are

$$p_{mm} - \beta[1 + (1 - \beta^2)u' - \beta^2 \frac{\sqrt{3}R}{2l} R\psi'] p_{mn} = \frac{P}{3}, \tag{7.4a}$$

$$p_{mm} R\psi' - \beta[\frac{\sqrt{3}R}{2l}(1 - \beta^2 u') - \frac{1}{2}\beta^2(1 + \frac{9R^2}{2l^2}) R\psi'] p_{mn} = 0 . \tag{7.4b}$$

The system is completed by joining in the members 'constitutive laws', eqns (2.9) and (2.11), omitting the step function in the latter.

In order to simplify eqns. (7.4) we need order estimations of u' and $R\psi'$. Accepting the restriction $\delta_{mm} = o(h^2)$, eqn. (2.13k), we find with the help of (7.2a) that $u' = o(h^2)$. Similarly, we adopt for $R\psi'$ the restriction $R\psi' = o(h^2)$. We shall see later that within the P-range of interest it is indeed always satisfied. This done we see from (7.4b) that the quantity p_{mn}/p_{mm} $(m \neq n)$ must also be of $o(h^2)$. Summing up the simplifying assumptions to be introduced we write

$$u' = o(h^2), \qquad R\psi' = o(h^2), \qquad p_{mn}/p_{mm} = o(h^2) . \tag{7.5a,b,c}$$

As done throughout this work $o(h^2)$ quantitites are neglected compared to $o(h^0)$ quantities. Accordingly the equilibrium relations (7.4) become

$$p_{mm} = \frac{P}{3}, \qquad p_{mm} R\psi' - \frac{\sqrt{3}R}{2l} p_{mn} = 0 . \tag{7.6a,b}$$

Let us now introduce all the non-dimensional quantities and normalization rules of Section 2.5 and, in addition, choose to normalize $R\psi'$ such that the corresponding normalized quantity is of $o(1)$:

$$\hat{\psi}^{\bullet} = \frac{\sqrt{3}}{\lambda^2}(\frac{l}{R})(R\psi') . \tag{7.7}$$

The notation used so far for the physical-dimensional quantities δ_{mn}, p_{mn}, u' ψ', and P will from now on be used to denote their non-dimensional normalized counterparts $\hat{\delta}_{mn}$, $\hat{p}_{mn}$, $\hat{u}^{\bullet}$, $\hat{\psi}^{\bullet}$ and $\hat{P}$. No confusion should arise because the former are now discarded. The simplified bay equations for the normalized quantities in their new notation are summarized below:

'STRAIN-DISPLACEMENT' :

$$\delta_{mm} = 2P_E(-u'), \tag{7.8a}$$

$$\delta_{mn} = 2P_E(u' + \frac{1}{2}\psi'), \quad m \neq n; \tag{7.8b}$$

EQUILIBRIUM:

$$p_{mm} = P, \tag{7.8c}$$

$$\frac{2}{3}\lambda^2 p_{mm}\psi' - p_{mn} = 0; \tag{7.8d}$$

'CONSTITUTIVE' :

$$\delta_{mm} = \frac{\varepsilon^2}{2}\left[\frac{1}{(1-p_{mm})^2} - \frac{1}{(1-p_o)^2}\right] + (p_{mm} - p_o), \tag{7.8e}$$

$$\delta_{mn} = \frac{1}{\kappa}(p_{mn} - \frac{1}{2}p_o), \quad m \neq n. \tag{7.8f}$$

The last two are copied from (2.34a,b) omitting the step function H.

To obtain the bay 'strains' equations we eliminate all the p_{mn}'s and δ_{mn}'s from equations (7.8). In doing so one must bear in mind that though neglecting p_{mn} with respect to P or p_{mm} is justified this may not be the case with respect to 1-P or 1-p_{mm}. Hence, when replacing p_{mm} in the first term of (7.8e) we use the better approximation $p_{mm} - p_{mn} = P$ rather than (7.8c). In application, however, the $o(h^2)$ term thus retained should be neglected in situations where 1-P is not too small. Upon introducing C_s from eqns. (4.6) the bay 'strains' become

$$u' = -\frac{p_o}{4\kappa P_E} - \frac{1}{2P_E}\left[\frac{\varepsilon^2/2}{(1-\frac{P}{1-(2/3)\lambda^2\psi'})^2} - (1-P) - C_s\right], \tag{7.9a}$$

$$\psi' = \frac{1}{(P_E - 4\nu P)}\left[\frac{\varepsilon^2/2}{(1-\frac{P}{1-(2/3)\lambda^2\psi'})^2} - (1-P) - C_s\right]. \tag{7.9b}$$

We now see that as long as P is not too close to 1, i.e. that the column is not too

close to local buckling, the dimensional ψ' is indeed of $o(h^2)$. We also make the following observations:

1. Comparing the square brackets in (7.9a,b) with the slackening load equation (4.5) we note that ψ' vanishes, as it should, when $P = P_s$, and u' assumes then its slackening value $-p_o/4\kappa P_E$.

2. ψ' is an increasing function of P, which means that the post-slackening torsional mode is stable.

3. Eqns. (7.8) and (7.9) were derived for a bay having only three active diagonals and therefore should not be used below slackening. This, together with the requirements $u' = o(1)$, $\psi' = o(1)$, establish their P-range of validity.

$$P_s \leq P \leq 1 - h\varepsilon/\sqrt{2}\,. \tag{7.10}$$

The initial post-slackening behavior can also be easily derived. To within first orders in h and $(P - P_s)$ we obtain

$$u' = -\frac{p_o}{4\kappa P_E} - \frac{1}{2P_E}\left(1 + \frac{\varepsilon^2}{(1-P_s)^3}\right)(P - P_s)\,, \tag{7.11a}$$

$$\psi' = \frac{1}{P_E - 4\nu P}\left(1 + \frac{\varepsilon^2}{(1-P_s)^3}\right)(P - P_s)\,. \tag{7.11b}$$

A typical $P-\psi'$ equilibrium path is shown qualitatively in Figure 7-2. Its interaction with the global buckling line is not as yet known.

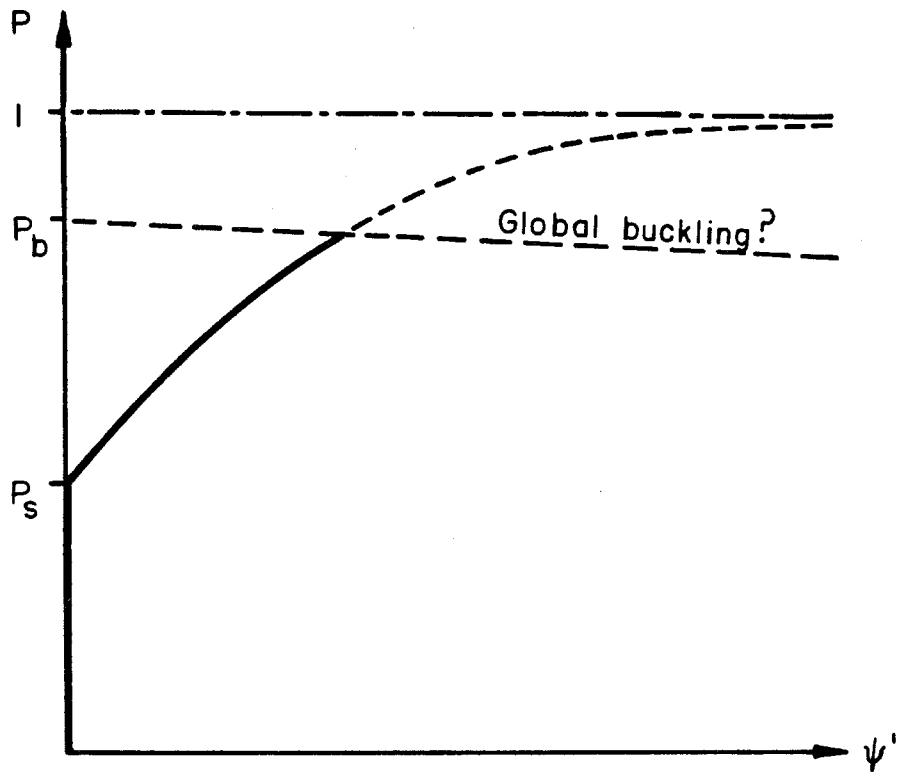

Figure 7-2. Pre- and post-slackening bay twisting (qualitative).

8. ON THE EFFECT OF LONGERONS CONTINUITY

This chapter is intended to provide support to assumption (13) of Section 2.1, namely, that treating the longerons as if they were discontinuous, their segments being pinned to each other, does not under usual circumstances affect the resulting column behavior significantly; also, to establish the limitations of this assumption and the changes that arise in the behavior when it is violated.

To keep matters within reasonable bounds we do the analysis under the ideal column assumptions. There is no loss of generality in this since longeron continuity modifies only the longeron 'constitutive relation' which is essentially the same in the ideal and non-ideal cases. In the first section we establish the continuous-longerons ideal-column equations. The results are then used to estimate the relative importance of the continuity terms and to calculate an approximate LBL as modified by longerons continuity.

8.1 The Continuous-Longerons Ideal-Column Equations

The sole cause for differences in behavior between columns having continuous and discontinuous-pinned longerons lies in the fact that in the former the longeron segments do sustain end bending moments necessary to maintain continuity. In the absence of such moments end-slope mismatch between two adjacent segments will arise due to the difference between their axial loads as well as due to the global curvature. If the longeron segments are slender and the causes of the mismatch are slight the moments required to correct it are small, certainly small enough so as not interfere with global column equilibrium. This is true also in the string-diagonaled column inasmuch as the diagonals leave almost no shear to be carried by longeron bending. Thus, the only way through which these moments can influence the global behavior is by modifying the

longeron segment constitutive law. This law will now involve not only the axial load p but also the unknown end moments. An additional set of equations, arising from inter-segment matching, will take care of the additional unknowns. An assumption implied in the following derivation is that local imperfection and local deflection of all longerons and all segments occur in planes parallel to the x-z plane.

8.1.1 The Modified Constitutive Relation: Figure 8-1 depicts an imperfect segment of longeron number m, located in bay i between battens i-1 and i. Isolating the segment and placing it on simple supports as in the figure requires introduction of an axial load $p_i^{(mm)}$ and the end bending moments $m_{i-1}^{b(mm)}$ and $m_i^{b(mm)}$.

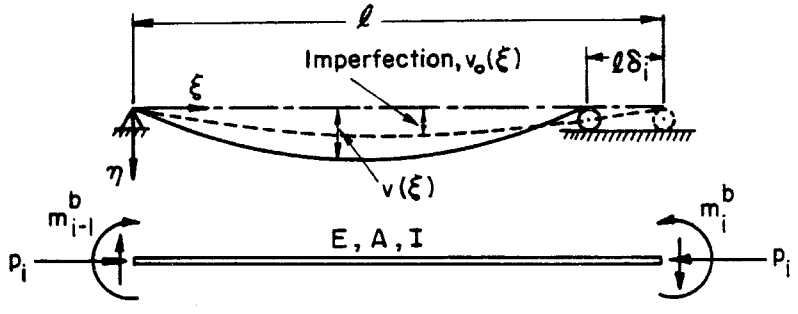

Figure 8-1. The longeron segment.

For simplicity of notation we omit the longeron index m wherever safe. Figure 8–1 also defines the local coordinate system (ξ, η), the shortening $l\delta_i$, the deflection v, and other geometrical and structural quantities - all physical-dimensional.

The differential equation governing the segment deflection $v(\xi)$ is

$$v'' + \frac{p_i}{EI} v = v_o''(\xi) - \frac{m_{i-1}^b}{EI}(1 - \frac{\xi}{l}) - \frac{m_i^b}{EI}(\frac{\xi}{l}) . \tag{8.1}$$

To guarantee the continuity of local imperfection across battens we express it with respect to the local coordinates as $v_o(\xi) = (-1)^i \varepsilon \sin \pi\xi/l$. Upon introducing $p_e = \pi^2 EI/l^2$ and also

$$\chi_i \equiv \sqrt{p_i / p_e} \tag{8.2}$$

the solution satisfying boundary conditions $v(o) = v(l) = 0$ becomes

$$v(\xi) = \frac{(-1)^i \varepsilon}{1 - \frac{p_i}{p_e}} \sin \frac{\pi\xi}{l} +$$

$$+ \frac{1}{p_i} \{ \frac{m_{i-1}^b \sin \chi_i (\pi - \frac{\pi\xi}{l}) + m_i^b \sin \chi_i \frac{\pi\xi}{l}}{\sin \pi\chi_i} - m_{i-1}^b (1 - \frac{\xi}{l}) - m_i^b \frac{\xi}{l} \} . \tag{8.3}$$

Let us now introduce the following normalizations, the first three of which were already used in previous chapters:

$$\hat{p}_i \equiv p_i / p_e = \chi_i^2 = o(1) , \tag{8.4a}$$

$$\hat{\delta}_i \equiv \delta_i (l^2 / \pi^2 \rho^2) = o(1) , \tag{8.4b}$$

$$\hat{\varepsilon} \equiv \varepsilon / (\sqrt{2}\rho) = o(1) , \tag{8.4c}$$

$$\hat{v} \equiv v / (\sqrt{2}\rho) = o(1) , \tag{8.4d}$$

$$\hat{\xi} \equiv \pi\xi / l = o(1) , \tag{8.4e}$$

$$\hat{m}_i^b \equiv m_i^b / (\sqrt{2}\rho p_e) . \tag{8.4f}$$

The order of magnitude of $\hat{v}$ is according to assumption (16) of Section 2.1.

As done in previous cases we will henceforth deal with only the normalized quantities, therefore we can omit the 'hats' and use the old notation for the new quantities. Eqn. (8.3) will now read

$$v(\xi) = \frac{(-1)^i\varepsilon}{1-p_i}\sin\xi + \frac{1}{\chi_i^2}\{\frac{m_{i-1}^b \sin\chi_i(\pi-\xi) + m_i^b \sin\chi_i\xi}{\sin\pi\chi_i} - \frac{1}{\pi}[\,m_{i-1}^b(\pi-\xi) + m_i^b\xi\,]\}. \quad (8.5)$$

Two features of this solution are of interest in this work. The first are the end-slopes $v_{i-1}'^b$ and $v_i'^b$ defined as the derivatives of $v(\xi)$ with respect to ξ at $\xi = 0$ and $\xi = \pi$ respectively:[1]

$$\begin{Bmatrix} v_{i-1}'^b \\ -v_i'^b \end{Bmatrix} = \frac{(-1)^i\varepsilon}{1-p_i}\begin{Bmatrix} 1 \\ 1 \end{Bmatrix} + \frac{\pi}{6}\begin{bmatrix} 2g_1(\chi_i) & g_2(\chi_i) \\ g_2(\chi_i) & 2g_1(\chi_i) \end{bmatrix}\begin{Bmatrix} m_{i-1}^b \\ m_i^b \end{Bmatrix} \quad (8.6)$$

where the functions $g_1(\chi)$ and $g_2(\chi)$ are given by

$$g_1(\chi) \equiv \frac{3}{\pi\chi}(\frac{1}{\pi\chi} - \mathrm{ctg}\,\pi\chi), \qquad g_2(\chi) = \frac{6}{\pi\chi}(\frac{1}{\sin\pi\chi} - \frac{1}{\pi\chi}). \quad (8.7a,b)$$

The second is the relative shortening δ_i (Figure 8-1), calculated using dimensional quantities as $p_i/(EA) + (1/l)\int_0^l (v'^2/2)d\xi$, then normalized according to (8.4b) and expressed in normalized quantities:

$$\delta_i = \frac{\varepsilon^2}{2}[\,\frac{1}{(1-p_i)^2} - 1\,] + p_i + \frac{2/\pi}{(1-p_i)^2}(-1)^i\varepsilon(m_i^b + m_{i-1}^b)$$

$$+ h_1(\chi_i)(m_i^b + m_{i-1}^b)^2 + h_2(\chi_i)(m_i^b - m_{i-1}^b)^2, \quad (8.8)$$

where the functions $h_1(\chi)$ and $h_2(\chi)$ are defined as

$$h_1(\chi) = \frac{1}{4\chi^2}\cdot\frac{\pi\chi - \sin\pi\chi}{\pi\chi + \pi\chi\cos\pi\chi}, \qquad h_2(\chi) = \frac{1}{4\chi^2}(\frac{-4}{\pi^2\chi^2} + \frac{\pi\chi + \sin\pi\chi}{\pi\chi - \pi\chi\cos\pi\chi}). \quad (8.9a,b)$$

Equation (8.8) is the modified longeron-segment constitutive relation sought. The first two terms are independent of the end moments and are identical to those of the ideal column (eqn. (2.34a) with p_o=0). The rest are modifications due to longeron continuity.

1. The result (8.6), apart from having an imperfection term, is the same as Timoshenko's [16], Section 1.6.

8.1.2 The Case $p_i=1$: First we note that as $p\to 1$ ($\chi\to 1$) the functions g_1, g_2, h_1, and h_2 show the following behavior:

$$2g_1 \sim \frac{12}{\pi^2}\left[\frac{1}{1-p}+\frac{1}{2}\right], \qquad g_2 \sim \frac{12}{\pi^2}\left[\frac{1}{1-p}-\frac{1}{2}\right], \tag{8.10a,b}$$

$$h_1 \sim \frac{2}{\pi^2}\frac{1}{(1-p)^2}, \qquad h_2 \sim \left(\frac{1}{8}-\frac{1}{\pi^2}\right). \tag{8.10c,d}$$

These and other singularities appearing in (8.6) and (8.8) suggest that the segment must collapse upon p=1. Whereas this is certainly true if the end moments are prescribed and arbitrary it cannot be the case in a continuous longeron if p=1 occurs at only isolated segments; for then neighboring segments for which $p\neq 1$ lend stiffness to the singular one through the end moments, in an amount just necessary to preserve continuity. In other words, the end moments are determined so as to exactly counteract the effect of ε. Using (8.10) in either line of (8.6) or (8.8) we find the condition on the moments to be

$$m_i^b + m_{i-1}^b = -\frac{\pi}{2}(-1)^i\varepsilon, \qquad p_i = 1\,. \tag{8.11}$$

This satisfied, all singular terms in (8.6) and (8.8) intercancel and we obtain

$$v_i'^b = v_{i-1}'^b = -(m_i^b - m_{i-1}^b)/\pi, \quad p_i = 1\,; \tag{8.12a}$$

$$\delta_i = \frac{\varepsilon^2}{2} + 1 + \left(\frac{1}{8}-\frac{1}{\pi^2}\right)(m_i^b - m_{i-1}^b)^2\,, \quad p_i = 1\,; \tag{8.12b}$$

Strikingly, the deflection resembles that of the second (full-wave) buckling mode.

8.1.3 The End-Moments Equations: If eqn (8.8) is included in the column system it brings with it three additional unknowns. These are the sequences of i, m_i^b, belonging to the three longerons. By imposing matching conditions between each two adjacent segments we obtain, for each longeron, the required additional equation. This one will hold for $p\neq 1$; the case p=1 is covered by (8.11).

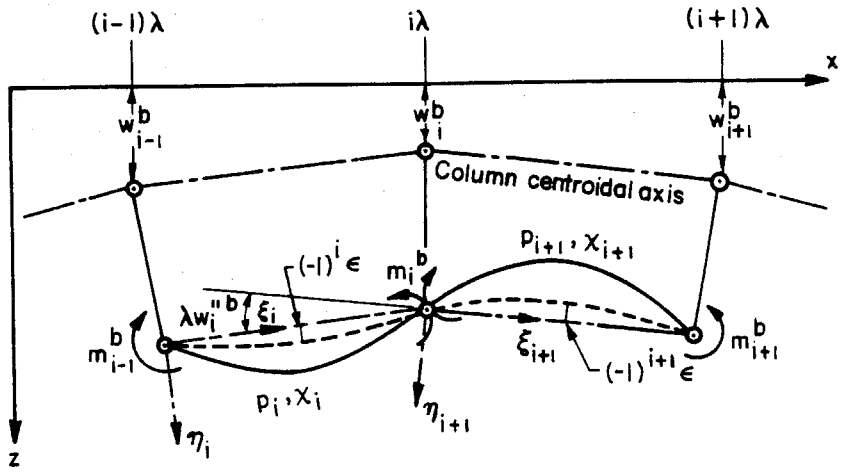

Figure 8-2. Matching of two adjacent longeron segments (even i).

Figure 8-2 depicts two adjacent longeron segments to be matched. Each has its own *local* coordinate system (ξ, η). As a result of global curvature the axes ξ_i and ξ_{i+1} are inclined relative to each other by an angle $\lambda w_i''^b$, where (see w_i' definition (2.2b))

$$w_i''^b \equiv \frac{1}{\lambda}(w_i' - w_{i-1}') \tag{8.13}$$

is a deflection 'second derivative' measure pertaining to a batten point. The slopes of segment i at batten i and of segment i+1 at batten i, both relative to the ξ_i axis, can now be written from (8.6), taking account of this angle,

$$\text{Segment i:} \quad v_i'^b = \frac{(-1)^i\varepsilon}{1-p_i} - \frac{\pi}{6}[\, g_2(\chi_i)\, m_{i-1}^b + 2g_1(\chi_i)\, m_i^b \,],$$

$$\text{Segment i+1:} \quad v_i'^b = \frac{(-1)^i\varepsilon}{1-p_{i+1}} + \frac{\pi}{6}[\, 2g_1(\chi_{i+1})\, m_i^b + g_2(\chi_{i+1})\, m_{i+1}^b \,] + \lambda w_i''^b .$$

Matching the two slopes we obtain[2]

2. Apart from the imperfection term, eqn. (8.14) is equivalent to Timoshenko's [16], eqn. (1-46).

$$\frac{\pi}{6}\{g_2(\chi_i)\,m_{i-1}^b + 2[g_1(\chi_i)+g_1(\chi_{i+1})]\,m_i^b + g_2(\chi_{i+1})\,m_{i+1}^b\} =$$

$$= -(-1)^i \varepsilon \frac{p_{i+1}-p_i}{(1-p_i)(1-p_{i+1})} - \lambda w_i''^b \,. \qquad (8.14)$$

This is a linear, second order, variable coefficients difference equation for the segment-end bending moments m_i^b. The two boundary conditions required for it arise from the vanishing of these moments at the column end battens

$$m_o^b = 0\,, \qquad m_N^b = 0\,. \qquad (8.15a,b)$$

For a continuous longeron, local buckling is a condition on the χ_i's under which the boundary conditions (8.15), though being homogeneous, cannot suppress the homogeneous solution of (8.14). The form of (8.14) (i.e., g_1, $g_2 > 0$; $g_2(\chi_i) \sim g_2(\chi_{i+1})$ as $\lambda \to 0$) suggest that m_i^b is then an alternating sequence. Else, if the case is other than local buckling, the homogeneous solution *is* suppressed and we expect m_i^b to comprise two sequences; an alternating one driven by the first term on the right hand side of (8.14), and a slowly-varying one responding to $\lambda w_i''^b$. It is advantageous to have to deal with only slowly-varying sequences. To this end we decompose m_i^b, for local buckling as well as for the general case, as follows:

$$m_i^b = (-1)^i \mu_i^{(1)b} + \mu_i^{(2)b}\,, \qquad (8.16)$$

where the $\mu_i^{(j)b}$ sequences, now slowly varying,[3] satisfy the following system:

$$\frac{\pi}{6}\{g_2(\chi_i)\,\mu_{i-1}^{(1)b} - 2[g_1(\chi_i)+g_1(\chi_{i+1})]\mu_i^{(1)b} + g_2(\chi_{i+1})\,\mu_{i+1}^{(1)b}\} = \frac{\varepsilon(p_{i+1}-p_i)}{(1-p_i)(1-p_{i+1})}; \qquad (8.17a)$$

$$\frac{\pi}{6}\{g_2(\chi_i)\,\mu_{i-1}^{(2)b} + 2[g_1(\chi_i)+g_1(\chi_{i+1})]\mu_i^{(2)b} + g_2(\chi_{i+1})\,\mu_{i+1}^{(2)b}\} = -\lambda w_i''^b; \qquad (8.17b)$$

3. Except, maybe, within narrow 'boundary layers'.

$$\mu_0^{(1)b} = 0, \quad \mu_N^{(1)b} = 0; \quad \mu_0^{(2)b} = 0, \quad \mu_N^{(2)b} = 0. \qquad (8.17c\text{-}f)$$

In consistence with the general approach of this work, namely, treating sequences as if they were continuous functions, we now would like to find a system of *differential* equations, with appropriate boundary conditions, the solutions of which will approximate the μ-sequences satisfying (8.17) at a set of discrete points. It is convenient here to depart from the former practice of choosing these points at the bay modes and to choose them at the battens instead. Accordingly, if q_i is a general segment-inherent quantity (e.g., p_i, χ_i, δ_i) and q_i^b is a general batten-inherent quantity (e.g., $\mu_i^{(j)b}$, w_i^b) their conversion scheme will be the following:

$$q(x) \leftrightarrow q_i^b \equiv \frac{1}{2}(q_{i+1} + q_i), \qquad (8.18a)$$

$$q'(x) \leftrightarrow q_i'^b \equiv \frac{1}{\lambda}(q_{i+1} - q_i) \text{ or } \frac{1}{2\lambda}(q_{i+1}^b - q_{i-1}^b), \qquad (8.18b)$$

$$q''(x) \leftrightarrow q_i''^b \equiv \frac{1}{\lambda}(q_{i+1}' - q_i') \text{ or } \frac{1}{\lambda^2}(q_{i+1}^b - 2q_i^b + q_{i-1}^b), \qquad (8.18c)$$

where q_i' is defined as in eqns. (2.2). Using these the system (8.17) becomes

$$p = p(x), \quad \chi = \chi(x), \quad w = w(x), \quad \mu_1 = \mu_1(x), \quad \mu_2 = \mu_2(x); \qquad (8.19a)$$

$$\frac{\lambda^2}{2}[g_2(\chi)\mu_1']' - [2g_1(\chi) - g_2(\chi)]\mu_1 = \frac{3\lambda}{\pi} \cdot \frac{\varepsilon p'}{(1-p)^2 - (\lambda^2/4)p'^2}; \qquad (8.19b)$$

$$\frac{\lambda^2}{2}[g_2(\chi)\mu_2']' + [2g_1(\chi) + g_2(\chi)]\mu_2 = -\frac{3\lambda}{\pi}w''; \qquad (8.19c)$$

$$\mu_1(0) = 0, \quad \mu_1(\pi) = 0; \quad \mu_2(0) = 0, \quad \mu_2(\pi) = 0. \qquad (8.19d)$$

These are the sought end-moment equations. The end moments themselves are calculated from (8.16) letting $\mu_i^{(j)b} = \mu_j(x_i^b)$.

With a few exceptions eqns. (8.19) can be simplified further by neglecting the $O(\lambda^2)$ terms compared to the $O(\lambda^0)$ ones. It cannot be done in (8.19b) for narrow

$O(\lambda)$ 'boundary layers' near the end battens, since there μ'' must be large enough to settle the dispute existing between the boundary conditions and the behavior of the driving sequence. Another exception is the local buckling case, in which the $O(\lambda^2)$ term is responsible for the non-trivial solution. None of these reservations, however, apply to (8.19c). Thus, provided due awareness is given to the above exceptions, we can write

$$\mu_1 = \frac{-3\lambda/\pi}{2g_1(\chi)-g_2(\chi)} \cdot \frac{\varepsilon p'}{(1-p)^2}, \tag{8.20a}$$

$$\mu_2 = \frac{-3\lambda/\pi}{2g_1(\chi)+g_2(\chi)} \cdot w'' . \tag{8.20b}$$

(Note that $2g_1-g_2$ and $2g_1+g_2$ are positive in $0 \leq x < \pi$.) We see that under most circumstances μ_1 and μ_2 are point-functions of p, p', and w'', moreover, that they are of $o(\lambda)$.

8.1.4 The Continuous-Longerons Ideal-Column Equations: Before we can summarize the equations applicable to an ideal column having continuous longerons we have to give the constitutive relation (8.8) a form compatible with the developments of Section 8.1.3. We take the following steps: (1) Expressing the moments m_i^b in terms of the slowly-varying $\mu_i^{(j)b}$ using (8.16); (2) eliminating $\mu_{i-1}^{(j)b}$ and $\mu_{i+1}^{(j)b}$ in favor of $\mu_i^{(j)b}$ using combinations of (8.18); (3) deriving $\delta_i^b \equiv (\delta_{i+1}+\delta_i)/2$; (4) using the assumptions $(\lambda/2)p' << 1-p$ and $\mu_j'' = o(\lambda^o)$ to allow neglection of high-order-in-λ terms; (5) treating the batten-related sequences of i as if they were functions of x. As a result of these operations the following constitutive relation is obtained:

$$\delta = \frac{\varepsilon^2}{2}\left[\frac{1}{(1-p)^2}-1\right] + p + \frac{2\lambda}{\pi}\varepsilon\left\{\frac{\mu_1'}{(1-p)^2}-\left[\frac{\mu_2}{(1-p)^2}\right]'\cos\frac{\pi x}{\lambda}\right\} + \\ + 4h_1(\chi)\mu_2^2 + 4h_2(\chi)\mu_1^2 \tag{8.21}$$

where μ_1 and μ_2 are solutions of (8.19) or (8.20) and the alternating factor $(-1)^i$ is replaced by the cosine function. The most remarkable finding in (8.21) is that due to mutual cancellation between δ_i and δ_{i+1} the alternating term in (8.21) is one order higher than its originator, the third term of (8.8).

The assumptions made in deriving (8.21) - unavoidable ones if progress were to be made - are essentially the same as those involved in (8.20). Hence there is no point in using the more general (8.19) in conjunction with (8.21), and we can look upon (8.20) and (8.21) as constituting part of the continuous-longerons ideal column equations. From a global point of view, the inexactitude of (8.20), (8.21) at the boundary layers and at isolated points of $p_i \sim 1$ is purely local and cannot influence the global behavior to a significant extent. Thus, somewhat below the LBL, eqns. (8.20) and (8.21) can be applied throughout the span. Close to or above the LBL their validity breaks down because long stretches of $p \sim 1$ are expected.

Once (8.20) and (8.21) are written for each longeron, the continuous-longerons ideal-column system is completed by adding the ideal column relations

$$p_{11} = P(1+2w), \quad P_{22} = P_{33} = P(1-w), \quad P_E(w'' - w_o'') + \frac{1}{3}(\delta_{11} - \delta_{22}) = 0.$$

and boundary conditions $w(o)=w(\pi)=0$. No attempt is made in this work to obtain solutions of this system.

8.2 Effects of Longerons Continuity

Let us now use the results of the previous section in order to draw some conclusions as to importance of longerons continuity. If the longerons are truly

discontinuous then $\mu_1=\mu_2=0$ and (8.21) reduces to the ideal constitutive relation. The whole column system then reduces to the ideal case. We can thus estimate the importance of the effect by just looking at the relative magnitudes in (8.21) - whenever it is applicable - of the terms representing continuity.

In the region of applicability of (8.21), where $1/(1-p)^2 = o(1)$ throughout the span except at isolated points, eqns. (8.20) give μ_1 and μ_2 of $o(h)$. Substituting them into (8.21) we see immediately that whatever ε is the longeron continuity effect on the segment shortening is of $o(h^2)$ compared to $o(1)$ of the leading effect. Within the framework of the present theory this effect is negligible. We have thus justified assumption (13) of Section 2.1 for equilibrium points not too close to the LBL.

Is that assumption also applicable close or above the LBL? We are not as well-equipped to answer this question as we were to the previous one. Let us therefore obtain some idea of the answer by means of calculating an approximation to the actual a-P locus of local buckling - the *continuous-longerons LBL*.

The continuous-longerons LBL is expected to have higher P-values than those of the usual one. This is due to the aforementioned fact that segments having $p<1$, through their end-moments, can check the $p=1$ segment deflections from growing indefinitely. (The two LBLs should intersect at $a=0$ since there all segments attain $p=1$ simultaneously.) The longeron has therefore to be analyzed for buckling as an indivisible unit, the governing equation being the homogeneous one associated with (8.14), (8.15),

$$g_2(\chi_i)\, m^b_{i-1} + 2[g_1(\chi_i) + g_1(\chi_{i+1})]\, m^b_i + g_2(\chi_{i+1})\, m^b_{i+1} = 0\,; \qquad (8.22a)$$

$$m^b_0 = 0\,, \qquad m^b_N = 0\,. \qquad (8.22b,c)$$

This choice is motivated by the fact that the solution must in any case be numerical and finite-difference equations are more suitable for that.

To obtain an exact LBL, one must solve the complete column system in order to find the exact $\chi(x)$. This is beyond our intentions. Instead we *assume* a deflection shape $w(x)$ and derive $\chi(x)$ using ideal column relations. A reasonable assumption for an $\varepsilon=0$ column is the usual $w(x)=a\sin x$, which for longeron 11 leads to

$$\chi_i = \sqrt{P[\,1+2a\sin(i-\tfrac{1}{2})\lambda\,]} \tag{8.23}$$

There remains to solve the eigenvalue problem (8.22), (8.7), (8.23) for the eigenvalue $P(a;\lambda)$. The following crude shooting technique has been found effective:

1. Use symmetry with respect to the midspan to consider only one halfspan. Integration of (8.22a) proceeds from the midspan towards an end.

2. Choose a and guess P. calculate χ_i from (8.23) and $g_1(\chi_i)$ and $g_2(\chi_i)$ from (8.7) for all bays in the halfspan.

3. To start integrating one must have two m_i^b's, their i's differing by at most 2. These are chosen at two battens located symmetrically about the midspan and symmetry then implies that they are either equal (if N is odd) or opposite (if N is even). Their absolute value is chosen, for convenience, as 1.

4. Once 2 m_i^b's are known, a third can be found using (8.22a). In this way an alternating sequence m_i^b is produced which satisfies (8.22b,c) only if $P=P_{LBL}$ (or higher critical loads). If $P\neq P_{LBL}$ but fairly close to it, and if the number of bays is large enough, the sequence seems first to converge to zero but later starts to diverge very fast.

5. The bay number at which divergence starts is *extremely* sensitive to the choice of P. So much so that if the number of bays is large enough a sufficient accuracy of P_{LBL} can be obtained without ever caring about satisfying (8.22b,c) but only about keeping the point of divergence far from the

midspan. The point of divergence as a function of P serves to control the improvement of P.

The scheme described above has been used to calculate an approximate continuous-longerons LBL for a 19-bays column (λ =0.165). This is about the least slender column which can still be considered slender. The results are shown in Figure 8-3. It is seen that the continuous-longerons LBL is indeed higher than the discontinuous one and intersecting with the latter at a=0. Clearly, the P-difference (~ 7% at a=1) must be considered of $o(\lambda)$ rather than of $o(\lambda^2)$, (λ^2=2.7%). It is thus concluded that *close to the LBL* the error committed by treating continuous longerons as if they were discontinuous, though small and conservative, is nevertheless not negligible according to the standards set in this work. Luckily, equilibrium paths of real columns approach the LBL only past the limit-load point, which is their most practically-important feature.

Also shown (qualitatively) in Figure 8-3 is the expected behavior of the continuity error along an equilibrium path. As long as the path is well below the LBL the error is small, of $o(h^2)$. As the path approaches the LBL the error increases gradually. Finally, as $a \to \infty$, the error becomes that existing between the two different LBL's, i.e., of $o(h)$.

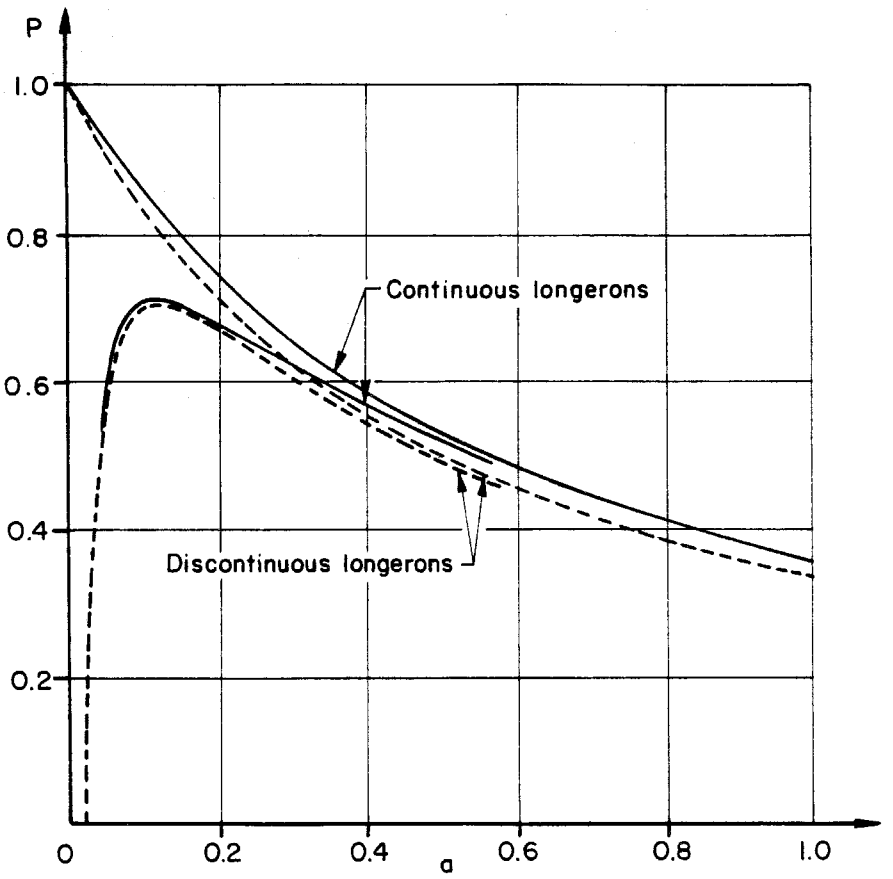

Figure 8-3. Effects of longeron continuity, 19-bays column.

9. CONCLUDING REMARKS

Let us here summarize the main results obtained in the present work:

1. Equations (2.37), (2.38) together with the boundary conditions (2.40) constitute a well posed problem, the solution of which yields the displacement unknowns u', ϑ, γ, and w. Once these are obtained, their substitution into (2.31) gives the local 'strains', δ_{mn}. The internal 'stresses', p_{mn}, are found partly from (2.37e,f) or (2.38e,f) and the rest from (2.32). These solutions are physically valid inasmuch as the assumptions of Section 2.1 are satisfied. They are then of $o(h)$ accuracy. A partially decoupled system, valid for region I only, is given in eqns. (2.42). For closed-form treatment the displacement unknowns may be viewed as continuous functions of x and the primes, accordingly, as ordinary derivatives. With few exceptions, only such results were presented here. Numerical solutions, not included in this work, were also obtained by treating the displacement unknowns and their primed associates according to their exact finite difference definitions, normalized versions of (2.1) and (2.2). The method used was finite difference integration combined with shooting technique.

2. If $o(h)$ quantities are removed from (2.37), (2.38) and infinite shear rigidity is postulated, the result is a greatly simplified system we called the 'ideal column'. Its behavior is determined by the solution of a single ordinary nonlinear differential equation (3.2a). The ideal column turned out to be a powerful tool for revealing the most important behavioral features of more complicated systems and for obtaining quick $o(h^0)$-accuracy results. It allowed us to proceed to great depths using a closed form approach. Among the results were: (i) The local buckling line and the nature of local buckling in the deflected state (Section 3.2); (ii) the phenomena around the first and

second bifurcation points (Sections 3.3, 3.4); (iii) exact solution and equilibrium path of the globally-perfect case (Eqns. (3.18b), (3.20)); (iv) asymptotic study of that solution which led to understanding of the post-buckling behavior and to the construction of a simple and accurate equilibrium path working formula (Eqns. (3.33), (3.31b)); (v) the latter afforded a quick access to the column practically most important property, its maximum load-carrying capacity P_m (Eqns. (3.34)).

3. The main subject of the work was, however, the more complicated non-ideal column. In Chapter 4 we dealt with its behavior in the undeflected or only slightly deflected situations. The complete qualitative picture was given in Figures 4-1 and 4-3. Whereas in the perfect ideal column we had two bifurcation points, $P = P_E$ (global buckling) and $P = 1$ (local buckling), two more were found to exist in the perfect general column: $P = P_s$ (slackening, where the column goes into a torsion mode, Chapter 7) and $P = P^*$, where the column bifurcates globally, its bays becoming what we called critical. P_E itself was modified to become P_E^*. Each one of these loads is an upper bound on the column load-carrying capacity. This was stated in eqn. (4.20c) which forms a basis for optimal design of columns. The various bifucration loads in the presence of local imperfections and their imperfection sensitivities were analyzed in detail: P_s (eqn. (4.5)) in Section 4.2 and P_b (eqns. (4.17), (4.11a)) in Section 4.4. Initial post buckling and global imperfection sensitivity were also studied. The question of what happens first, buckling or slackening, was answered in Section 4.8.

4. In Chapter 5 we followed slackening phenomena into the a-P plane. This was done by means of slackening loci in that plane which signified the occurrence of their specific phenomena when intersected by proper equilibrium paths. In particular, we dealt with midspan slackening, end-bay

slackening, slackening onset and slackening of the back diagonals. We usually treated these problems to a lesser accuracy, $o(h^0)$, than we did in other topics. The picture that emerged was summarized in Section 5.5. Slackening phenomena in the a-P plane are of little practical interest since, if $P_s > P_b$ the validity of equations (2.37), (2.38) was never compromised by a type of slackening (i.e. back diagonals) which contradicted the assumptions done in their derivation.

5. Unlike in the ideal case, the closed-form approach succeeded to construct only a partial picture of the behavior of the general deflected column. The most remarkable item achieved is the complete solution for the all-region-I, locally-perfect case. The behavior discovered, though quantitatively close to that of the ideal column, was qualitatively very different. The onset of criticality locus, eqn. (6.8b), was found to constitute an upper bound on the column strength in addition to the one imposed by the LBL. The load associated with it, P_c^* - a deflected generalization of P* - was given by eqns. (6.14)-(6.16). Those details of behavior we did obtain, together with the ideal-column results, allowed us to construct, by way of interpolation and generalization, a somewhat artificial but very useful equilibrium path formula (eqns. 6.27). Comparison with exact numerical solutions showed it to perform quite well.

6. The behavior in post-slackening in cases where slackening precedes global buckling was analyzed in Chapter 7. It was found that the column goes into a torsional mode in which each bay is independent of the others, three of its diagonals are slack while the other three are taut. This mode was found to be stable and to require only negligible diagonal forces.

7. In deriving equations (2.37), (2.38) the longerons were treated as if they were

discontinuous, their segments being pinned to each other, i.e., the segments end bending moments were assumed to be of negligible consequence. Chapter 8 attempted to verify the validity and establish the limitations of this assumption. It was found to be valid (i.e., to cause an $o(h^2)$ error) as long as the equilibrium path did not approach the LBL too closely. If it did the error became of $o(h)$. From an engineering standpoint, however, the important (limit point) part of the equilibrium path is usually well below the LBL. By calculating the buckling load of a continuous longeron bent globally in a prescribed sine shape we also obtained an indication as to the way the LBL is modified by longeron continuity.

In concluding we would like to mention that results obtained by pure numerical solutions of eqns. (2.37), (2.38), (i.e., finite-difference integration combined with shooting technique), and which could not be incorporated in this work, brought up neither new facts nor contradictions to the body of results obtained in closed form. The ideal-column theory represented by eqns (3.33), (3.31b) was found to be extremely accurate compared to numerical results employing the same assumptions. Also, the qualitative picture of diagonal slackening in the a-P plane was fully confirmed. On these grounds it is believed that although the analysis has been in a sense incomplete (e.g., no solutions consisting of multiple regions were attempted) the picture obtained is by no means lacking in essentials.

The greatest limitation of the theory is its inapplicability (or its uncertain applicability) to the important cases of columns having longeron segments which are rigidly of flexibly clamped to the battens. It seems that the methods used here (see preface to this work) are in principle unsuited to tackle this problem and heavier numerical involvement must be allowed.

What probably can be done but has not been attempted in this work is the investigation of the triplex interaction between global buckling, local buckling and slackening, especially when $P^* \sim P_E^* \sim 1$. This requires a system of equations broader than (2.37), (2.38), which accounts for all possible displacements, out-of-plane ones as well as those included in (2.37), (2.38). The future may see this work done.

REFERENCES

[1] Hagler, T., "Building Large Space Structures in Space," *Astronautics and Aeronautics*, Vol. 14, No. 5, May 1976.

[2] Card, M.C. and Boyer, W.J., "Large Space Structures - Fantasies and Facts," Proc. AIAA/ASME/ASCE/AHS 21st Structures, Structural Dynamics and Materials Conference, Part 1, 1980.

[3] Huckins, E.K., "A Case for Large Space Systems Technology," Society of Allied Weight Engineers, 39th Annual Conference, St. Louis, Missouri, May 1980 (SAWE Paper 1372).

[4] Carlisle, R.F. and Dibattista, J.D., "The Role of Large Space Systems," AAS/AIAA Annual Meeting on Space Enhancing Technological Leadership, Boston, Massachusetts, Oct. 1980 (AAS Paper 80-275).

[5] Brodsky, R.F. and Morais, B.G., "Space 2020: The Technology, the Missions Likely 20-40 Years from Now," *Astronautics and Aeronautics*, Vol. 20, No. 5, May 1982.

[6] *Large Space Systems Technology - 1980*, Second Annual Technical Review, NASA Langley Research Center, Hampton, Virginia, Nov. 1980 (NASA CP 2168).

[7] *Large Space Systems Technology - 1981*, Third Annual Technical Review, NASA Langley Research Center, Hampton, Virginia, Nov. 1981 (NASA CP 2215).

[8] *Modeling, Analysis and Optimization Issues for Large Space Structures*, Proceedings of a workshop, Williamsburg, Virginia, May 1982 (NASA CP 2258).

[9] *Structural Dynamics and Control of Large Space Structures - 1982*, Proceeding of a workshop, NASA Langley Research Center, Hampton, Virginia, Jan. 1982 (NASA CP 2266).

[10] *Large Space Antenna Systems Technology - 1982*, Proceeding of a Conference, Hampton, Virginia, Nov. 1982 (NASA CP 2269).

[11] Hedgepeth, J.M., "Critical Requirements for the Design of Large Space Structures," NASA Contractor Report 3484, Nov. 1981.

[12] "Development of a Composite Geodetic Structure for Space Construction. Phase I Final Report," McDonnel Douglas Astronautics Company, MDC G8079, Oct. 1979.

[13] "Interim Report for Study of Wrap-Rib Antenna Design," Lockheed Missiles and Space Company, LMSC-D714653, July 1981.

[14] Koiter, W.T., *The Stability of Elastic Equilibrium*, Thesis, Delft Technische Hogeschool, The Netherlands, Translation: Air Force Flight Dynamics Laboratory, Technical Report AFFDL-TR-70-25.

[15] Tvergaard, V., "Buckling Behavior of Plate and Shell Structures," *Theoretical and Applied Mechanics:* Proceedings of the 14th IUTAM Congress, Delft, the Netherlands, Aug. 1976, W.T. Koiter (ed.) North Holland, 1977.

[16] Timoshenko, S.P. and Gere, J.M., *Theory of Elastic Stability*, McGraw-Hill Book Company, New York, 2nd edition, 1961.

[17] van der Neut, A., 'The Interaction of Local Buckling and Column Failure of Thin-Walled Compression Members," Proceedings of the 12th International Congress on Applied Mechanics, Stanford, 1968, Springer-Verlag 1969.

[18] Koiter, W.T. and Kuiken, G.D.C., 'The Interaction Between Local Buckling and Overall Buckling on the Behavior of Built-Up Columns," Report 447, Delft Technische Hogeschool, The Netherlands, May 1971 (N71-35139).

[19] *Pignataro, M. and Rizzi, N.*, "On the Interaction Between Local and Overall Buckling of an Asymmetric Portal Frame," *Meccanica*, Vol. 18 No. 2, June 1983.

[20] Thompson, J.M.T. and Hunt, G.W., *A General Theory of Elastic Stability*, John Wiley & Sons, New York, 1973.

[21] Thompson, J.M.T. and Lewis, G.M., "On the Optimum Design of Thin-Walled Compression Members," *Journal of the Mechanics and Physics of Solids*, Vol. 20, No. 2, May 1972.

[22] Bleich, F., *Buckling Strength of Metal Structures*, Mc-Graw-Hill Book Company, New York, 1952.

[23] *Noor, A.K. and Peters, J.M.*, 'Recent Advances in Reduction Methods for Instability Analysis of Structures," *Computers & Structures*, Vol. 16, Nos. 1-4, pp. 67-80, 1983.

[24] Bleich, F. and Melan, E., *Die gewöhnlichen und partiellen* Differenzengleichungen der Baustatik, Julius Springer, Berlin 1927.

[25] von Karman, T. and Biot, M.A., *Mathematical Methods in Engineering*, McGraw-Hill Book Company, New York, 1940.

[26] Wah, T., 'The Buckling of Gridworks," *Journal of Mechanics and Physics of Solids*, Vol. 13 No. 1, February 1965.

[27] Forman, S.E. and Hutchinson, J.W., 'Buckling of Reticulated Shell Structures," *International Journal of Solids and Structures*, Vol. 6 No. 7, July 1970.

[28] Anderson, M.S., 'Buckling of Periodic Lattice Structures," *AIAA Journal*, Vol. 19 No. 6, June 1981.

[29] Crawford, R.F. and Hedgepeth, J.M., 'Effects of Initial Waviness on the Strength and Design of Built-up Structures," *AIAA Journal*, Vol. 13 No. 5, May 1975.

[30] Byskov, E., "Applicability of an Asymptotic Expansion for Elastic Buckling Problems with Mode Interaction," *AIAA Journal*, Vol. 17 No 6, June 1979.

[31] Mikulas, M.M., 'Structural Efficiency of Long, Lightly Loaded Truss and Isogrid Columns for Space Applications," NASA TM 78687, July 1978 (N78-33480).

[32] Anderson, M.S., 'Buckling of Imperfect Periodic Structures," *COLLAPSE, The Buckling of Structures in Theory and Practice*, J.M.T. Thompson, and G.W. Hunt (eds.), Cambridge University Press, 1983.

[33] Crawford, R.F. and Benton, M.D., 'Strength of Initially Wavy Lattice Columns," *AIAA Jorunal*, Vol. 18 No. 5, May 1980.

[34] Timoshenko, Young, and Weaver, *Vibration Problems in Engineering*, John Wiley & Sons, New York, 1974 pp. 175-177.

[35] Budianski, B., 'Theory of Buckling and Post-Buckling Behavior of Elastic Structures," *Advances in Applied Mechanics*, Vol. 14, Academic Press, New York, 1974, pp. 2-63.